



UNIVERSIDADE FEDERAL DO CEARÁ
CENTRO DE CIÊNCIAS
DEPARTAMENTO DE QUÍMICA ANALÍTICA E FÍSICO-QUÍMICA
PROGRAMA DE PÓS-GRADUAÇÃO EM QUÍMICA

LEONARDO PAES DA SILVA

**SULFONAMIDES DERIVED FROM ANACARDIC ACID AS POTENTIAL
ANTICHAGASIC: A THEORETICAL APPROACH BASED ON MOLECULAR
DOCKING, MOLECULAR DYNAMICS, AND DENSITY FUNCTIONAL THEORY
CALCULATIONS**

FORTALEZA

2021

LEONARDO PAES DA SILVA

SULFONAMIDES DERIVED FROM ANACARDIC ACID AS POTENTIAL
ANTICHAGASIC: A THEORETICAL APPROACH BASED ON MOLECULAR
DOCKING, MOLECULAR DYNAMICS, AND DENSITY FUNCTIONAL THEORY
CALCULATIONS

Dissertação apresentada ao Programa de Pós-Graduação em Química da Universidade Federal do Ceará como requisito parcial à obtenção do título de mestre em Química. Área de concentração: Físico-Química.

Orientador: Prof. Dr. Pedro de Lima Neto.
Coorientador: Prof. Dr. Emmanuel Silva Marinho.

FORTALEZA

2021

Dados Internacionais de Catalogação na Publicação
Universidade Federal do Ceará
Biblioteca Universitária

Gerada automaticamente pelo módulo Catalog, mediante os dados fornecidos pelo(a) autor(a)

- S581s Silva, Leonardo Paes da.
Sulfonamides derived from anacardic acid as potential antichagasic : a theoretical approach based on molecular docking, molecular dynamics, and density functional theory calculations. / Leonardo Paes da Silva. – 2021.
80 f. : il. color.
- Dissertação (mestrado) – Universidade Federal do Ceará, Centro de Ciências, Programa de Pós-Graduação em Química, Fortaleza, 2021.
Orientação: Prof. Dr. Pedro de Lima Neto.
Coorientação: Prof. Dr. Emmanuel Silva Marinho.
1. Sulfonamide. 2. Density functional theory. 3. Molecular docking. 4. Molecular dynamics. I. Título.
CDD 540
-

LEONARDO PAES DA SILVA

SULFONAMIDES DERIVED FROM ANACARDIC ACID AS POTENTIAL
ANTICHAGASIC: A THEORETICAL APPROACH BASED ON MOLECULAR
DOCKING, MOLECULAR DYNAMICS, AND DENSITY FUNCTIONAL THEORY
CALCULATIONS

Dissertação apresentada ao Programa de Pós-Graduação em Química da Universidade Federal do Ceará como requisito parcial à obtenção do título de Mestre em Química. Área de concentração: Físico-Química.

Aprovada em: ____/____/____.

BANCA EXAMINADORA

Prof. Dr. Pedro de Lima Neto (Orientador)

Universidade Federal do Ceará (UFC)

Prof. Dr. Emmanuel Silva Marinho (Coorientador)

Universidade Estadual do Ceará (UECE)

Prof. Dr. Tércio de Freitas Paulo

Universidade Federal do Ceará (UFC)

Prof. Dr. Márcia Machado Marinho

Universidade Estadual do Ceará (UECE)

To God, my parents, and friends.

ACKNOWLEDGMENTS

I recognize my insignificance, and in front of the LORD, I owe gratitude for my life and for giving me the opportunity to fulfill my mission each day.

To my dear mother Leonizia Paes, my father Pedro Edson and Miguel Paes.

To professors Pedro de Lima Neto and Emmanuel Silva Marinho, for believing in my potential and for the direction and incentive in academic life, since graduation. Without them, I would not have gotten where I am and where I want to be.

To my colleagues in the lab and life: Lucas Lima, Francisco Wagner, Ámison Rick, Lucas Coutinho, Emmanuele Marinho, Renato Veríssimo.

All the members of the GQT (Grupo de Química Teórica), who contributed in lab experience.

To professor Norberto de Kássio Vieira Monteiro, professor Márcia Machado Marinho, professor Hélcio Silva dos Santos, professor Alexandre Magno Rodrigues Teixeira, Jacilene Silva, who kindly contributed to the conclusion of this dissertation article.

This study was financed in part by the Coordenação de Aperfeiçoamento de Pessoal de Nível Superior – Brasil (CAPES) – Finance Code 001.

“Coragem fez de mim, um grande lutador
Mesmo sendo sofredor acredito no amor
Amor de um homem que andou pegando a paz
Jejuou no deserto, falou não pro Satanás
Aquele ali sim, teve determinação
Não fraquejou com os irmãos
Você sabe, tem vários por aí que são covarde
Usa da maldade, falta com verdade
Final dos tempos está se aproximando
Falta fé, cresce o ódio, assim vive o ser humano”
(Sabotage)

ABSTRACT

Chagas disease (CD) is a tropical disease caused by the parasite *Trypanosoma cruzi*, transmitted by the barber insect. Currently, there are approximately 7 million infected people in the world, and it is estimated that 70 million people could contract this disease. The anacardic acid (AA) showed effectiveness *in silico* and *in vivo* tests. The antichagasic potential of five sulfonamide molecules, derived from anacardic acid, was evaluated from a molecular approach based on Density Functional Theory (DFT), Molecular Dynamics (MD), and Molecular Docking calculations. Methyl 2-methoxy-6- (8- (methylsulfonamide) octyl) benzoate (SA1); 2-methoxy-6- (8- (phenylsulfonamide) octyl) benzoate (SA2); methyl 2-methoxy-6- (8- (2methylphenyl sulfonamide) octyl) benzoate (SA3); methyl 2-methoxy-6- (8- (methylphenylsulfonamide)octyl)benzoate (SA4); methyl 2-(8-(2,5-dimethylphenylsulfonamide)octyl)-6-methoxybenzoate (SA5) were the investigated molecules. The DFT calculations were performed using the B3LYP/6-311+G (d, p) level of theory. The global and local reactivity data showed that SA1 shows the highest molecular reactivity, while SA2 is the most stable derivative. In addition, the structures of investigated molecules were confirmed by the linear correlations higher than 0.98 displayed between the experimental and calculated spectroscopic data (IR and NMR). Molecular docking of the molecules showed a greater prominence for the SA1, SA2, and SA4 molecules in the results of distances of ligand/cruzain. In molecular dynamics, SA4 obtained better stability due to greater interactions with important aminoacids of cruzain.

Keywords: sulfonamide; density functional theory; molecular docking; molecular dynamics.

RESUMO

A doença de Chagas é uma doença tropical causada pelo parasito *Trypanosoma cruzi*, transmitida pelo inseto barbeiro. Atualmente, há aproximadamente cerca 7 milhões de pessoas infectadas no mundo, além disso, calcula-se que 70 milhões de pessoas poderão contrair essa doença. O ácido anacárdico (AA) mostrou efetividade em teste *in silico* e *in vivo*. O potencial antichagásico de cinco moléculas sulfonamidas, derivadas do ácido anacárdico, foi avaliado o potencial reativo dos derivados moléculas em uma abordagem molecular baseada na Teoria Funcional da Densidade (DFT). Na Dinâmica molecular (MD) e nos cálculos de Docking molecular foi verificado a interação desses derivados, com a enzima alvo (cruzaína). Metil 2-metoxi-6- (8-(metilsulfonamida) octil) benzoato (SA1); Metil 2-metoxi-6-(8-(fenilsulfonamida) octil) benzoato (SA2); Metil 2-metoxi-6- (8- (2-metilfenil sulfonamida) octil) benzoato (SA3); metil 2-metoxi-6- (8- (metilfenilsulfonamida) octil) benzoato (SA4); metil 2- (8- (2,5- dimetilfenilsulfonamida) octil) -6-metoxibenzoato (SA5) foram as moléculas investigadas. Os cálculos do DFT foram realizados utilizando o nível teórico B3LYP/6-311+G (d, p). As estruturas das moléculas investigadas foram confirmadas pelas correlações lineares superiores a 0,98 entre os dados espectroscópicos experimentais calculados de Infravermelho (IV) e Ressonância Magnética Nuclear (RMN) do carbono. Os dados de reatividade global e local mostraram que SA1 mostra a maior reatividade molecular, enquanto SA2 é a derivada mais estável. Além disso, o Docking molecular das moléculas mostrou destaques para as moléculas SA1, SA2 e SA4 nos resultados das distâncias de interação ligante/cruzaína, e no desempenho da dinâmica molecular, SA4 obteve melhor estabilidade com o sítio, devido a uma maior quantidade de interações com importantes aminoácidos da cruzaína.

Palavras-chave: sulfonamida; teoria do funcional da densidade; docking molecular; dinâmica molecular.

LIST OF FIGURES

Figure 1 –	The linear correlation between the experimental wavenumbers and theoretical wavenumbers for the fundamental vibrational modes of the AA derivatives molecules at the B3LYP/6-311+G (d, p) level of theory. (a) SA1; (b) SA2; (c) SA3; (d) SA4; (e) SA5	28
Figure 2 –	Structure 2D of the AA derivatives molecules structured with the central A ring and the variations of derivatives on the R radical, highlighting the secondary aromatic B ring	29
Figure 3 –	Optimized geometries of the AA molecule and their derivatives SA1-SA5 for the B3LYP/6-311+G (d, p) level of theory	30
Figure 4 –	Linear correlation with the experimental ¹³ C isotropic shielding and the calculated isotropic magnetic shielding at B3LYP/6–311+G (d, p) in Chloroform. (a) SA1; (b) SA2; (c) SA3; (d) SA4; (e) SA5	31
Figure 5 –	Frontier Molecular Orbitals (HOMO and LUMO) and the energy gap (ΔE) calculated for the AA and Derivates (SA1-5) at B3LYP/6–311+G (d, p) level of theory	33
Figure 6 –	Calculated isosurfaces for the Electronic Fukui functions using the electronic density and computed at B3LYP/6–311+G (d, p) computational level	35
Figure 7 –	Calculated Molecular Electrostatic Potential (MEP) at B3LYP/6-311+G(d,p) level of theory for the SA1- SA5 molecules	36
Figure 8 –	Interaction complex of the receptor cruzain with ligands VS1 (a), BZN (b), SA1 (c), SA2 (d), SA3 (e), SA4 (f), SA5(g), AA (h)	37
Figure 9 –	SA1 (A), SA2 (B), SA3 (C), SA4 (D), SA5 (E), AA (F) and BZN (G) molecular interactions with cruzain	39
Figure 10 –	Determination of root mean square deviation (RMSD) of unbounded 1F29 (black) and 1F29-SA1 (red), 1F29-SA2 (green), 1F29-SA3 (blue), 1F29-SA4 (yellow), 1F29-SA5 (brown), and 1F29-BZN (cyan) complexes	40
Figure 11 –	Energies of interaction present in the 1F29-SA1, 1F29-SA2, 1F29-SA3, 1F29-SA4, 1F29-SA5, and 1F29-BZN complexes, with standard deviation	41

Figure 12 – Interactions presents in the (a) 1F29-SA1, (b) 1F29-SA2, (c) 1F29-SA3, (d) 1F29-SA4, (e) 1F29-SA5, and (f) 1F29-BZN complexes 42

LIST OF TABLES

Table – 1	Binding residue/protein distances in angstroms.....	38
-----------	---	----

LIST OF ABBREVIATIONS AND ACRONYMS

AA	Anacardic Acid
Ala	Alanine
Asn	Asparagine
BZN	Benznidazol
Cys	Cysteine
DFT	Density Functional Theory
Gln	Glutamine
Gly	Glycine
Gromacs	Groningen Machine for Chemical Simulation
His	Histidine
Lys	Lysine
MD	Molecular Dynamics
Met	Methionine
PLIP	Protein-Ligand Interaction Profile
PDB	Protein Data Bank
RMSD	Root MeanSquare Deviation
SA1	Methyl 2- methoxy-6- (8- (methylsulfonamide) octyl) benzoate
SA2	Methyl 2-methoxy-6- (8- (phenylsulfonamide) octyl) benzoate
SA3	Methyl 2-methoxy-6- (8- (2methylphenylsulfonamide)octyl)benzoate
SA4	Methyl 2-methoxy-6-(8- (methylphenylsulfonamido)octyl) benzoate
SA5	Methyl 2-(8-(2,5- dimethylphenylsufonamido)octyl)-6-methoxybenzoate
Trp	Tryptophan
Val	Valine

VS1

Vinyl Sulfone I

SUMMARY

1	INTRODUCTION.....	14
2	SULFONAMIDES DERIVED FROM ANACARDIC ACID AS POTENTIAL ANTICHAGASIC: A THEORETICAL APPROACH BASED ON MOLECULAR DOCKING, MOLECULAR DYNAMICS, AND DENSITY FUNCTIONAL THEORY CALCULATIONS	17
3	CONCLUSIONS	62
	REFERENCE	64
	APPENDIX A – AUTHOR'S CURRICULUM DATA.....	66
	APPENDIX B – PAPERS PUBLISHED.....	71
	APPENDIX C – ELSEVIER AND RSC'S AUTHOR RIGHTS	79

1 INTRODUCTION

Neglected diseases are endemic tropical diseases that prevail under poverty conditions and help maintain inequality because they are potent obstacles to national development (POSENATO; LUÍS, *et al.*, [S.d.]). They mainly affect the poor in Africa, Asia, and Latin America. As examples of neglected diseases, we can mention dengue fever, Chagas disease, schistosomiasis, leishmaniasis, malaria, tuberculosis. According to the World Health Organization (WHO), more than 1 billion people are infected with one or more neglected diseases, representing one-one-sixth of the world's population. Together they cause 500,000 to 1 million deaths each year. Although funding has been provided for research related to neglected diseases, the knowledge generated has not been translated into advances in treatments such as new drugs, diagnostic methods, and vaccines (“Doenças negligenciadas: estratégias do Ministério da Saúde”, 2010). One of the reasons for this is that the pharmaceutical industry's interest in the topic is low, the reason being that the profitability potential of the industry is low because the affected population is low-income, and most of them are in developing countries (BRITO; FALCÃO, *et al.*, 2021).

Despite the growing demand for safe and effective medicines, neglected diseases represent a low priority for the pharmaceutical industry. Low investment in research and development (R&D) results in few drugs and vaccines for neglected diseases. Moreover, many of the drugs were developed more than half a century ago and are highly toxic (KESSELHEIM, 2019).

Chagas Disease (CD) is caused by human infection with the protozoan *Trypanosoma cruzi* (*T. cruzi*). Insects called " blood-sucking insect " are the primary vectors involved in the spread of this disease. The infection mainly occurs by inoculating the bite site with protozoa present in the insect intestine. However, there are other forms of transmission. This disease can also be transmitted orally through food contaminated by parasites, mainly its feces (WHO).

CD is identified with an acute phase lasting about two months. The symptoms of this phase include fever, inflammation at the inoculation site, unilateral eyelid edema, lymphadenopathy, and hepatosplenomegaly (BRITO *et al.*, 2021). In addition, a high number of parasites circulate in the blood, but symptoms are absent or mild and nonspecific in most cases. In the chronic phase, parasites are mainly hidden in the heart and digestive muscles. As a result, as many as 30% of patients have heart disease, and up to 10% have digestive system disease (usually enlarged esophagus or colon), neurological disease, or mixed disease. In

addition, the infection can cause sudden death due to arrhythmia or progressive heart failure caused by the destruction of the myocardium and its nervous system (MARTINS-MELO *et al.*, 2014).

There are treatments available for CD. Benznidazole (BZN) and Nifurtimox are commonly recommended. In Brazil, where the infected population is equivalent to 4.6 million people with *T. cruzi* infection (MARTINS-MELO, RAMOS, *et al.*, 2014), the only available drug is BZN. This drug is almost 100% effective in curing the disease if administered soon after infection at the beginning of the acute phase, including cases of congenital transmission (WHO). However, BZN is effective in the chronic phase of the disease. In addition, the most common side effects are rash, digestive intolerance, anorexia, asthenia, headache, and sleep disturbances (FERREIRA, *et al.*, 2019). In more severe cases, skin reactions, fever, atopic dermatitis, erythematosis, light-sensitive rashes, purpura, weight loss, and gastrointestinal disturbances occur within the first weeks of treatment (CLAYTON, 2010).

More and more researches are being done into the use of natural medicines that effectively treat and cure diseases. Natural products have shown great potential as drugs (CHEUKA, MAYOKA, *et al.*, 2016). Natural drugs are being studied for the treatment of CD, and one of the examples is *Lychnophora trichocarpha*, a native plant from Brazilian savanna (Cerrado), indicating results in decreasing the amount of *T. cruzi* in the host's blood (SÜLSEN, PUENTE, *et al.*, 2016).

Alternatively, the use of cashew tree derivatives *Anacardium occidentale L* has been gaining space for potential drugs. Studies indicate good results as antidiabetic (JAISWAL, *et al.*, 2017; SU, *et al.*, 2019), antioxidant, larvicidal e antiacetylcholinesterase (OLIVEIRA, *et al.*, 2011), antimicrobial (K., H. *et al.*, 2014) e antifungal (SANTOS, *et al.*, 2011). The anacardic acid (AA) is one of the main components of the cashew nut shell liquid (CNSL) (PAULA, *et al.*, 2020), can be utilized as a sub-product of industrial residues. Furthermore, besides showing promising results as an antioxidant for biofuels (PAULA, *et al.*, 2020, RANGEL, *et al.*, 2021), the AA has also been shown to have biological activities, showing promising results in enzyme inhibition of Glyceraldehyde 3-phosphate (GAPDH) of *T. cruzi*, an enzyme essential of the glycolytic pathway of the antichagasic parasite, in tests with the evolutive forms of the parasite, in epimastigotes and trypomastigotes (ALVES, 2018).

Furthermore, computational resources significantly contribute to searching for new potential candidates to combat the disease (DE AZEVEDO JR., 2010). In the works of Marinho (MARINHO, *et al.*, 2019; MARINHO, *et al.*, 2020; MARINHO, *et al.*, 2021), they showed the pharmacological potential of AA as an antichagasic through molecular docking. The studies

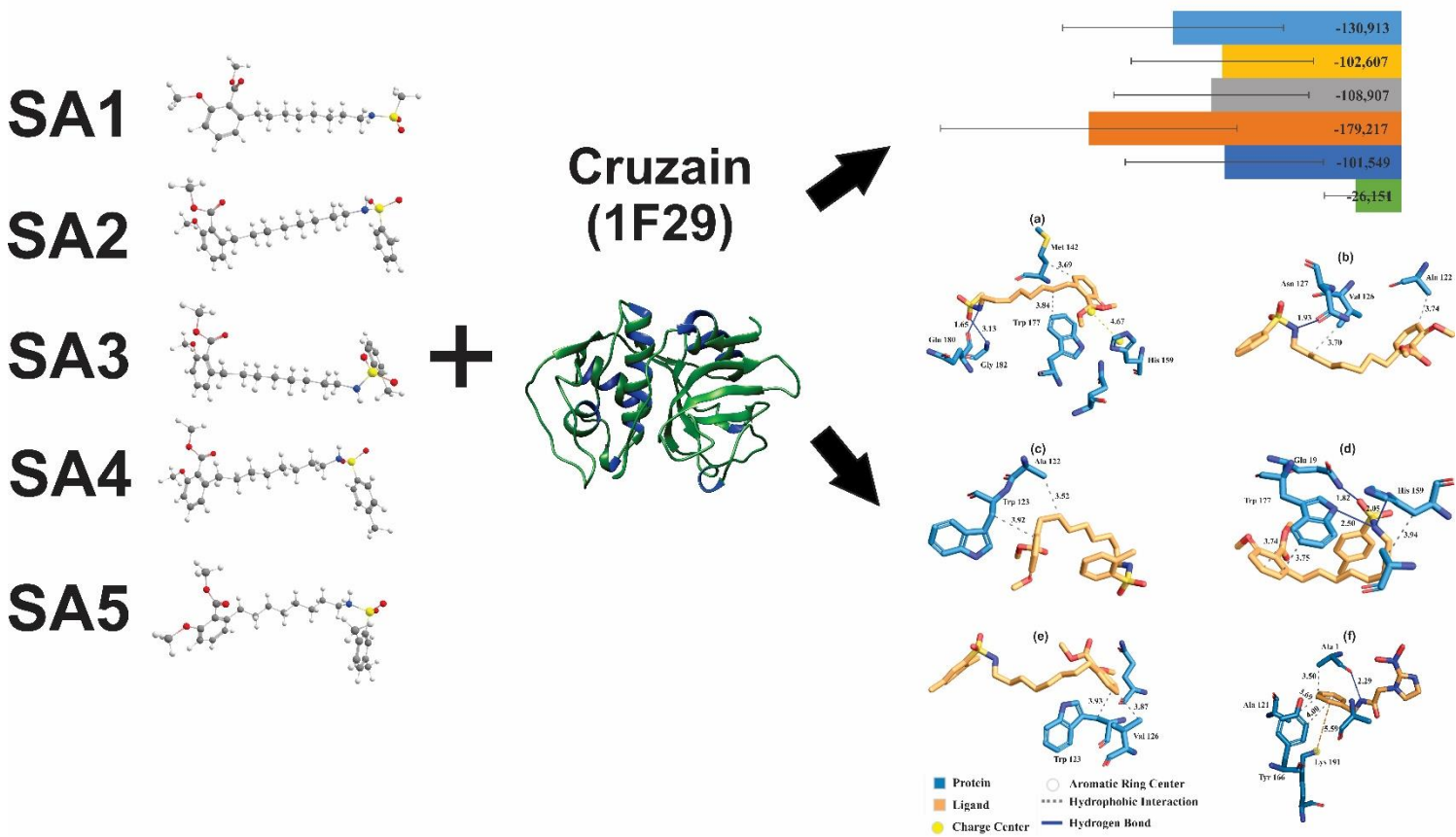
showed an excellent interaction of AA with the enzyme cruzain, responsible for the proteolytic activity involved in several vital processes and are present in all stages of the evolutionary cycle of the parasite. It was also evaluated in silico the interaction of AA with the enzyme TcGAPHD. In the glycolytic pathway of the parasite, this enzyme is responsible for the conversion of glyceraldehyde-3-phosphate into 1,3-bisphosphoglycerate in the presence of nicotinamide adenine dinucleotide (NAD)⁺ inorganic phosphate (MARINHO; *et al.*, 2019; ZINSSER, *et al.*, 2014).

In a study by Reddy (REDDY; *et al.*, 2012), synthesis, Infrared (IR), and Nuclear Resonance Magnetic (NMR) spectroscopical identifications of C-8 sulfonamide derivatives of anacardic acid were performed. They showed their antibacterial activity on *Escherichia coli*, *Pseudomonas aeruginosa*, *Staphylococcus aureus* and *Streptococcus pyogenes* bacterial strains.

In this perspective, this work aims to investigate the antichagasic potential of anacardic acid sulfonamide derivatives, characterizing their global and local reactivity by the density functional theory method. Furthermore, to identify the possible sites of reactivity of these molecules with cruzain and investigate the stability of the interactions of SA1-SA5 molecules with cruzain sites through molecular dynamics, comparing them with the drug BZN.

Chapter 1

Sulfonamides derived from anacardic acid as potential antichagasic: a theoretical approach based on Molecular Docking, Molecular Dynamics, and Density Functional Theory calculations





PCCP

Sulfonamide derived from anacardic acid as potential anti-sores: a theoretical approach based on Molecular Docking, Molecular Dynamics, and Density Functional Theory calculations

Journal:	<i>Physical Chemistry Chemical Physics</i>
Manuscript ID	CP-ART-08-2021-003995.R1
Article Type:	Paper
Date Submitted by the Author:	n/a
Complete List of Authors:	da Silva, Leonardo; Universidade Federal do Ceará, Química Analítica e Físico-Química Wagner Queiroz Neto, Francisco; Universidade Federal do Ceará, Analítica e Físico Química Bezerra, Lucas; Universidade Federal do Ceara, Química Analítica e Físico-Química Silva, Jacilene; Universidade Regional do Cariri Monteiro, Norberto; Federal University of Ceará Technology Centre, Marinho, Marcia; Universidade Federal do Ceará, Departamento de Farmácia; dos Santos, Helcio; Universidade Estadual Vale do Acaraú Teixeira, Alexandre; Universidade Regional do Cariri Marinho, Emmanuel; Universidade Estadual do Ceará Lima-Neto, Pedro; Universidade Federal do Ceara, Quimica Analitica e Físico-Química

SCHOLARONE™
Manuscripts

RESUMO

A doença de Chagas é uma doença tropical causada pelo parasito *Trypanosoma cruzi*, transmitida pelo inseto barbeiro. Atualmente, há aproximadamente cerca 7 milhões de pessoas infectadas no mundo, além disso, calcula-se que 70 milhões de pessoas poderão contrair essa doença. O ácido anacárdico (AA) mostrou efetividade em teste em teste *in silico* e *in vivo*. O potencial antichagásico de cinco moléculas sulfonamidas, derivadas do ácido anacárdico, foi avaliado o potencial reativo dos derivados moléculas em uma abordagem molecular baseada na Teoria Funcional da Densidade (DFT). Na Dinâmica Molecular (MD) e nos cálculos de Docking molecular foi verificado a interação desses derivados, com a enzima alvo (cruzaína). Metil 2-metoxi-6- (8-(metilsulfonamida) octil) benzoato (SA1); Metil 2-metoxi-6-(8-(fenilsulfonamida) octil) benzoato (SA2); Metil 2-metoxi-6- (8- (2-metilfenil sufonamida) octil) benzoato (SA3); metil 2-metoxi-6- (8- (metilfenilsulfonamida) octil) benzoato (SA4); metil 2- (8- (2,5- dimetilfenilsufonamida) octil)-6-metoxibenzoato (SA5) foram as moléculas investigadas. Os cálculos do DFT foram realizados utilizando o nível teórico B3LYP/6-311+G (d, p). As estruturas das moléculas investigadas foram confirmadas pelas correlações lineares superiores a 0,98 entre os dados espectroscópicos experimentais calculados de Infra-Vermelho (IV) e Ressonancia Magnética Nuclear (RMN) do Carbono. Os dados de reatividade global e local mostram que SA1 mostra a maior reatividade molecular, enquanto SA2 é a derivada mais estável. Além disso, o Docking molecular das moléculas mostrou destaques para as moléculas SA1, SA2 e SA4 nos resultados das distâncias de interação ligante/cruzaína, e no desempenho da dinâmica molecular, SA4 obteve melhor estabilidade com o sítio, devido a uma maior quantidade de interações com importantes aminoácidos da cruzaína.

Palavras-chave Sulfonamida; Teoria do Funcional da Densidade; Docking Molecular; Dinâmica Molecular.

ABSTRACT

Chagas disease (CD) is a tropical disease caused by the parasite *Trypanosoma cruzi*, transmitted by the barber insect. Currently, there are approximately 7 million infected people in the world, and it is estimated that 70 million people could contract this disease. The anacardic acid (AA) showed effectiveness *in silico* and *in vivo* tests. The antichagasic potential of five sulfonamide molecules, derived from anacardic acid, was evaluated from a molecular approach based on Density Functional Theory (DFT), Molecular Dynamics (MD), and Molecular Docking (docking) calculations. Methyl 2-methoxy-6-(8-(methylsulfonamide) octyl) benzoate (SA1); 2-methoxy-6-(8-(phenylsulfonamide) octyl) benzoate (SA2); methyl 2-methoxy-6-(8-(2methylphenyl sulfonamide) octyl) benzoate (SA3); methyl 2-methoxy-6-(8-(methylphenylsulfonamide)octyl)benzoate (SA4); methyl 2-(8-(2,5-dimethylphenylsulfonamide)octyl)-6-methoxybenzoate (SA5) were the investigated molecules. The DFT calculations were performed using the B3LYP/6-311+G (d, p) level of theory. The structures of investigated molecules were confirmed by the linear correlations higher than 0.98 displayed between the experimental and calculated spectroscopic data (IR and NMR). The global and local reactivity data showed that SA1 shows the highest molecular reactivity, while SA2 is the most stable derivative. In addition, the molecular docking of the molecules showed a greater prominence for the SA1, SA2, and SA4 molecules in the results of distances of ligand/cruzain. In molecular dynamics, SA4 obtained better stability due to greater interactions with important amino acids of cruzain.

Keywords Sulfonamide; Density Functional; Molecular Docking; Molecular Dynamics.

1 Introduction

In 21 countries in Latin America, the World Health Organization (WHO) considers Chagas disease to be endemic, affecting Asia and Africa. (SCHMUNIS, 2007) WHO estimates that between six and seven million people are infected with the parasite called *Trypanosoma cruzi* (*T. cruzi*). The Chagas disease is one of the leading causes of heart disease in Latin America, and the bite transmits it by the blood-sucking insect known as Triatominae, or "kissing bugs." The parasite can evade the host's defense system through its antioxidant enzymes; increase in B lymphocytes, Hypergammaglobulinemia, and production of antibodies that do not help in the parasite cancellation, the existence of specific molecules in the parasite's membrane that also help in the inefficiency of the host's defense system in fighting the parasite. (CARDOSO; REIS-CUNHA; BARTHOLOMEU, 2016)

Some molecules are used to combat disease wounds. Among them, benznidazole is commonly used. Although this antichagasic drug was developed over 50 years ago, its mechanism of action is not yet fully discovered. It may work by covalent modification of macromolecules by nitroreduced intermediates or other nitroreduced interactions with parasite components. (OLIVEIRA *et al.*, 2008) However, it leads to several side effects for the user, which include skin reactions, fever, atopic dermatitis, erythematous, light-sensitive rashes, purpura, weight loss, and gastrointestinal disorders, hypersensitivity symptoms, dermatitis with rash, generalized fever with edema, lymphadenopathy, muscle, and joint pain, bone marrow depression, thrombocytopenic purpura and agranulocytosis, the most severe manifestation, polyneuropathy, paresthesia and polyneuritis of the peripheral nerves. (COURA; DE CASTRO, 2002) For these reasons, alternative sources of antichagasic drugs are sought, which perform well, causing less risk to the patient.

According to the Food and Agriculture Organization (FAO), in the years 2016 and 2017, around 8 million tons of cashew nuts were produced worldwide, and 5.7 million hectares were used for production worldwide, (PAULA *et al.*, 2020) wherefrom cashew nuts phenolic compounds can be obtained, such as cardol, cardanol and Anacardic Acid (AA). The AA, one of the main constituents of cashew nuts, is a potential candidate for antichagasic activity since tests with the evolutionary forms of *T. cruzi* epimastigotes and trypomastigotes of trypanocidal activity showed results in inhibition of essential enzymes in the evolutionary cycle of *T. cruzi*. (HAMAD; MUBOFU, 2015; MARINHO *et al.*, 2019; MUROI; KUBO, 1996; PEREIRA *et al.*, 2008) One of these enzymes is cruzain, primarily responsible for the proteolytic activity

involving several vital processes, such as host cell infection, replication, and metabolism during the parasite's life cycle.(MARINHO, 2020)

Besides, new easy-to-use syntheses of the Sulfonamide family (SA) were performed, where they are directly derived from (AA), in which they showed antibacterial activity (*viz.* *E. coli* (MTCC443)), *P. aeruginosa* (MTCC424), *S. aureus* (MTCC96) e *S. pyogenes* (MTCC443).(REDDY *et al.*, 2012) In addition to their biological activities such as gastric protection, antitumor, antioxidant, antibiotics, antimicrobial activity, and soy lipoxygenase-1 inhibitory activity.(HAMAD; MUBOFU, 2015; KUBO *et al.*, 1993)

Computational studies on molecules are a way of predicting an application as an antichagasic, in which through simulations, properties that corroborate its applicability can be obtained.(MARINHO *et al.*, 2019) Therefore, the study of the following molecules: methyl 2-methoxy-6- (8- (methylsulfonamide) octyl) benzoate (SA1); 2-methoxy-6- (8- (phenylsulfonamide) octyl) benzoate (SA2); methyl 2-methoxy-6- (8- (2methylphenyl sulfonamide) octyl) benzoate (SA3); methyl 2-methoxy-6- (8- (methylphenylsulfonamide) octyl) benzoate (SA4); methyl2-(8-(2,5-dimethylphenylsufonamide)octyl)-6 methoxybenzoate (SA5), checking their interactions with the enzyme cruzain , which is primarily responsible for a proteolytic activity involving several essential processes in the process of parasite internalization into mammalian cells, playing an important role.

Therefore, using the Density Functional Theory (DFT), a comparison was made about the global reactivities of each molecule (ionic potential, electro-affinity, Gap, electronegativity, global hardness, Softness, global electrophilicity). Also, the local reactivity, verified by the functions of the Electronic Fukui. In Molecular Docking and Molecular Dynamics (MD), the cruzain enzyme was used. Through MD simulations, it is possible to obtain the interaction between SA's molecules and cruzain their active site.

2 Materials

2.1 Quantum chemical calculations

To determine the optimized molecular geometry of the molecules was utilized, the microspecies majority was checked at pH 7.4 in MarvinSketch 18.30 version using a calculation plugin for achieving the lowest energy conformer.(CSIZMADIA, 2019) The Density Functional Theory (DFT) method was carried out in the Gaussian 09 program(FRISCH *et al.*,

2009) using Becke's three-parameter hybrid functional and the Lee, Yang, and Parr correlation functional (B3LYP)(BECKE, 1993) with the basis set triple zeta of Pople with polarization in the d and p atomic orbitals and a diffuse functions for the non-hydrogen atoms 6-311+G(d, p). After the geometrical optimization, the fundamental vibrational spectra were computed at the same level of theory to confirm that all the obtained molecular geometries can be used to determine the molecular properties of the compounds SA1-SA5 with the absence of negative vibrational frequencies, were theoretically assigned using the scaling factor of 0.9679 in the calculated wavenumbers,(ALMEIDA-NETO *et al.*, 2020; ANDERSSON; UVDAL, 2005) confirming the state of minimum energy. Then, the ^1H and ^{13}C NMR spectra were computed at B3LYP/6-311+G (d, p) level of theory in Chloroform an implicit solvent using the Polarizable Continuum Model with the Integral Equation Formalism (IEF-PCM)(DITCHFIELD; HEHRE; POPLE, 1971; MCWEENY, 1962; WOLINSKI; HINTON; PULAY, 1990) solvation model available in Gaussian 09. The tetramethylsilane (TMS) was used as a reference compound to compute the chemical shift for the carbon (δ_C) atoms using the following expressions: $\delta_C = \sigma_{H(TMS)} - \sigma_{H(calc)}$, where the quantity σ_C are the calculated shielding constant for the carbon. To understand the chemical behavior of the compounds, the energies of the Frontier Molecular Orbitals (FMO) were computed at B3LYP/6-311+G (d, p) computational performed with the dielectric constant of water, with the IEF-PCM solvation model. From this calculation, the energy value of these molecular orbitals was used to calculate the quantum reactivity descriptors(FUKUI, 1982): the HOMO-LUMO energy gap (ΔE_{gap} , equation 1); By Koopmans' theorem,(KOOPMANS, 1934) the ionization potential (I , equation 2) and the electron affinity (A , equation 3); From the work of Chermette; Iczkowski and Margrave,(CHERMETTE, 1999; ICZKOWSKI; MARGRAVE, 1961) the electronegativity (χ , equation 4); In Pearson's work, the global hardness (η , equation 5), and the global softness (S , equation 6) that was proposed by Yang and Parr;(YANG; PARR, 1985) The global electrophilicity index (ω , equation 7) introduced by Parr and Szentpály(PARR; SZENTPÁLY; LIU, 1999) and the global nucleophilicity index (ε , equation 8) proposed in the work of Chattaraj.(PARR; CHATTARAJ, 1991)

$$\Delta E_{GAP} = E_{LUMO} - E_{HOMO} \quad (1)$$

$$I = -E_{HOMO} \quad (2)$$

$$A = -E_{LUMO} \quad (3)$$

$$\chi = \frac{I + A}{2} \quad (4)$$

$$\eta = \frac{I - A}{2} \quad (5)$$

$$\sigma = \frac{1}{\eta} \quad (6)$$

$$\omega = \frac{\chi^2}{2\eta} \quad (7)$$

$$\varepsilon = \frac{1}{\omega} \quad (8)$$

To complete the chemical reactivity characterization, the Electronic Fukui functions (f)(BULAT *et al.*, 2004) were computed from the electronic density of the computed FMO according to the equations 9 – 11 for the nucleophilic attack, electrophilic attack, and radical attack, respectively.(BETTENS *et al.*, 2020) The isosurfaces were obtained using the Multiwfn program(LU; CHEN, 2012) and rendered by the VESTA software.(MOMMA; IZUMI, 2011)

$$f^+ \approx v_{LUMO} \quad (9)$$

$$f^- \approx v_{HOMO} \quad (10)$$

$$f^0 \approx \frac{\rho_{HOMO} + \rho_{LUMO}}{2} \quad (11)$$

The Condensed Fukui functions (f_k) were determined using the Hirshfeld charge(HIRSHFELD, 1977) analysis obtained from the optimized geometry for each molecule for the nucleophilic attack (f_k^+ , equation 12), electrophilic attack (f_k^- , equation 13), and radical attack (f_k^0 , equation 14). Also, the Δf index (equation 15) was computed for the SA1-A5 molecules. When the index is positive ($\Delta f > 0$), the reactive site has nucleophilic character and a negative value for the index ($\Delta f < 0$), it is associated with a reactive site which has a electrophilic character.(ALMEIDA-NETO *et al.*, 2020; MORELL; GRAND; TORO-LABBÉ, 2005; PAULA *et al.*, 2020)

$$f_k^+ = q_k(N + 1) - q_k(N) \quad (12)$$

$$f_k^- = q_k(N) - q_k(N - 1) \quad (13)$$

$$f_k^0 = \frac{q_k(N + 1) - q_k(N - 1)}{2} \quad (14)$$

$$\Delta f = f_k^+ - f_k^- \quad (15)$$

Where $q_k(N + 1)$, $q_k(N)$, and $q_k(N - 1)$ are the Hirshfeld charge in the atom k for the anionic, neutral, and cationic species. Finally, the Molecular Electrostatic Potential (MEP) was computed at the B3LYP/6-311+G (d, p) computational level for the title molecules. The isosurfaces for each electrostatic map were rendered by the Gabedit program.(ALLOUCHE, 2011)

2.2 Molecular Docking

The structure of cruzain receptor (PDB 1F29) was obtained from the Protein Data Bank, identified as "*Crystal Structure Analysis of cruzain Bound to a Vinyl Sulfone Derived Inhibitor (I)*", deposited at 2.15 Å resolution, determined by X-Ray Diffraction, classified as a hydrolase, in the organism *Trypanosoma Cruzi* and expressed in the *Escherichia coli* system.(BRINEN *et al.*, 2000)

The enzyme preparation was performed by removing the H₂O molecules. The inhibitor derived from vinyl sulfone I (VS1) is present in the PDB file using the UCSF Chimera code,(PETTERSEN *et al.*, 2004) thus eliminating the interference they could cause in the molecular docking result. Next step, the polar hydrogens were added to the protein structure using the Autodock Tools code with the residues removed.(MORRIS *et al.*, 2009; SANNER, 1999) Then, ligand and enzyme were saved in PDBQT format for further reading in the software AutoDock Vina(ALLOUCHE, 2012) Docking simulations were performed using the AutoDock Vina code (version 1.1.2) with three-way multithreading.(ALLOUCHE, 2012) Docking simulations were performed using the AutoDock Vina code (version 1.1.2) with three-way multithreading.(BRINEN *et al.*, 2000) The grid box was centered in protein with the parameters of 112Å x 58Å x 80Å and dimensions (x, y, z) = (11.514, -5.628, 11.363), and 100 independent simulations were performed, obtaining ten poses each. Data were obtained for comparison by performing simulations with the same parameters with benznidazole (BZN) (PubChem CID 31593), a nitroimidazole-derived drug with antiprotozoal activity, used for the treatment of Chagas disease⁴¹, with the natural inhibitor anacardic acid (AA) and with the vinyl sulfone I (VS1) derived inhibitor co-crystallized on the target enzyme. Discovery Studio Visualizer(DASSAULT SYSTÈMES BIOVIA, 2019) and UCSF Chimera(PETTERSEN *et al.*, 2004) analyzed the results.

2.3 Molecular Dynamics simulation

The Gromacs (GRoningen MAchine for Chemical Simulation) 2019.2 package *software*(BERENDSEN; VAN DER SPOEL; VAN DRUNEN, 1995) was used for performing all simulations by molecular dynamics (MD). CHARMM27(MACKERELL; BANAVALI; FOLOPPE, 2000) was the force field chosen for these simulations; ligands SA1, SA2, SA3, SA4, and SA5 were parameterized through SwissParam.(ZOETE *et al.*, 2011) Six triclinic boxes simulation was created for systems containing only protein 1F29 and 1F29-SA1, 1F29-

SA2, 1F29-SA3, 1F29-SA4, 1F29-SA5, 1F29-BZN complexes. Subsequently, 7360 water molecules described by the TIP3P model (JORGENSEN *et al.*, 1983), were additional, while for the neutralization of the system, 13 sodium ions were added.

The geometry of systems was optimized using two algorithms. The *steepest descent* (ARFKEN; WEBER; HARRIS, 2013) is followed by the *conjugate gradient* (BORGIA; COYLE; ZWIERS, 2007) with energy tolerance of 10 kJ mol⁻¹ nm⁻¹ and step size of 10⁻⁴ nm. Subsequently, two shorts 10 ns simulations were performed in each step equilibrium. The ensemble NVT used the V-rescale method (BUSSI; DONADIO; PARRINELLO, 2007) with a temperature of 310 K, while the ensemble NPT used the Parrinelo-Rahman barostat (PARRINELLO; RAHMAN, 1981) at a pressure of 1.0 bar. The production step MD was simulated in 200 ns through Leap-Frog integrator; (VAN GUNSTEREN; BERENDSEN, 1988) the same temperature and pressure used in the previous step were maintained. The server Protein-Ligand Interaction Profile (PLIP) (SALENTIN *et al.*, 2015) was utilized to analyze interactions of 1F29-SA1, 1F29-SA2, 1F29-SA3, 1F29-SA4, 1F29-SA5 and, 1F29-BZN complexes.

3 Results

3.1 Structural and spectroscopic analysis

The linear correlation between the calculated wavenumbers and the experimental wavenumbers of AA derivatives, obtained from Reddy *et al.*, (REDDY *et al.*, 2012) were made for each derivate. The results are shown in Fig.1. For the analysis of theoretical-experimental correlation, the coefficient of determination (R²) was computed. For the SA1-SA5 molecules (Fig. 2), the values of R² were found to be 0.9984 for the SA1, 0.9991 for the SA2, 0.9991 for the SA3, 0.9991 for the SA4, and 0.9994 for the SA5. These results indicate that the simulated molecules can describe with excellent agreement the experimental spectroscopic data. All the

scaled frequencies calculated have been detailed for each type of vibration in table S1.

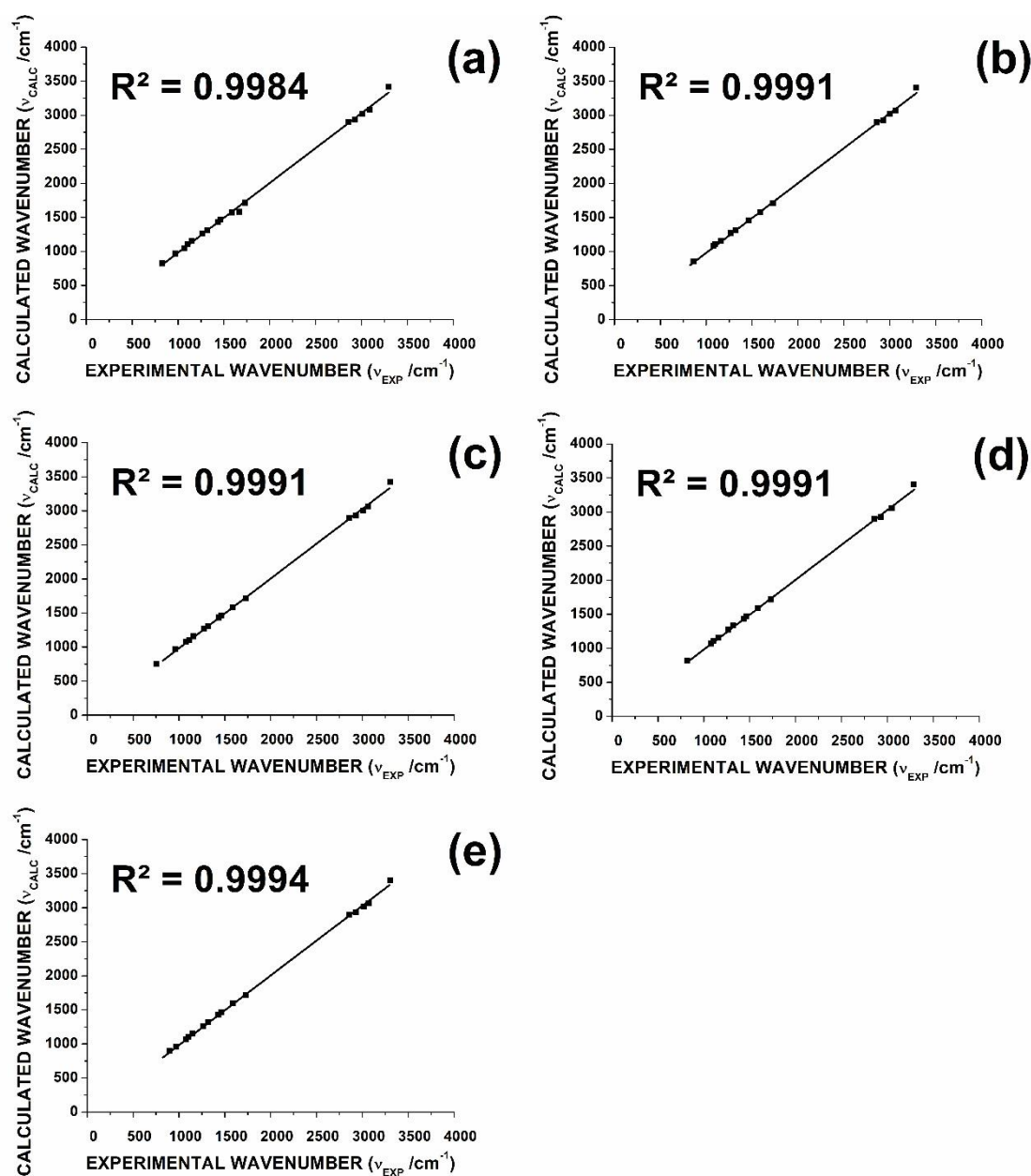


Fig. 1. The linear correlation between the experimental wavenumbers and theoretical wavenumbers for the fundamental vibrational modes of the AA derivatives molecules at the B3LYP/6-311+G (d, p) level of theory. (a) SA1; (b) SA2; (c) SA3; (d) SA4; (e) SA5.

The structure of the molecules SA1-SA5 (Fig. 2 and Fig. 3) was analyzed by performing a conformational scan of the dihedral angles of the most stable conformation. For scan calculations, the basis 6-31G (d, p) was used. The main scanning dihedral angles were Scan 1 C6-C1-C7-C8 (Fig. S1) // Scan 2 C22-C21-C20-S25 (Fig S2) // Scan 3 C5-C6-C9-O12 (Fig S3) //. The energy range shows the conformation of the minimum energy geometry of the

molecules. The energy varies up to 16 kcal.mol^{-1} , where the lowest local minima occur by the dihedral rotation of C1-C2-O7-C8 bonds.

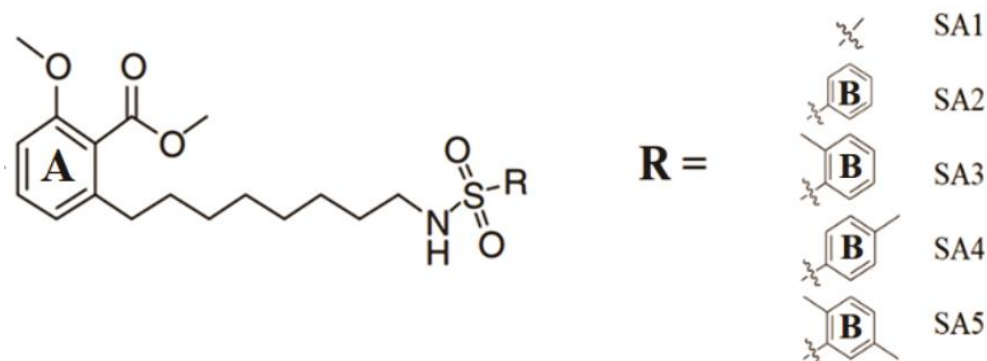


Fig. 2. Structure 2D of the AA derivatives molecules structured with the central A ring and the variations of derivatives on the R radical, highlighting the secondary aromatic B ring.

The initial, lowest energy point is the reference structure for comparison of the structures obtained from the conformations of the angular variation performed in 10 steps of 36° in each molecule and each scan Fig. S1-S3. The scans confirm the energy minimum used for the following calculations, besides observing points of energy minima.

The ^{13}C NMR isotropic shielding was computed for the five derivatives at the B3LYP/6-311+G(d, p) level of theory and GIAO(WOLINSKI; HINTON; PULAY, 1990) (gauge-independent atomic orbitals) method was used using Chloroform as an implicit solvent. The experimental values of the isotropic shielding were obtained from the work of Reddy *et al.* (REDDY *et al.*, 2012). The linear correlations between theoretical and the experimental values of the isotropic shielding are shown in Fig. 4. The coefficient of determination R^2 values was higher than 0.98, which implies an excellent agreement between the calculated molecule and the experimental data.

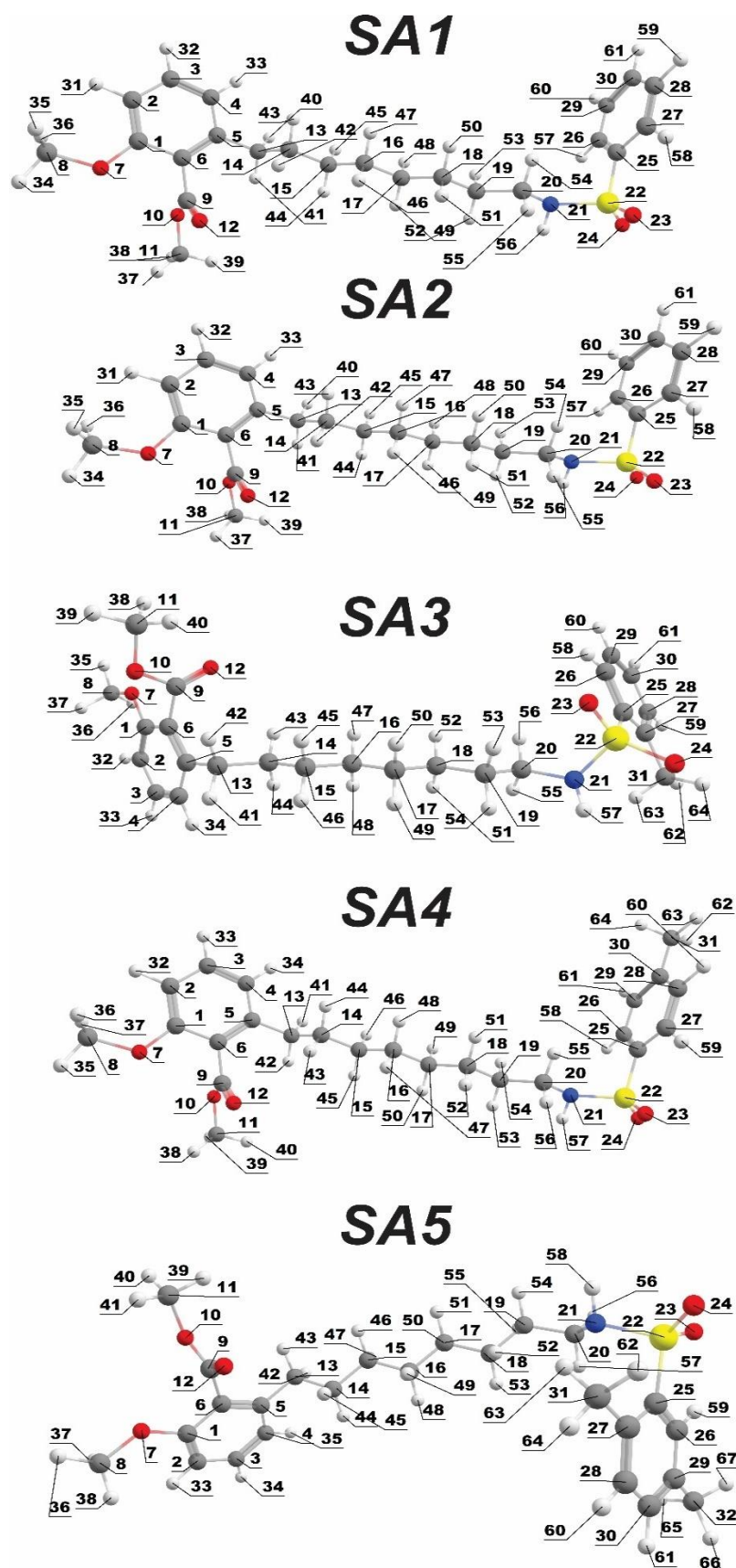


Fig. 3. Optimized geometries of the AA molecule and their derivatives SA1-SA5 for the B3LYP/6-311+G (d, p) level of theory.

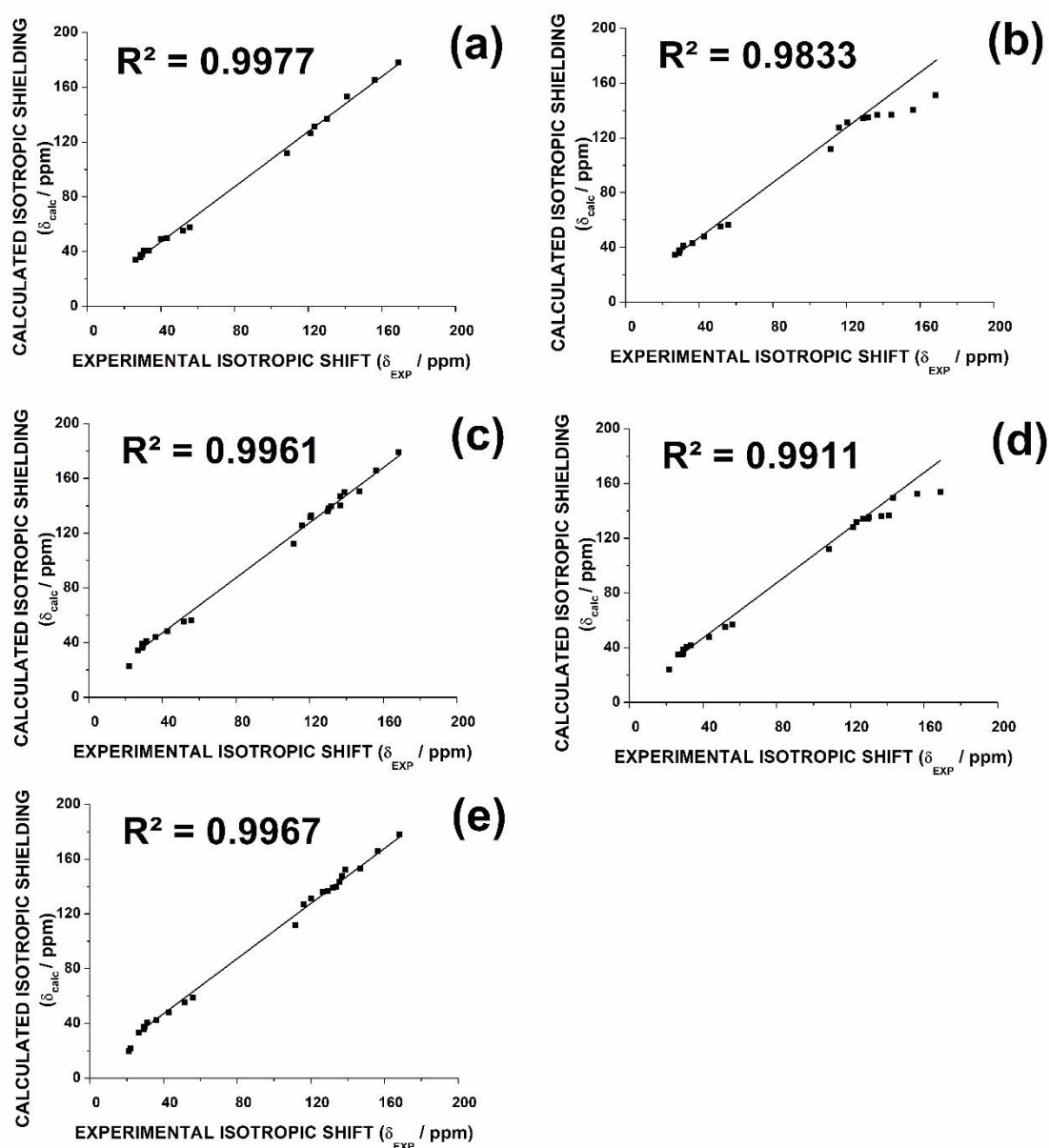


Fig. 4. Linear correlation with the experimental ^{13}C isotropic shielding and the calculated isotropic magnetic shielding at B3LYP/6-311+G (d, p) in Chloroform. (a) SA1; (b) SA2; (c) SA3; (d) SA4; (e) SA5.

3.2 Frontier Molecular Orbital and global quantum reactivity descriptors analysis

The Frontier Molecular Orbitals were computed at B3LYP/6-311+G(d,p) computational level and obtained from the SA1-SA5 optimized geometries (Fig 2), and the rendered isosurfaces are shown in Fig. 5. It can be seen that for all the five derivatives, the HOMO is distributed mainly in the benzene ring and the methoxy group that is common for all the molecules. For the SA1 derivative, the LUMO is spread over mainly in the benzene ring and the ester group. For the other four derivatives, the LUMO is spread over mainly in the benzene ring added to the sulfonamide group, as shown in Fig. 5. The chemical reactivity can be predicted

by the energy values of the HOMO and the LUMO since higher is the energy value of the HOMO orbital, higher is the susceptibility of the molecule to donate electronic density and lower is the energy of the LUMO orbital, higher is the susceptibility of the molecule to accept electronic density. (Koopmans, 1934) The energy values computed for the SA1-SA5 derivatives are shown in Table 1, together with the values for those two molecular orbitals for the AA molecule. According to the data in Table 1 in respect to the HOMO energy value, the predicted order for the chemical reactivity is $SA3 > SA4 > SA2 > SA5 > SA1 > AA$. Hence, the chemical modifications on the AA molecule enhanced the chemical reactivity. The LUMO energy values predict the following order for the chemical reactivity: $SA1 > AA > SA5 > SA4 > SA3 > SA2$. According to this result, only the SA1 derivative has an electrophilic character lower than the AA molecule. The Ionization potential (I) and the electron affinity (A) are related to the nucleophilic character and the electrophilic, respectively, and they are directly related to the HOMO and LUMO, respectively. Besides the HOMO and LUMO energy values, the energy gap (ΔE) between those two molecular orbitals is frequently used to measure chemical reactivity. According to the HOMO-LUMO energy gap data from the Table 1, the predicted order for the reactivity is $SA2 > SA3 > SA4 > SA5 > AA > SA1$. This result shows that SA2-5 derivatives are more reactive than the AA molecule, and only the SA1 exhibited less reactive than the precursor molecule.

The HOMO-LUMO energy gap is related to the concept of hard and soft molecules: the higher the energy gap, the higher is the hard character, and the lower the energy gap, the higher is the soft character of a molecule. Hence, the data obtained from the quantum descriptors global hardness (η) and global softness (σ) show that the predicted order for the chemical reactivity is the same as the energy gap.

Electronegativity corresponds to the tendency to attract electronic density, where a high value indicates a strong electronic attraction. Thus, the value of SA2 was the highest identified, followed by the sequence in descending order: $AA > SA4 > SA3 > SA5 > SA1$.

Finally, the quantum descriptors electrophilicity index (ω) and nucleophilicity index (ε) are related to the electrophilic and nucleophilic character, respectively. The order predicted by the electrophilicity index is $SA2 > SA3 > SA4 > AA > SA5 > SA1$. The order predicted by the nucleophilicity index is $SA1 > SA5 > AA > SA4 > SA3 > SA2$, which is the opposite from the obtained from the electrophilicity index. Therefore, the chemical reactivity of these derivatives is ruled by the electrophilic character of the molecule, hence the SA2

molecule should be the most reactive molecule when compared to the other derivatives and the AA molecule.

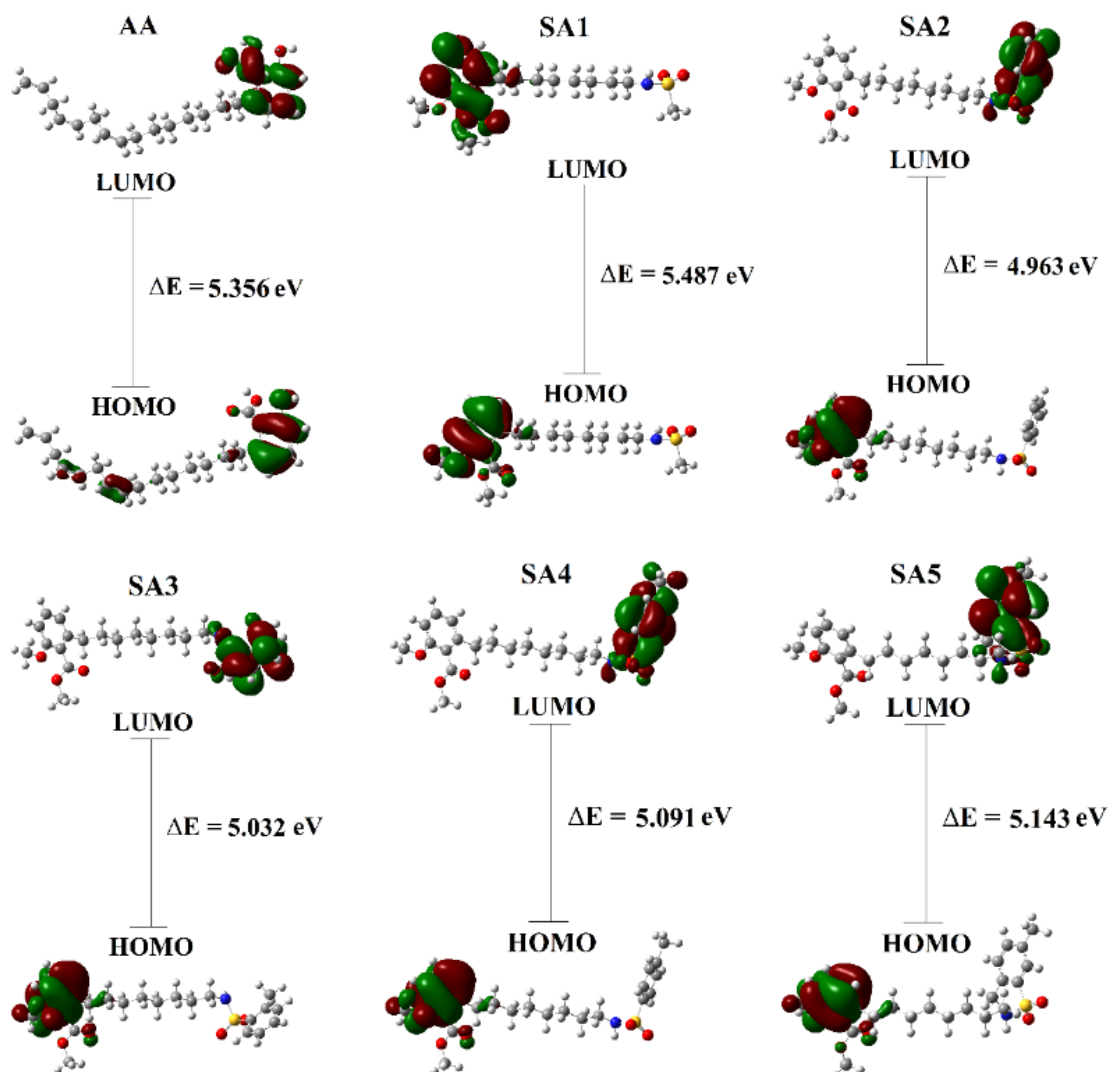


Fig. 5. Frontier Molecular Orbitals (HOMO and LUMO) and the energy gap (ΔE) calculated for the AA and Derivates (SA1-5) at B3LYP/6-311+G (d, p) level of theory.

3.4 Local quantum reactivity descriptors

The reactivity at a specific molecule site can be described by the Fukui functions (Electronic and Condensed) analysis and the Δf index (local reactivity descriptors). (MORELL; GRAND; TORO-LABBÉ, 2005) The results of the isosurfaces of 0.03 from the electronic Fukui functions for the nucleophilic attack (f_k^+) and electrophilic attack (f_k^-) are shown in Fig. 6 for the five derivatives of the AA molecule. It was common for all the five molecules that the regions with tendency for a nucleophilic and electrophilic attacks were, respectively, the ester group and the benzene ring since the ester group has higher electronic density spread over this

group which can be used to donate electronic density and the benzene ring has empty molecular orbitals that can be used to accept the electronic density and this negative charge is delocalized due to the resonance effect. Also, the Condensed Fukui functions and the Δf index were computed using the Hirshfeld charge population analysis for the nucleophilic attack (f_k^+) and electrophilic attack (f_k^-). (LIU; RONG; LU, 2014; OLÁH; ALSENOY; SANNIGRAHI, 2002; ROY, 2003) The results for the SA1-A5 derivatives are shown in Tables S1 – S5 in the Supplementary Material. According to these results, for the SA1 molecule, the atoms that are more susceptible for a nucleophilic attack are C3, C5, C8, C9, O10, C11, O12, C17, C18, C19, C20 and the atoms more susceptible for an electrophilic attack are C1, C2, C4, C6, O7, C13, C14, C15, C16, N21, S22, O23, O24, and C25; for the SA2 molecule, the atoms that are more susceptible for a nucleophilic attack are C3, C5, C8, C9, O10, C11, and O12 and the atoms more susceptible for an electrophilic attack are C1, C2, C4, C6, O7, C13, C14, C15, C16, C17, C18, C19, C20, N21, S22, O23, O24, C25, C26, C27, C28, C29, and C30; for the SA3 molecule, the atoms that are more susceptible for a nucleophilic attack are C3, C5, C8, C9, O10, C11, O12, C18, C19, C20, S22, O23, C25, C26, C27, C28, C29, C30, and C31 and the atoms more susceptible for an electrophilic attack are C1, C2, C4, C6, C7, C13, C14, C15, C16, C17, N21, and O24; for the SA4 molecule, the atoms that are more susceptible for a nucleophilic attack are C3, C5, C8, C9, O10, C11, O12, C13, C15, C17, C18, C19, C20, S22, C25, C26, C27, C28, C29, C30, and C31 and the atoms more susceptible for an electrophilic attack are C1, C2, C4, C6, O7, C14, C16, N21, O23, and O24; for the SA5 molecule, the atoms that are more susceptible for a nucleophilic attack are C3, C5, C8, C9, O10, C11, O12, C18, C19, C20, N21, S22, C25, C26, C27, C28, C29, C30, C31, and C32 and the atoms more susceptible for an electrophilic attack are C1, C2, C4, C6, O7, C13, C14, C15, C16, C17, O23, and O24.

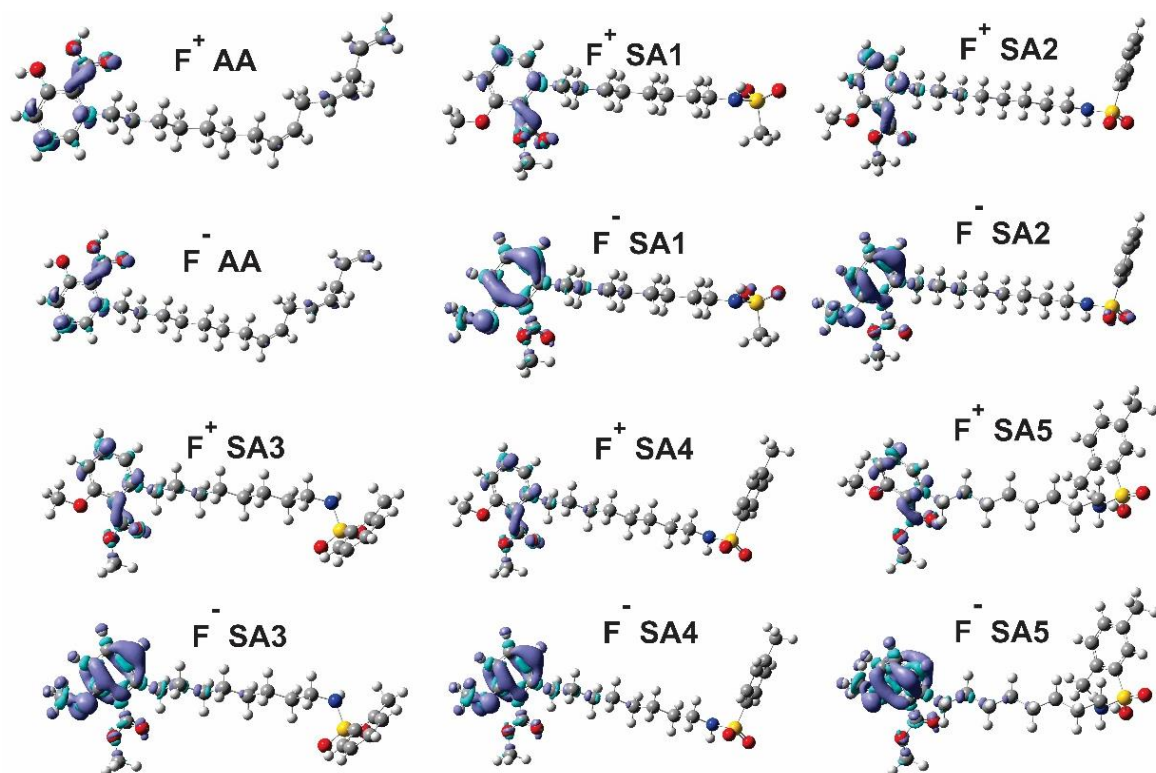


Fig. 6. Calculated isosurfaces for the Electronic Fukui functions using the electronic density and computed at B3LYP/6-311+G (d, p) computational level.

3.5 Molecular Electrostatic Potential (MEP)

The Molecular Electrostatic Potential (MEP) was determined for the SA1-SA5 molecules, and the rendered isosurfaces are shown in Fig. 7. It can be seen from Fig. 7 a color variation from red to blue. The order of color trend red \rightarrow orange \rightarrow yellow \rightarrow green \rightarrow blue represents the tendency of nucleophilicity to electrophilicity on a scale of -0.05 eV to 0.05 eV, respectively. The regions of the MEP with greater localized electronic density (negatively charged region) will tend to be red, which is associated with a nucleophilic character. The regions with less localized electronic density (positively charged) will be blue, related to an electrophilic character. Fig. 7 shows that the ester group and the oxygen atom from the sulfonamide group have a higher electronic density concentration, indicating that it is favorable to donate the electronic density (nucleophilic character). While the methoxy group, methyl (SA1), and phenyl (SA2-SA5) of the sulfonamide are regions with low electronic density concentration, which indicates a tendency to receive electronic density (electrophilic character). This result is directly related to the Electronic Fukui functions: the red-colored regions in the MEP of the SA1-5 indicate a negative charge that can donate a nucleophilic attack, and the

benzene ring can accept extra electronic density since the negative charge is distributed over the entire aromatic ring as shown in the MEP in Fig. 7.

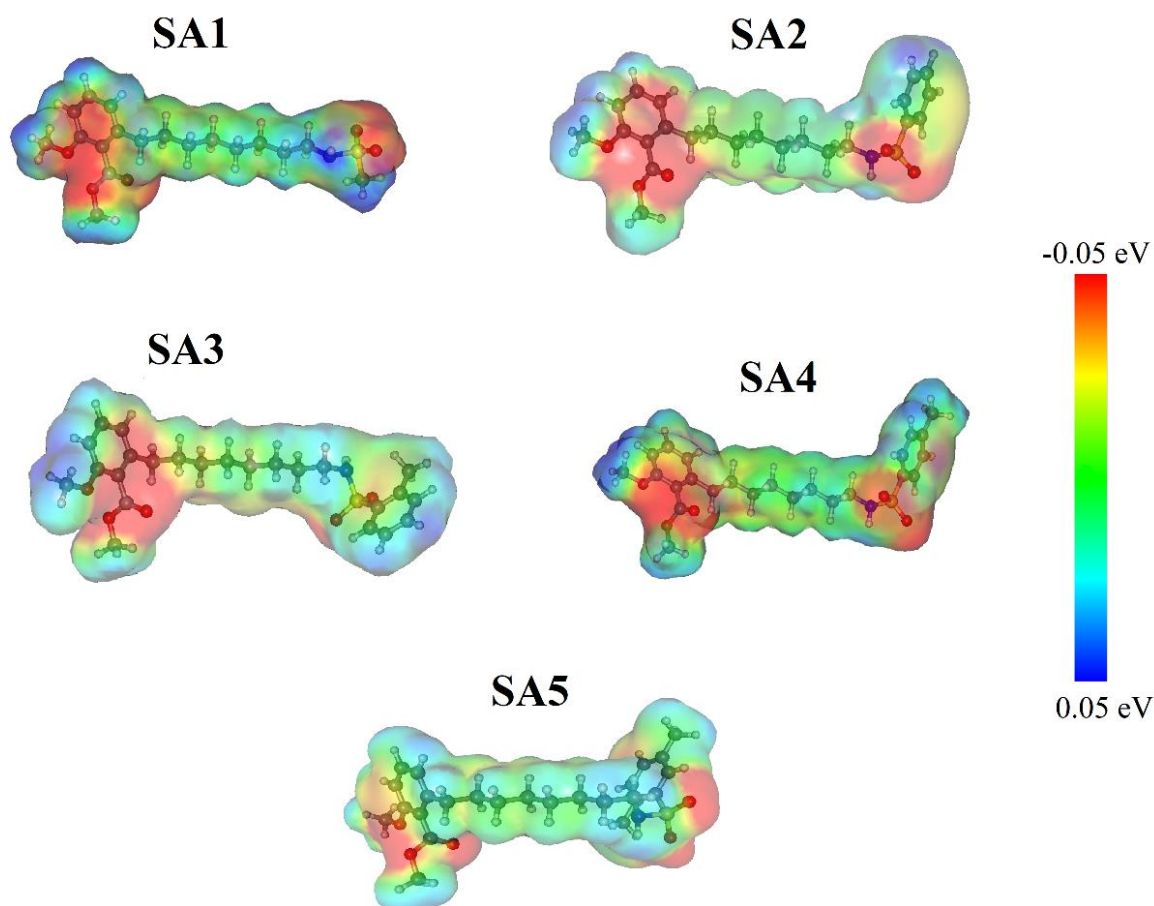


Fig. 7. Calculated Molecular Electrostatic Potential (MEP) at B3LYP/6-311+G(d,p) level of theory for the SA1- SA5 molecules.

3.6 Molecular Docking

Molecular docking simulations were performed with the cruzain receptor to investigate the potential *in silico* antichagasic effect of the anacardic acid-derived ligands (SA1, SA2, SA3, SA4 and SA5). All the analyzed ligands showed RMSD (Root Mean Square Deviation) values within the ideal parameter, less than 2.0 Å, (YUSUF *et al.*, 2008) in the order of 1.885 Å (SA1), 1.748 Å (SA2), 1.219 Å (SA3), 1.435 Å (SA4), 1.740 Å (SA5), 1.709 Å (AA), 1.700 Å (BZN) and 1.658 Å (VS1 redocking) indicating the statistical validation of the simulations. In addition, affinity energy was used as a criterion to evaluate the protein/ligand complexes formed, being considered ideal values, those below -6.0 kcal/mol. (SHITYAKOV; FÖRSTER, 2014). The ligands evaluated showed affinity energy with the cruzain receptor in the order of -4.2 kcal.mol⁻¹ (SA1), -4.5 kcal.mol⁻¹ (SA2), -3.9 kcal.mol⁻¹ (SA3), -4.9 kcal.mol⁻¹

¹ (SA4), -4.8 kcal/mol (SA5), -3.9 kcal/mol (AA), -5.0 kcal/mol (BZN) and -7.2 kcal/mol (VS1 redocking). It can be pointed out that the affinity values of the SA1, SA2, SA4, and SA5 derivatives were better than the anacardic acid (AA). The coupling of the ligands can be observed in Fig. 8.

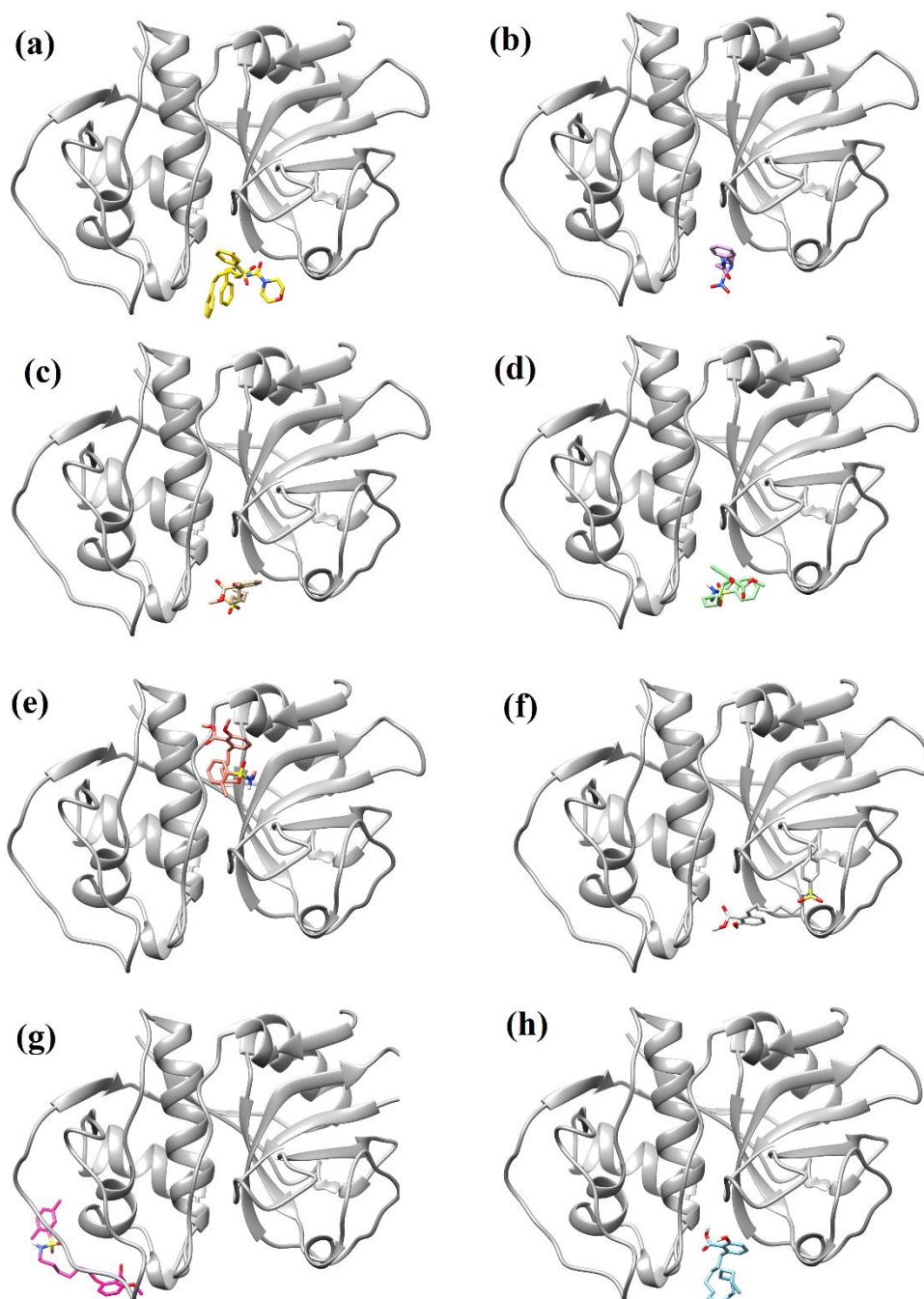


Fig. 8: Interaction complex of the receptor cruzain with ligands VS1 (a), BZN (b), SA1 (c), SA2 (d), SA3 (e), SA4 (f), SA5(g), AA (h).

Table 2 shows the binding distances between the amino acid residues of the enzyme and the ligand molecules, in which it was possible to observe that the ligands SA1, SA2, and

AA were close to the binding site of BZN and VS1 (inhibitor co-crystallized in the enzyme PDB), and therefore close to the active site, it was also observed that in the redocking the co-crystallized inhibitor docked in the same region of cruzain, validating the docking simulations performed.

SA1 and SA2 performed better and closer to the site residues (His159, Cys25, Asn175, Gln19, and Trp177). SA3, SA4, and SA5 showed higher values than the reference values (BZN and VS1 PDB), which may be related to the presence of methylation in the structures' phenyl radical, SA3 ortho-methylated, SA4 para-methylated, and SA5 ortho-methylated.

Table 2. Binding residue/protein distances in angstroms

Residue	SA1	SA2	SA3	SA4	SA5	AA	BZN	VS1 PDB	VS1
								Native	Redocking
His159	3.1	3.7	16.0	6.9	15.3	7.1	3.1	3.1	3.4
Cys 25	3.7	3.5	15.6	7.9	10.8	8.0	4.3	2.6	3.7
Asn 175	6.7	7.0	8.2	6.8	18.6	6.8	6.5	6.8	6.9
Gln 19	3.1	3.0	13.5	4.9	11.4	3.7	3.3	3.2	3.0
Trp 177	3.6	3.5	10.9	3.5	15.8	3.4	2.6	3.2	3.9

From the analysis of molecular interactions (Fig. 9.), it was observed that the ligands SA2 and BZN presented two interactions with the residue of the active site of the enzyme Cys25, being a Conventional Hydrogen Bond with SA2 and a Hydrophobic interaction with BZN. The interactions were also observed with Trp177, a highly conserved residue in the enzyme, presenting π - π Stacked interactions with the ligands SA1, SA2, SA4, AA, and BZN. The Amide-Pi Stacked interaction with SA2 and Hydrophobic interaction with SA4 (table S7). The ligands SA3 and SA5 are docked in different regions. Thus no interactions with the residues of the cruzain active site were observed. For the SA1, SA2, and SA4 compounds, the interaction between the amino acid Trp177 with the benzene ring of these molecules is a π - π stacked type since this group is more susceptible to accept electronic density predicted by the Electronic Fukui functions.

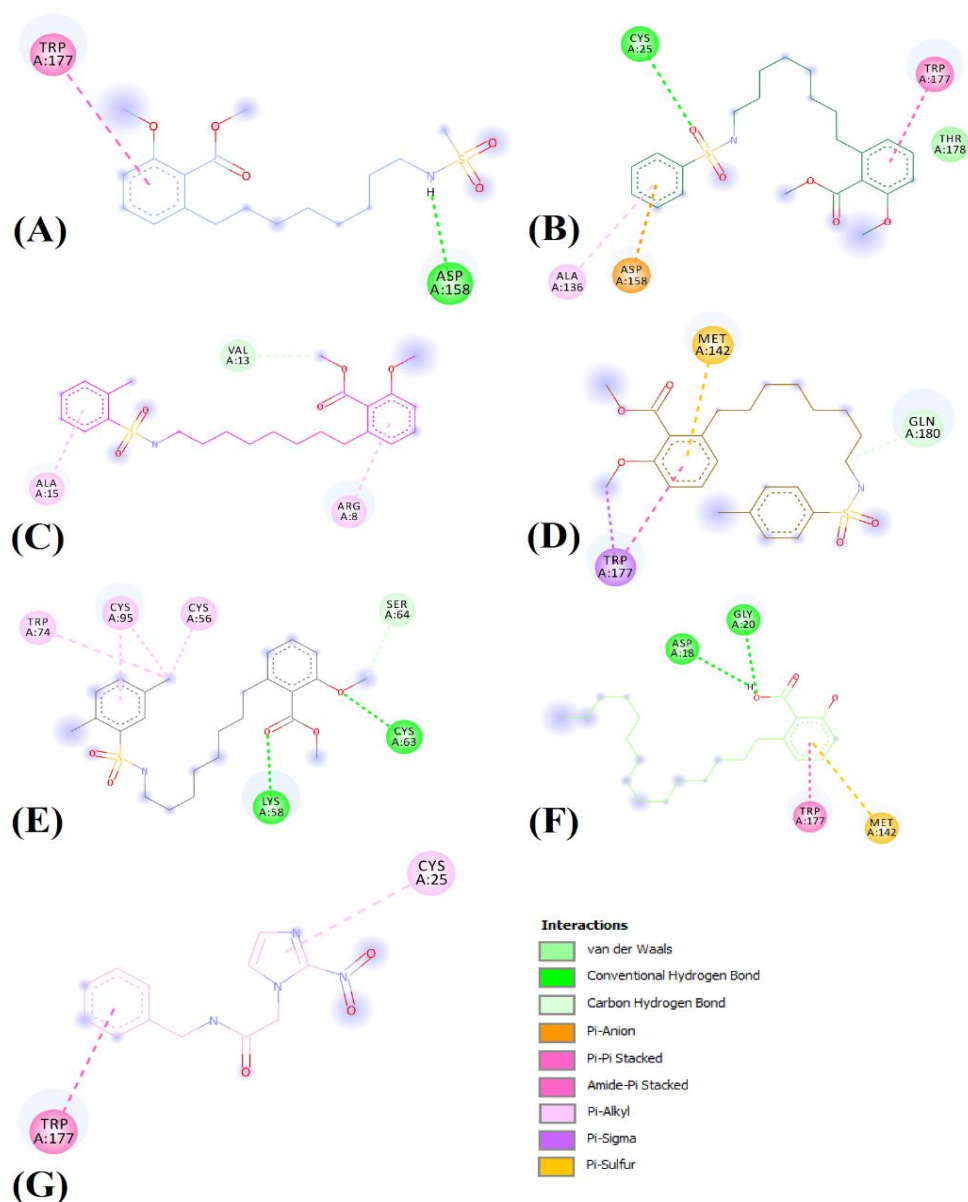


Fig. 9: SA1 (A), SA2 (B), SA3 (C), SA4 (D), SA5 (E), AA (F) and BZN (G) molecular interactions with cruzain.

3.7 Molecular Dynamics Analysis

The root mean square deviation (RMSD) is used to analyze whether the system has reached equilibrium. Fig. 10 showed similar values RMSD for the protein 1F29 and for the 1F29-SA1, 1F29-SA2, 1F29-SA3, 1F29-SA4, 1F29-SA5 complexes. The protein and the complexes cited above reached equilibrium at the beginning of MD simulations. The 1F29-BZN complex showed the highest values RMSD and reached the equilibrium from 50 ns. Therefore, the ligand BZN had fewer stable interactions with the protein 1F29 concerning the

other ligands (SA1, SA2, SA3, SA4, and SA5). The following analyzes will be carried out only in the equilibrium time interval previously recorded.

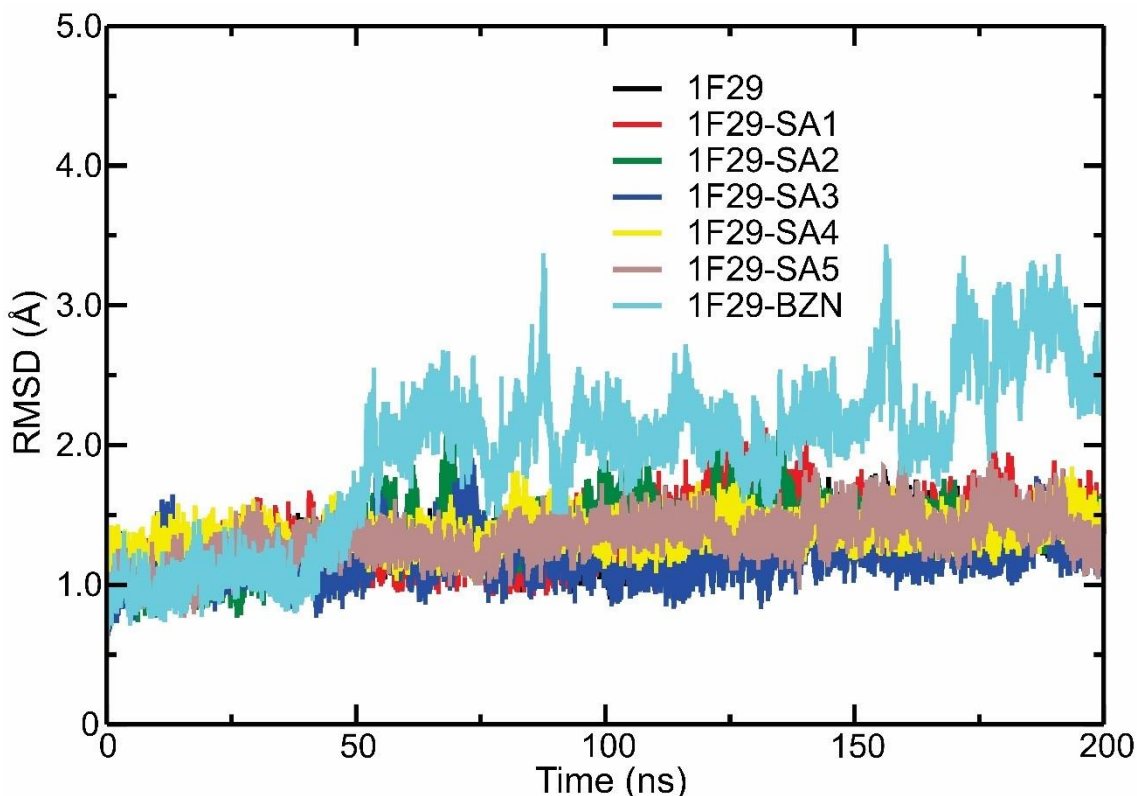


Fig. 10: Determination of root mean square deviation (RMSD) of unbounded 1F29 (black) and 1F29-SA1 (red), 1F29-SA2 (green), 1F29-SA3 (blue), 1F29-SA4 (yellow), 1F29-SA5 (brown), and 1F29-BZN (cyan) complexes.

The Coulomb and Lennard-Jones short-range energies were calculated and have been added between receptor 1F29 with SA1, SA2, SA3, SA4, SA5, and BZN ligands, shown in Fig. 11. 1F29-SA1, 1F29-SA2, 1F29-SA3, and 1F29-SA5 complexes showed similar interaction energies, in the value of $-130.913 \text{ kJ mol}^{-1}$ (63.314), $-102.607 \text{ kJ mol}^{-1}$ (52.214), $-108.907 \text{ kJ mol}^{-1}$ (55.580), $-101.549 \text{ kJ mol}^{-1}$ (56.744), respectively. When compared to the interaction energies of the above complexes, the 1F29-SA4 complex has the highest interaction energy of $-179.217 \text{ kJ mol}^{-1}$ (85.031), while that the 1F29-BZN has the smaller interaction energy in the value of $-26.151 \text{ kJ mol}^{-1}$ (18.105).

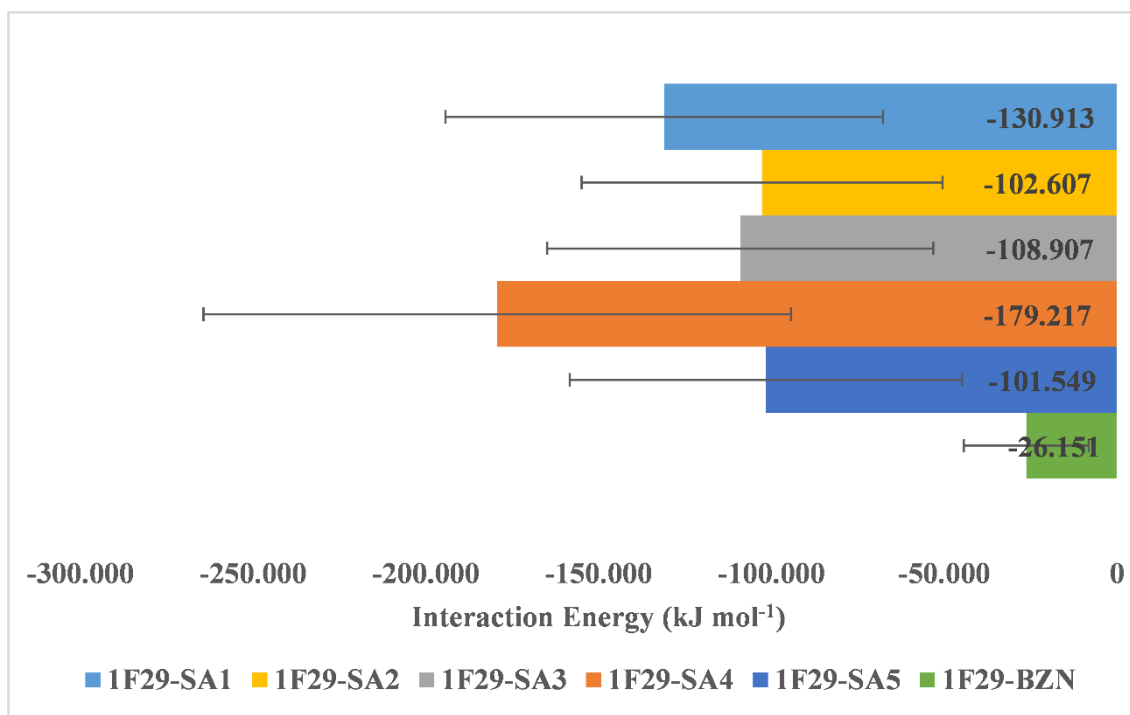


Fig. 11: Energies of interaction present in the 1F29-SA1, 1F29-SA2, 1F29-SA3, 1F29-SA4, 1F29-SA5, and 1F29-BZN complexes, with standard deviation.

The Fig. 12 shows the main interactions calculated between complexes analyzed in its last simulation frame (200 ns). SA1 ligand presented two hydrogen bonds with Gln 180 and Gly 182 amino acids, with distance 1.65 Å and 3.13 Å, respectively (Fig. 12a); moreover, two hydrophobic interactions occurred between Trp 177 and Met 142 with SA1 ligand, with values of 3.84 Å and 3.69 Å, respectively. His 159 shows a charge center with SA1, with a distance of 4.67 Å. 1F29-SA3 (Fig. 12c) and 1F29-SA5 (Fig. 12e) complexes show only hydrophobic interactions. The first one with Ala 122 (3.52 Å) and Trp 123 (3.92 Å); and second one with Trp 123 (3.93 Å), Val 126 (3.87 Å). The 1F29-SA2 complex interacts hydrophobically with Val 126 and Ala 122 amino acids residues, with a distance of 3.70 Å and 3.74 Å, respectively (Fig. 12b). Moreover, the ligand SA2 showed a hydrogen bond with Asn 127, with a distance of 1.93 Å. The BZN ligand (Fig. 12f) interacts hydrophobically with the Ala 1 (3.50 Å), Ala 121 (3.69 Å), Tyr 166 (4.00 Å) amino acids. Besides, was registered a charge center with the Lys 191 (5.59 Å) amino acid and one hydrogen bond with the Ala 1 (2.29 Å) amino acid. Between 1F29 and SA4 (Fig. 12d), there are three hydrophobic interactions with Trp 177 and His 159 (distance of 3.74 Å, 3.75 Å, and 3.94 Å, respectively); Moreover, two hydrogen bonds uncharged of moderate strength were registered with the amino acids Gln 19 (1.82 Å), His 159

(2.05 Å), and a weak one with Trp 177 (2.50 Å). These bonds are responsible for the high interaction energy observed for this complex concerning the others (1F29-SA1, 1F29-SA2, 1F29-SA3, and 1F29-SA5), this intermolecular force contributes from 11 to 60 kJ mol⁻¹ in the interaction energy (ELEMANS; LEI; DE FEYTER, 2009). Besides, this intermolecular force is the strongest and most influential in molecular recognition (DONG; DAVIS, 2021).

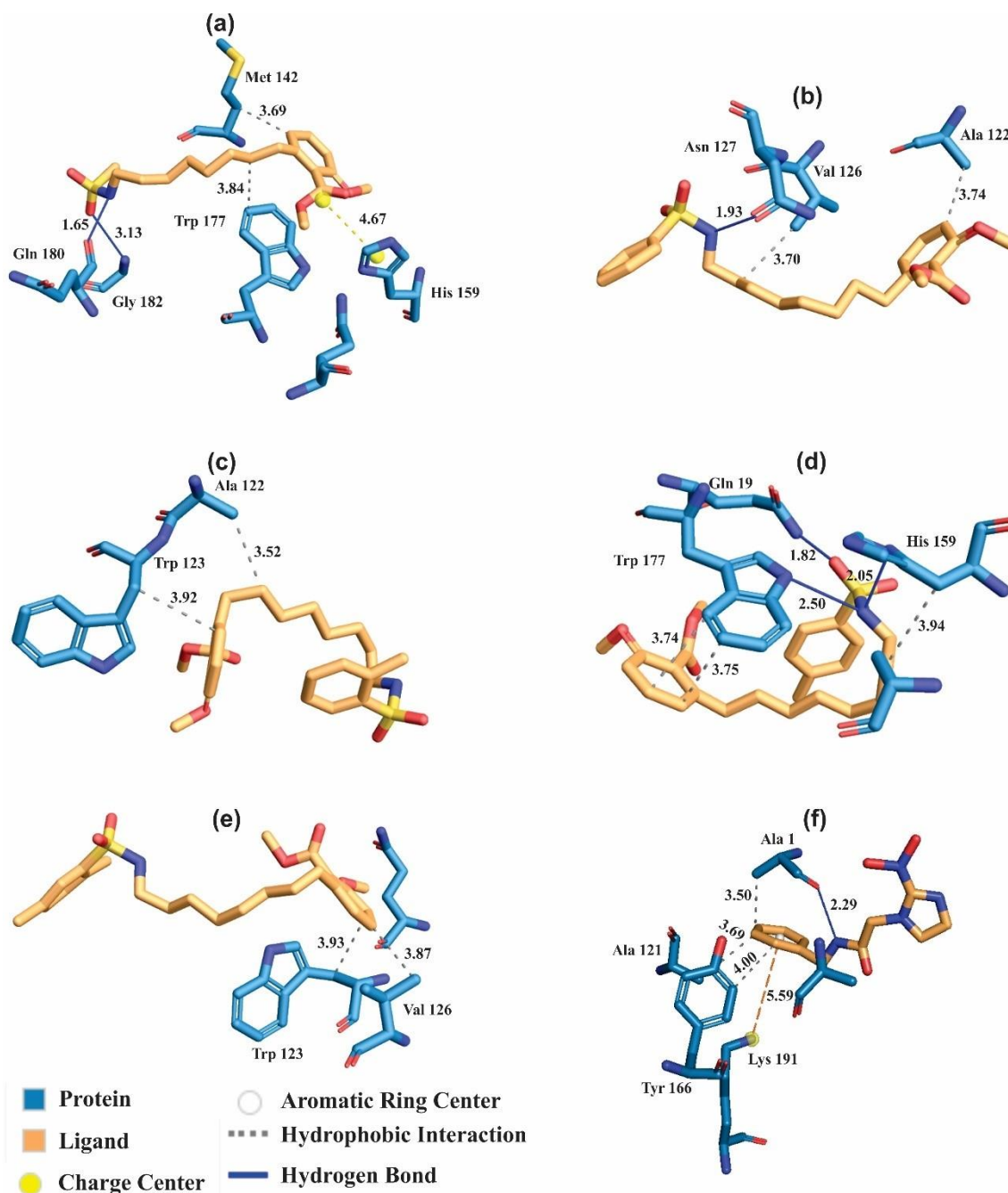


Fig. 12: Interactions presents in the (a) 1F29-SA1, (b) 1F29-SA2, (c) 1F29-SA3, (d) 1F29-SA4, (e) 1F29-SA5, and (f) 1F29-BZN complexes.

Conclusions

Quantum chemical calculations using the DFT method at the B3LYP/6-311+G (d, p) level were performed to compare with the experimental and theoretical spectroscopic data measured in NMR and IR. It was verified that the calculated structural data showed an excellent concordance with those experimental ones. The reactivity analysis observed that modification of the anacardic acid (AA) to the SA1-SA5 derivatives improved the overall reactivity. In molecular docking, it was indicated that the SA1, SA2, and SA4 molecules performed better in their interactions with the cruzain. They maintain an excellent interaction with the residues of the enzyme, indicating that the chemical substitutions made to the AA favor the interaction with the cruzain. The results of molecular dynamics indicate that the SA4 ligand showed high interaction energy with the 1F29 protein due to two moderate and one weak hydrogen bond uncharged in this complex. Thus, we can conclude that the anacardic acid derivatives could be promised as drugs for treating Chagas disease.

Conflicts of interest

There are no conflicts to declare.

Acknowledgments

The authors thank the financial support given by the following Brazilian funding agencies: Coordenação de Aperfeiçoamento de Pessoal de Nível Superior (CAPES), Conselho Nacional de Desenvolvimento Científico e Tecnológico (CNPq) and Fundação Cearense de Apoio ao Desenvolvimento Científico e Tecnológica (FUNCAP). The authors are grateful to the Centro Nacional de Processamento de Alto Desempenho (CENAPAD) of the Federal University of Ceará (UFC) by computational resources offered.

Referencies

ALLOUCHE, A. Software News and Updates Gabedit — A Graphical User Interface for Computational Chemistry Softwares. **Journal of computational chemistry**, v. 32, p. 174–182, 2012. Disponível em: <https://doi.org/10.1002/jcc>

ALLOUCHE, A. R. Gabedita - A graphical user interface for computational chemistry softwares. **Journal of Computational Chemistry**, v. 32, n. 1, p. 174–182, 2011. Disponível em: <https://doi.org/10.1002/jcc.21600>

ALMEIDA-NETO, F. W. Q.; DA SILVA, L. P.; FERREIRA, M. K. A.; MENDES, F. R. S.; DE CASTRO, K. K. A.; BANDEIRA, P. N.; DE MENEZES, J. E. S. A.; DOS SANTOS, H. S.; MONTEIRO, N. K. V.; MARINHO, E. S.; DE LIMA-NETO, P. Characterization of the structural, spectroscopic, nonlinear optical, electronic properties and antioxidant activity of the N-{4'-[(E)-3-(Fluorophenyl)-1-(phenyl)-prop-2-en-1-one]}-acetamide. **Journal of Molecular Structure**, v. 1220, p. 128765, 2020. Disponível em: <https://doi.org/10.1016/j.molstruc.2020.128765>

ANDERSSON, M. P.; UVDAL, P. New scale factors for harmonic vibrational frequencies using the B3LYP density functional method with the triple- ζ basis Set 6-311+G(d,p). **Journal of Physical Chemistry A**, v. 109, n. 12, p. 2937–2941, 2005. Disponível em: <https://doi.org/10.1021/jp045733a>

ARFKEN, G. B.; WEBER, H. J.; HARRIS, F. E. **Mathematical Methods for Physicists**. [S. l.: s. n.]. Disponível em: <https://doi.org/10.1016/C2009-0-30629-7>

BECKE, A. D. Density-functional thermochemistry. III. The role of exact exchange. **The Journal of Chemical Physics**, v. 98, n. 7, p. 5648–5652, 1993. Disponível em: <https://doi.org/10.1063/1.464913>

BERENDSEN, H. J. C.; VAN DER SPOEL, D.; VAN DRUNEN, R. GROMACS: A message-passing parallel molecular dynamics implementation. **Computer Physics Communications**, v. 91, n. 1–3, p. 43–56, 1995. Disponível em: [https://doi.org/10.1016/0010-4655\(95\)00042-E](https://doi.org/10.1016/0010-4655(95)00042-E)

BETTENS, T.; ALONSO, M.; DE PROFT, F.; HAMLIN, T. A.; BICKELHAUPT, F. M. Ambident Nucleophilic Substitution: Understanding Non-HSAB Behavior through Activation Strain and Conceptual DFT Analyses. **Chemistry - A European Journal**, v. 26, n. 17, p. 3884–3893, 2020. Disponível em: <https://doi.org/10.1002/chem.202000272>

BORGIA, G.; COYLE, B.; ZWIERS, P. B. Evolution of colorful display. **Evolution**, v. 61, n. 3, p. 708–712, 2007. Disponível em: <https://doi.org/10.1111/j.1558-5646.2007.00051.x>

BRINEN, L. S.; HANSELL, E.; CHENG, J.; ROUSH, W. R.; MCKERROW, J. H.; FLETTERICK, R. J. A target within the target: Probing cruzain's P1' site to define structural determinants for the Chagas' disease protease. **Structure**, v. 8, n. 8, p. 831–840, 2000. Disponível em: [https://doi.org/10.1016/S0969-2126\(00\)00173-8](https://doi.org/10.1016/S0969-2126(00)00173-8)

BRITO, A.; FALCÃO, L.; MATIAS, A.; BRITO, R.; LIMA, R. Um Doenças Negligenciadas: Doença de Chagas e os aspectos atuais do tratamento. **Revista de Ensino, Ciência e Inovação em Saúde**, v. 2, n. 1, p. 9–17, 2021. Disponível em: <https://doi.org/10.51909/RECIS.V2I1.69>. Acesso em: 25 out. 2021.

BULAT, F. A.; CHAMORRO, E.; FUENTEALBA, P.; TORO-LABBÉ, A. Condensation of Frontier Molecular Orbital Fukui Functions. **Journal of Physical Chemistry A**, v. 108, n. 2, p. 342–349, 2004. Disponível em: <https://doi.org/10.1021/jp036416r>

BUSSI, G.; DONADIO, D.; PARRINELLO, M. Canonical sampling through velocity rescaling. **Journal of Chemical Physics**, v. 126, n. 1, 2007. Disponível em: <https://doi.org/10.1063/1.2408420>

CARDOSO, M. S.; REIS-CUNHA, J. L.; BARTHOLOMEU, D. C. **Evasion of the immune**

response by trypanosoma cruzi during acute infection. [S. l.: s. n.] Disponível em: <https://doi.org/10.3389/fimmu.2015.00659>

CHERMETTE, H. Chemical reactivity indexes in density functional theory. **Journal of Computational Chemistry**, v. 20, n. 1, p. 129–154, 1999. Disponível em: [https://doi.org/10.1002/\(SICI\)1096-987X\(19990115\)20:1<129::AID-JCC13>3.0.CO;2-A](https://doi.org/10.1002/(SICI)1096-987X(19990115)20:1<129::AID-JCC13>3.0.CO;2-A)

COURA, J. R.; DE CASTRO, S. L. **A critical review on chagas disease chemotherapy.** [S. l.: s. n.] Disponível em: <https://doi.org/10.1590/S0074-02762002000100001>

CSIZMADIA, P. **MarvinSketch and MarvinView: Molecule Applets for the World Wide Web.** [S. l.: s. n.] Disponível em: <https://doi.org/10.3390/ecsoc-3-01775>

DASSAULT SYSTÈMES BIOVIA. **Discovery Studio Visualizer, Versão 16.1.0.** San Diego: [s. n.], 2019.

DITCHFIELD, R.; HEHRE, W. J.; POPLE, J. A. Self-consistent molecular-orbital methods. IX. An extended gaussian-type basis for molecular-orbital studies of organic molecules. **The Journal of Chemical Physics**, v. 54, n. 2, p. 720–723, 1971. Disponível em: <https://doi.org/10.1063/1.1674902>

DONG, J.; DAVIS, A. P. **Molecular Recognition Mediated by Hydrogen Bonding in Aqueous Media.** [S. l.: s. n.] Disponível em: <https://doi.org/10.1002/anie.202012315>

ELEMANS, J. A. A. W.; LEI, S.; DE FEYTER, S. **Molecular and supramolecular networks on surfaces: From two-dimensional crystal engineering to reactivity.** [S. l.: s. n.] Disponível em: <https://doi.org/10.1002/anie.200806339>

FRISCH, M. J. *et al.* **Gaussian 09, Revision B.01.** [S. l.: s. n.]

FUKUI, K. Role of frontier orbitals in chemical reactions. **Science**, v. 218, n. 4574, p. 747–754, 1982. Disponível em: <https://doi.org/10.1126/science.218.4574.747>

HAMAD, F. B.; MUBOFU, E. B. **Potential biological applications of bio-based anacardic acids and their derivatives.** [S. l.: s. n.] Disponível em: <https://doi.org/10.3390/ijms16048569>

HIRSHFELD, F. L. Bonded-atom fragments for describing molecular charge densities. **Theoretica Chimica Acta**, v. 44, n. 2, p. 129–138, 1977. Disponível em: <https://doi.org/10.1007/BF00549096>

ICZKOWSKI, R. P.; MARGRAVE, J. L. Electronegativity. **Journal of the American Chemical Society**, v. 83, n. 17, p. 3547–3551, 1961. Disponível em: <https://doi.org/10.1021/ja01478a001>

JORGENSEN, W. L.; CHANDRASEKHAR, J.; MADURA, J. D.; IMPEY, R. W.; KLEIN, M. L. Comparison of simple potential functions for simulating liquid water. **The Journal of Chemical Physics**, v. 79, n. 2, p. 926–935, 1983. Disponível em: <https://doi.org/10.1063/1.445869>

KESSELHEIM, A. S. Drug Development for Neglected Diseases — The Trouble with FDA Review Vouchers. <http://dx.doi.org/10.1056/NEJMp0806684>, v. 359, n. 19, p. 1981–1983, 2009. Disponível em: <https://doi.org/10.1056/NEJMP0806684>. Acesso em: 26 out. 2021.

KOOPMANS, T. Über die Zuordnung von Wellenfunktionen und Eigenwerten zu den Einzelnen Elektronen Eines Atoms. **Physica**, v. 1, n. 1–6, p. 104–113, 1934. Disponível em: [https://doi.org/10.1016/S0031-8914\(34\)90011-2](https://doi.org/10.1016/S0031-8914(34)90011-2)

KUBO, I.; MUROI, H.; HIMEJIMA, M.; YAMAGIWA, Y.; MERA, H.; TOKUSHIMA, K.; OHTA, S.; KAMIKAWA, T. Structure-Antibacterial Activity Relationships of Anacardic Acids. **Journal of Agricultural and Food Chemistry**, v. 41, n. 6, p. 1016–1019, 1993. Disponível em: <https://doi.org/10.1021/jf00030a036>

LIU, S.; RONG, C.; LU, T. Information conservation principle determines electrophilicity, nucleophilicity, and regioselectivity. **Journal of Physical Chemistry A**, v. 118, n. 20, p. 3698–3704, 2014. Disponível em: <https://doi.org/10.1021/jp5032702>

LU, T.; CHEN, F. Multiwfn: A multifunctional wavefunction analyzer. **Journal of Computational Chemistry**, v. 33, n. 5, p. 580–592, 2012. Disponível em: <https://doi.org/10.1002/jcc.22885>

MACKERELL, A. D.; BANAVALI, N.; FOLOPPE, N. Development and current status of the CHARMM force field for nucleic acids. **Biopolymers**, v. 56, n. 4, p. 257–265, 2000. Disponível em: [https://doi.org/10.1002/1097-0282\(2000\)56:4<257::AID-BIP10029>3.0.CO;2-W](https://doi.org/10.1002/1097-0282(2000)56:4<257::AID-BIP10029>3.0.CO;2-W)

MARINHO M.M, R. P.DOS SANTOS, E. M. BEZERRA, R. F. COSTA, C. S. FIGUEIRA, A. M. C. MARTINS, P de LIMA-NETO, E. S. MARINHO, V. N. FREIRE, E. L. ALBUQUERQUE, *Asian J. Pharm. Clin. Res.*, 2019, 183–189.

MARINHO, M. M. **EFEITO TRIPANOCIDA DE SUBSTÂNCIAS PRESENTES NO CAJUEIRO (*Anacardium occidentale*): UMA ABORDAGEM EXPERIMENTAL E TEÓRICA**. 2020. - Universidade Federal do Ceará, [s. l.], 2020.

MARTINS-MELO, F. R.; RAMOS, A. N.; ALENCAR, C. H.; HEUKELBACH, J. Prevalence of Chagas disease in Brazil: A systematic review and meta-analysis. **Acta Tropica**, v. 130, n. 1, p. 167–174, 2014. Disponível em: <https://doi.org/10.1016/J.ACTATROPICA.2013.10.002>

MCWEENY, R. Perturbation theory for the fock-dirac density matrix. **Physical Review**, v. 126, n. 3, p. 1028–1034, 1962. Disponível em: <https://doi.org/10.1103/PhysRev.126.1028>

MOMMA, K.; IZUMI, F. VESTA 3 for three-dimensional visualization of crystal, volumetric and morphology data. **Journal of Applied Crystallography**, v. 44, n. 6, p. 1272–1276, 2011. Disponível em: <https://doi.org/10.1107/S0021889811038970>

MORELL, C.; GRAND, A.; TORO-LABBÉ, A. New dual descriptor for chemical reactivity. **Journal of Physical Chemistry A**, v. 109, n. 1, p. 205–212, 2005. Disponível em: <https://doi.org/10.1021/jp046577a>

MORRIS, G. M.; RUTH, H.; LINDSTROM, W.; SANNER, M. F.; BELEW, R. K.; GOODSELL, D. S.; OLSON, A. J. Software news and updates AutoDock4 and AutoDockTools4: Automated docking with selective receptor flexibility. **Journal of Computational Chemistry**, v. 30, n. 16, p. 2785–2791, 2009. Disponível em: <https://doi.org/10.1002/jcc.21256>

MUROI, H.; KUBO, I. Antibacterial activity of anacardic acid and totarol, alone and in combination with methicillin, against methicillin-resistant *Staphylococcus aureus*. **Journal of Applied Bacteriology**, v. 80, n. 4, p. 387–394, 1996. Disponível em: <https://doi.org/10.1111/j.1365-2672.1996.tb03233.x>

OLÁH, J.; ALSENOY, C. Van; SANNIGRAHI, A. B. Condensed Fukui functions derived from stockholder charges: Assessment of their performance as local reactivity descriptors. **Journal of Physical Chemistry A**, v. 106, n. 15, p. 3885–3890, 2002. Disponível em: <https://doi.org/10.1021/jp014039h>

OLIVEIRA, M. de F.; NAGAO-DIAS, A. T.; OLIVEIRA DE PONTES, V. M.; SOUZA JÚNIOR, A. S. de; LUNA COELHO, H. L.; BRANCO COELHO, I. C. Tratamento etiológico da doença de Chagas no Brasil. **Revista de Patologia Tropical**, v. 37, n. 3, 2008. Disponível em: <https://doi.org/10.5216/rpt.v37i3.5063>

PARR, R. G.; CHATTARAJ, P. K. Principle of Maximum Hardness. **Journal of the American Chemical Society**, v. 113, n. 5, p. 1854–1855, 1991. Disponível em: <https://doi.org/10.1021/ja00005a072>

PARR, R. G.; SZENTPÁLY, L. V.; LIU, S. Electrophilicity index. **Journal of the American Chemical Society**, v. 121, n. 9, p. 1922–1924, 1999. Disponível em: <https://doi.org/10.1021/ja983494x>

PARRINELLO, M.; RAHMAN, A. Polymorphic transitions in single crystals: A new molecular dynamics method. **Journal of Applied Physics**, v. 52, n. 12, p. 7182–7190, 1981. Disponível em: <https://doi.org/10.1063/1.328693>

PAULA, R. S. F. *et al.* A potential bio-antioxidant for mineral oil from cashew nutshell liquid: an experimental and theoretical approach. **Brazilian Journal of Chemical Engineering**, v. 37, n. 2, p. 369–381, 2020. Disponível em: <https://doi.org/10.1007/s43153-020-00031-z>

PEREIRA, J. M.; SEVERINO, R. P.; VIEIRA, P. C.; FERNANDES, J. B.; DA SILVA, M. F. G. F.; ZOTTIS, A.; ANDRICOPULO, A. D.; OLIVA, G.; CORRÊA, A. G. Anacardic acid derivatives as inhibitors of glyceraldehyde-3-phosphate dehydrogenase from *Trypanosoma cruzi*. **Bioorganic and Medicinal Chemistry**, v. 16, n. 19, p. 8889–8895, 2008. Disponível em: <https://doi.org/10.1016/j.bmc.2008.08.057>

PETTERSEN, E. F.; GODDARD, T. D.; HUANG, C. C.; COUCH, G. S.; GREENBLATT, D. M.; MENG, E. C.; FERRIN, T. E. UCSF Chimera - A visualization system for exploratory research and analysis. **Journal of Computational Chemistry**, v. 25, n. 13, p. 1605–1612, 2004. Disponível em: <https://doi.org/10.1002/jcc.20084>

REDDY, N. S.; RAO, A. S.; CHARI, M. A.; KUMAR, V. R.; JYOTHY, V.; HIMABINDU, V. Synthesis and antibacterial activity of sulfonamide derivatives at C-8 alkyl chain of anacardic acid mixture isolated from a natural product cashew nut shell liquid (CNSL). **Journal of Chemical Sciences**, v. 124, n. 3, p. 723–730, 2012. Disponível em: <https://doi.org/10.1007/s12039-012-0253-1>

ROY, R. K. Stockholders charge partitioning technique. A reliable electron population analysis scheme to predict intramolecular reactivity sequence. **Journal of Physical**

Chemistry A, v. 107, n. 48, p. 10428–10434, 2003. Disponível em:
<https://doi.org/10.1021/jp035848z>

SALENTIN, S.; SCHREIBER, S.; HAUPT, V. J.; ADASME, M. F.; SCHROEDER, M. PLIP: Fully automated protein-ligand interaction profiler. **Nucleic Acids Research**, v. 43, n. W1, p. W443–W447, 2015. Disponível em: <https://doi.org/10.1093/nar/gkv315>

SANNER, M. F. **Python: A programming language for software integration and development**. [S. l.: s. n.]

SCHMUNIS, G. A. Epidemiology of Chagas disease in non-endemic countries: The role of international migration. In: 2007, **Memorias do Instituto Oswaldo Cruz**. [S. l.: s. n.] p. 75–85. Disponível em: <https://doi.org/10.1590/s0074-02762007005000093>

SHITYAKOV, S.; FÖRSTER, C. In silico predictive model to determine vector-mediated transport properties for the blood-brain barrier choline transporter. **Advances and Applications in Bioinformatics and Chemistry**, v. 7, n. 1, p. 23–36, 2014. Disponível em: <https://doi.org/10.2147/AABC.S63749>

VAN GUNSTEREN, W. F.; BERENDSEN, H. J. C. A Leap-Frog Algorithm for Stochastic Dynamics. **Molecular Simulation**, v. 1, n. 3, p. 173–185, 1988. Disponível em: <https://doi.org/10.1080/08927028808080941>

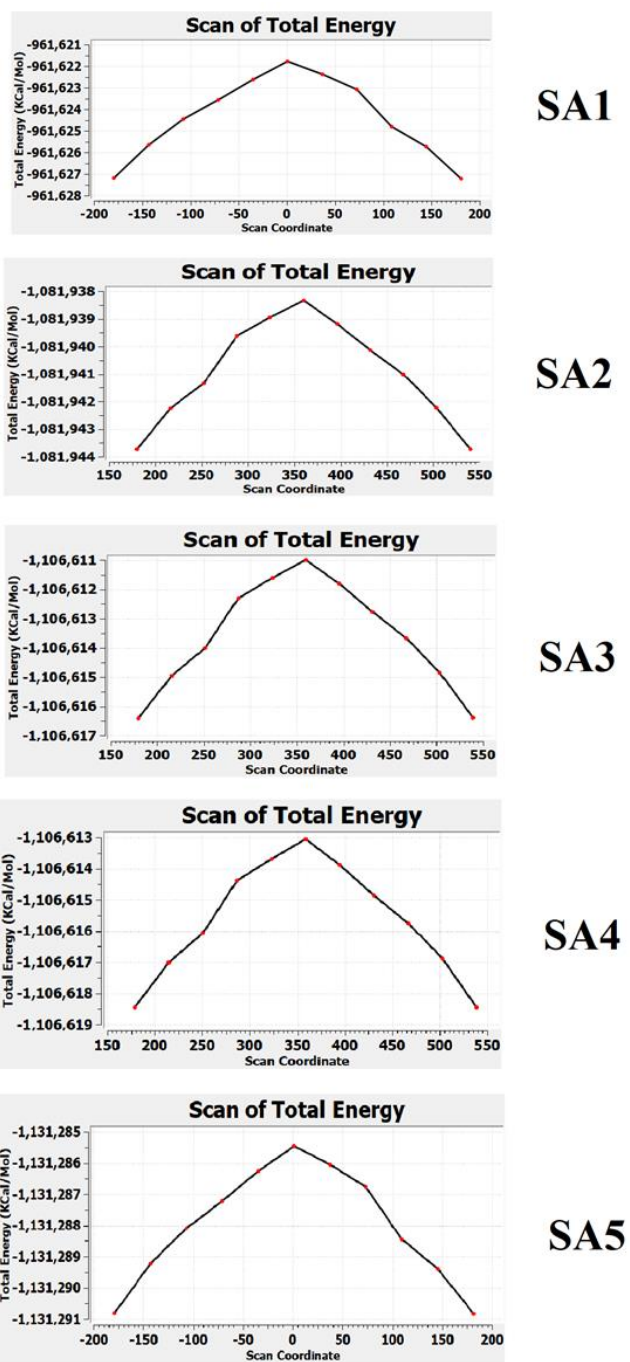
WOLINSKI, K.; HINTON, J. F.; PULAY, P. Efficient Implementation of the Gauge-Independent Atomic Orbital Method for NMR Chemical Shift Calculations. **Journal of the American Chemical Society**, v. 112, n. 23, p. 8251–8260, 1990. Disponível em: <https://doi.org/10.1021/ja00179a005>

YANG, W.; PARR, R. G. Hardness, softness, and the Fukui function in the electronic theory of metals and catalysis. **Proceedings of the National Academy of Sciences of the United States of America**, v. 82, n. 20, p. 6723–6726, 1985. Disponível em: <https://doi.org/10.1073/pnas.82.20.6723>

YUSUF, D.; DAVIS, A. M.; KLEYWEGT, G. J.; SCHMITT, S. An alternative method for the evaluation of docking performance: RSR vs RMSD. **Journal of Chemical Information and Modeling**, v. 48, n. 7, p. 1411–1422, 2008. Disponível em: <https://doi.org/10.1021/ci800084x>

ZOETE, V.; CUENDET, M. A.; GROSDIDIER, A.; MICHIELIN, O. SwissParam: A fast force field generation tool for small organic molecules. **Journal of Computational Chemistry**, v. 32, n. 11, p. 2359–2368, 2011. Disponível em: <https://doi.org/10.1002/jcc.21816>

Supplementary Material

**Fig S1.** Scan atoms : C6-C1-C7-C8

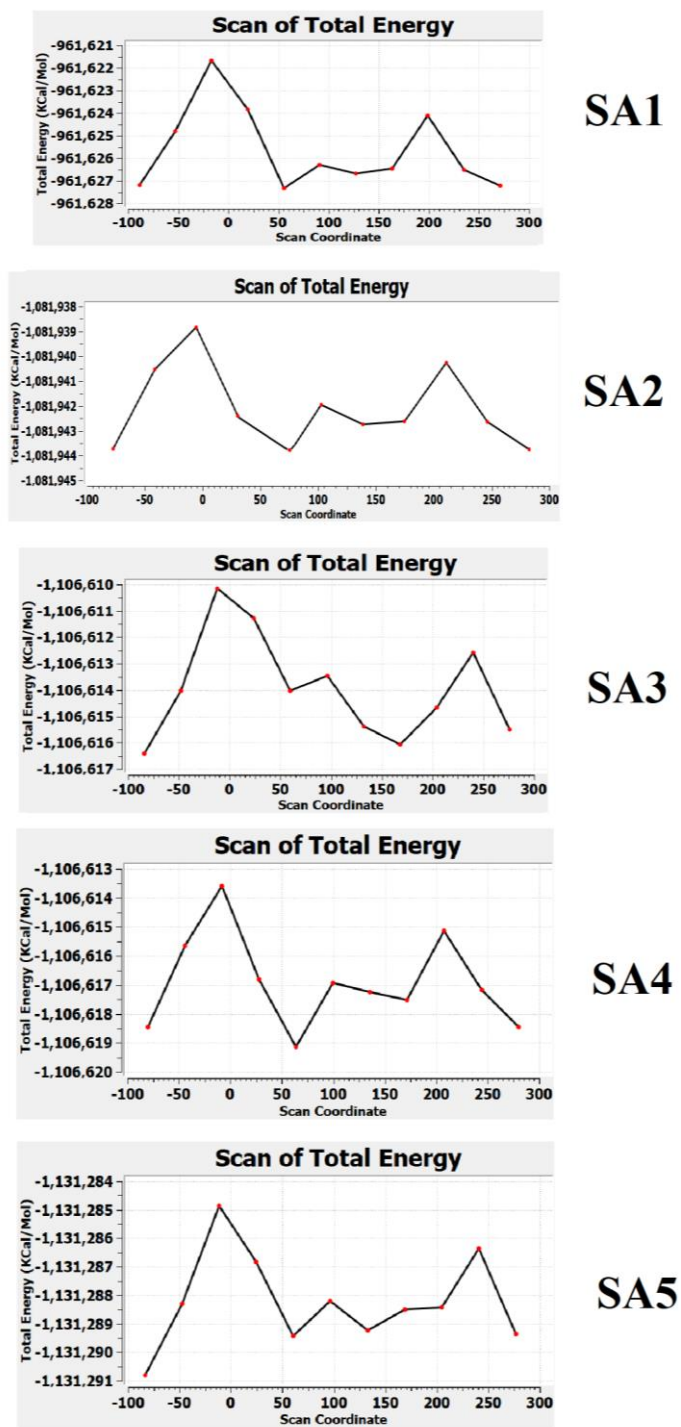
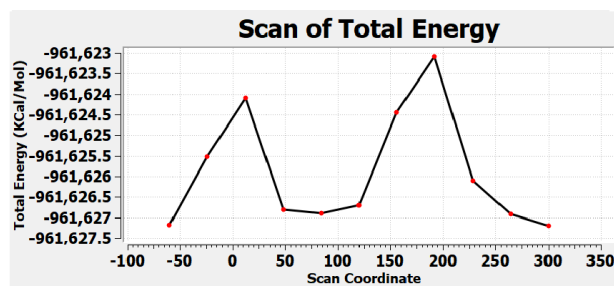
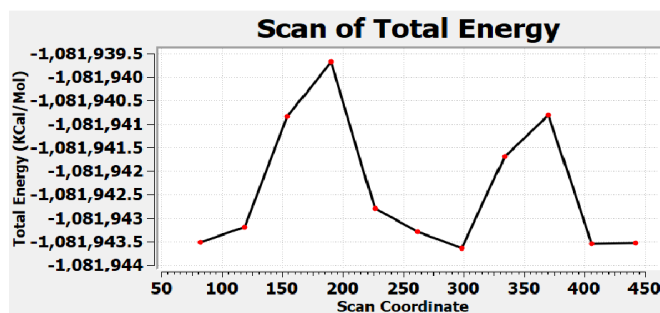


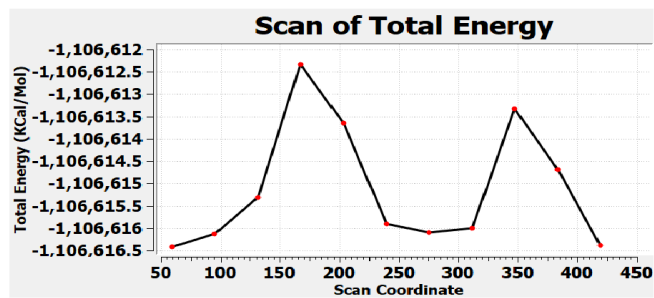
Fig S2. Scan atoms :: C22-C21-C20-S25



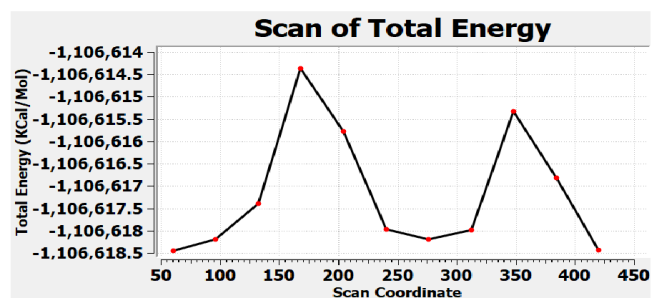
SA1



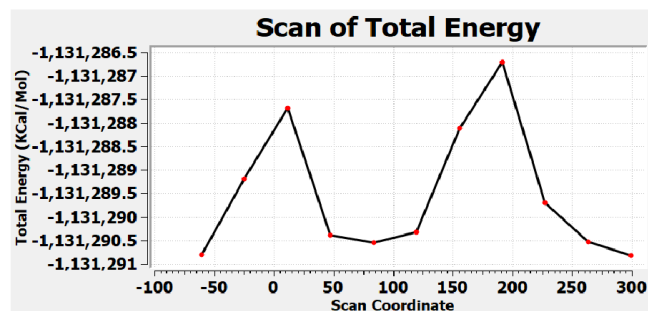
SA2



SA3



SA4



SA5

Fig S3. Scan atoms: C5-C6-C9-O12

Table S1. Scaled frequencies calculated for each type of vibration

Vibrational mode	SA1	SA2	SA3	SA4	SA5
Stretch N-H	3417.63	3408.47	3420.11	3405.52	3399.61
Bending C-N-H	1267.148 1332.401	1308.619	1269.816	1333.717	1071.618
Bending C-C-H	1156.16 1104.9 1267.148 1581.211 1568.575	1581.26 1105.825 853.0441	3061.736 1156.488 1105.287	1269.893 1156.861 1105.94 1066.188	1264.677 1156.616 962.8653
Stretch C-C ring benzenic	1581.211 1568.575	1581.26		813.5692	
Stretch C-H : metyl of ester	3021.024	3021.378		3054.329	
Bending C-H metyl of ester	968.0704 1435.705 1713.819	1714.372	1714.582 1156.488 754.3548	1714.545 1435.539 1156.861 1105.94 1066.188	1713.824 1264.677 1156.616 1105.64
Stretch H-C-H : aliphatic chain	2934.84 2895.308	2928.559 2895.612	2933.687 2894.5	2896.271	2928.766 2894.394
Bending C-C-H : aliphatic chain	1465.37 1332.401	1459.335 1308.619 1269.816 1105.825	1467.132 1307.943 1266.638 1105.287 754.3548	1467.494 1333.717 1269.893 1105.94 1066.188	1465.883 1323.172 1105.64 1071.618
Stretch C -C aliphatic chain	968.0704	1081.633	997.3531		962.8653
Bending C-C-C of aliphatic chain	823.1653 1067.955		1074.108		
Stretch C - O ether		1105.825	1105.287	1066.188	

Stretch C=O ester	1713.819	1714.372	1714.582	1714.545 813.5692	1713.824
Stretch S=O sulfonamide	1067.955		1074.108		1071.618
Stretch N-S	823.1653				
Stretch C-N			965.3381		
Stretch C-H ring benzenic (B)		3067.761			
Bending C-C-H ring benzenic (B)		1459.335 1159.965	1581.858 1266.638 754.3548	1584.804	1264.677 1594.059 1071.618 899.0091
Stretch C-C ring benzenic (B)			1581.858	1584.804	1264.677 1594.059
Stretch C-H methyl ring benzenic (B)			3061.736	2930.128	3017.77
Bending C-C-H methyl ring benzenic (B)			1432.124 1074.108		1432.708 1264.677 899.0091

Table S2. Condensed Fukui functions calculated by the Hirshfeld charge population for the SA1

Atom	f^+	f	f^-	Δf
1(C)	0.021598	0.06717	0.044384	-0.04557
2(C)	0.041137	0.065634	0.053386	-0.0245
3(C)	0.067449	0.052959	0.060204	0.01449
4(C)	0.029404	0.108969	0.069187	-0.07957
5(C)	0.037854	0.033058	0.035456	0.004796
6(C)	0.038625	0.04452	0.041573	-0.0059
7(O)	0.011843	0.096438	0.054141	-0.0846
8(C)	0.038253	0.025639	0.031946	0.012614
9(C)	0.041526	0.002986	0.022256	0.03854
10(O)	0.019997	0.006634	0.013316	0.013363

11(C)	0.021533	0.011692	0.016613	0.009841
12(O)	0.055092	0.040448	0.04777	0.014644
13(C)	0.00663	0.007879	0.007255	-0.00125
14(C)	0.004882	0.006261	0.005572	-0.00138
15(C)	0.004179	0.005659	0.004919	-0.00148
16(C)	0.002831	0.003633	0.003232	-0.0008
17(C)	0.004532	0.003791	0.004162	0.000741
18(C)	0.003713	0.002896	0.003305	0.000817
19(C)	0.00549	0.003112	0.004301	0.002378
20(C)	0.003856	0.002685	0.003271	0.001171
21(N)	3.7E-05	0.003586	0.001812	-0.00355
22(S)	0.007033	0.012308	0.009671	-0.00527
23(O)	0.008677	0.02911	0.018894	-0.02043
24(O)	0.005764	0.025559	0.015662	-0.0198
25(C)	0.003991	0.006742	0.005367	-0.00275
26(H)	0.053076	0.033011	0.043044	0.020065
27(H)	0.051267	0.035568	0.043418	0.015699
28(H)	0.026042	0.042979	0.034511	-0.01694
29(H)	0.050759	0.027326	0.039043	0.023433
30(H)	0.040424	0.027148	0.033786	0.013276
31(H)	0.056618	0.027168	0.041893	0.02945
32(H)	0.019198	0.012219	0.015709	0.006979
33(H)	0.025506	0.013582	0.019544	0.011924
34(H)	0.020095	0.009771	0.014933	0.010324
35(H)	0.008868	0.014123	0.011496	-0.00526
36(H)	0.016605	0.015438	0.016022	0.001167
37(H)	0.008618	0.004769	0.006694	0.003849
38(H)	0.002857	0.004451	0.003654	-0.00159
39(H)	0.006781	0.006469	0.006625	0.000312
40(H)	0.008202	0.00719	0.007696	0.001012
41(H)	0.00698	0.003621	0.005301	0.003359
42(H)	0.003735	0.003013	0.003374	0.000722
43(H)	0.006593	0.004142	0.005368	0.002451
44(H)	0.01371	0.003765	0.008738	0.009945
45(H)	0.010118	0.002684	0.006401	0.007434
46(H)	0.00591	0.00246	0.004185	0.00345
47(H)	0.020956	0.003152	0.012054	0.017804
48(H)	0.007257	0.003149	0.005203	0.004108
49(H)	0.013328	0.002425	0.007877	0.010903
50(H)	0.00451	0.002329	0.00342	0.002181
51(H)	0.00459	0.003606	0.004098	0.000984

52(H)	0.005356	0.005661	0.005509	-0.00031
53(H)	0.008199	0.006286	0.007243	0.001913
54(H)	0.002159	0.002984	0.002572	-0.00082

Table S3. Condensed Fukui functions calculated by the Hirshfeld charge population for the SA2

Atom	f^+	f^-	f^0	Δf
1(C)	0.022787	0.065793	0.04429	-0.04301
2(C)	0.042978	0.064484	0.053731	-0.02151
3(C)	0.075476	0.051838	0.063657	0.023638
4(C)	0.033255	0.106807	0.070031	-0.07355
5(C)	0.041891	0.032372	0.037132	0.009519
6(C)	0.042661	0.04343	0.043046	-0.00077
7(O)	0.009897	0.094306	0.052102	-0.08441
8(C)	0.035165	0.025113	0.030139	0.010052
9(C)	0.037851	0.002848	0.02035	0.035003
10(O)	0.017583	0.006555	0.012069	0.011028
11(C)	0.044694	0.011454	0.028074	0.03324
12(O)	0.054758	0.039397	0.047078	0.015361
13(C)	0.006799	0.007807	0.007303	-0.00101
14(C)	0.004769	0.006224	0.005497	-0.00146
15(C)	0.003913	0.005775	0.004844	-0.00186
16(C)	0.002324	0.003854	0.003089	-0.00153
17(C)	0.002449	0.004107	0.003278	-0.00166
18(C)	0.001325	0.003298	0.002312	-0.00197
19(C)	0.001112	0.003637	0.002375	-0.00252
20(C)	0.00087	0.003209	0.00204	-0.00234
21(N)	-0.00045	0.004199	0.001873	-0.00465
22(S)	0.001809	0.011975	0.006892	-0.01017
23(O)	0.001394	0.022662	0.012028	-0.02127
24(O)	0.004894	0.031368	0.018131	-0.02647
25(C)	-0.00087	-0.00034	-0.0006	-0.00053
26(C)	0.000349	0.001606	0.000978	-0.00126
27(C)	-7.8E-05	0.001167	0.000545	-0.00125
28(C)	0.001701	0.004393	0.003047	-0.00269
29(C)	0.002225	0.005238	0.003732	-0.00301
30(C)	0.002897	0.006647	0.004772	-0.00375
31(H)	0.031432	0.032437	0.031935	-0.00101
32(H)	0.046266	0.034905	0.040586	0.011361
33(H)	0.027096	0.042181	0.034639	-0.01509

34(H)	0.074081	0.02679	0.050436	0.047291
35(H)	0.028301	0.02658	0.027441	0.001721
36(H)	0.042639	0.026604	0.034622	0.016035
37(H)	0.050465	0.009553	0.030009	0.040912
38(H)	0.072583	0.013347	0.042965	0.059236
39(H)	0.03859	0.011905	0.025248	0.026685
40(H)	0.016289	0.015126	0.015708	0.001163
41(H)	0.008254	0.013886	0.01107	-0.00563
42(H)	0.002437	0.004208	0.003323	-0.00177
43(H)	0.007368	0.004895	0.006132	0.002473
44(H)	0.00657	0.006346	0.006458	0.000224
45(H)	0.007281	0.0073	0.007291	-1.9E-05
46(H)	0.002954	0.002981	0.002968	-2.7E-05
47(H)	0.004144	0.003819	0.003982	0.000325
48(H)	0.004285	0.00436	0.004323	-7.5E-05
49(H)	0.004344	0.00382	0.004082	0.000524
50(H)	0.002271	0.002928	0.0026	-0.00066
51(H)	0.001466	0.002567	0.002017	-0.0011
52(H)	0.001254	0.00311	0.002182	-0.00186
53(H)	0.002232	0.00353	0.002881	-0.0013
54(H)	0.001827	0.00259	0.002209	-0.00076
55(H)	0.00044	0.002415	0.001428	-0.00198
56(H)	0.001192	0.003349	0.002271	-0.00216
57(H)	0.001197	0.001902	0.00155	-0.00071
58(H)	0.00057	0.001348	0.000959	-0.00078
59(H)	0.002851	0.004088	0.00347	-0.00124
60(H)	0.00319	0.004671	0.003931	-0.00148
61(H)	0.003591	0.005083	0.004337	-0.00149

Table S4. Condensed Fukui functions calculated by the Hirshfeld charge population for the SA3

Atom	f^+	f	f^\bullet	Δf
1(C)	0.020678	0.073658	0.047168	-0.05298
2(C)	0.041593	0.070433	0.056013	-0.02884
3(C)	0.067136	0.058663	0.0629	0.008473
4(C)	0.030096	0.119049	0.074573	-0.08895
5(C)	0.039171	0.035886	0.037529	0.003285
6(C)	0.038872	0.04924	0.044056	-0.01037
7(O)	0.012196	0.105435	0.058816	-0.09324
8(C)	0.044482	0.027906	0.036194	0.016576

9(C)	0.040773	0.003513	0.022143	0.03726
10(O)	0.019505	0.0076	0.013553	0.011905
11(C)	0.020396	0.012779	0.016588	0.007617
12(O)	0.055399	0.046345	0.050872	0.009054
13(C)	0.006999	0.00842	0.00771	-0.00142
14(C)	0.004563	0.006698	0.005631	-0.00213
15(C)	0.003861	0.005832	0.004847	-0.00197
16(C)	0.002229	0.00343	0.00283	-0.0012
17(C)	0.00295	0.003219	0.003085	-0.00027
18(C)	0.00254	0.002058	0.002299	0.000482
19(C)	0.00223	0.001625	0.001928	0.000605
20(C)	0.00173	0.001165	0.001448	0.000565
21(N)	0.001128	0.001206	0.001167	-7.8E-05
22(S)	0.002914	0.002029	0.002471	0.000885
23(O)	0.000514	0.000342	0.000428	0.000172
24(O)	0.005944	0.008193	0.007069	-0.00225
25(C)	-0.00028	-0.00126	-0.00077	0.000982
26(C)	-0.00027	-0.00145	-0.00086	0.001181
27(C)	0.00142	0.000735	0.001078	0.000685
28(C)	0.004295	0.00303	0.003663	0.001265
29(C)	0.002653	0.000974	0.001814	0.001679
30(C)	0.004997	0.003561	0.004279	0.001436
31(C)	0.002819	0.000911	0.001865	0.001908
32(H)	0.058512	0.035631	0.047072	0.022881
33(H)	0.053348	0.038818	0.046083	0.01453
34(H)	0.026436	0.047017	0.036727	-0.02058
35(H)	0.061166	0.02965	0.045408	0.031516
36(H)	0.064889	0.029658	0.047274	0.035231
37(H)	0.047561	0.029485	0.038523	0.018076
38(H)	0.018437	0.010603	0.01452	0.007834
39(H)	0.023495	0.014737	0.019116	0.008758
40(H)	0.018237	0.013582	0.01591	0.004655
41(H)	0.017285	0.016774	0.01703	0.000511
42(H)	0.009683	0.01528	0.012482	-0.0056
43(H)	0.002188	0.004495	0.003342	-0.00231
44(H)	0.007286	0.005209	0.006248	0.002077
45(H)	0.005015	0.006616	0.005816	-0.0016
46(H)	0.007728	0.00768	0.007704	4.8E-05
47(H)	0.003219	0.002704	0.002962	0.000515
48(H)	0.003493	0.003623	0.003558	-0.00013
49(H)	0.004298	0.003895	0.004097	0.000403

50(H)	0.006526	0.003282	0.004904	0.003244
51(H)	0.00265	0.002169	0.00241	0.000481
52(H)	0.00643	0.001766	0.004098	0.004664
53(H)	0.005308	0.001441	0.003375	0.003867
54(H)	0.003323	0.002125	0.002724	0.001198
55(H)	0.003324	0.001316	0.00232	0.002008
56(H)	0.002963	0.001056	0.00201	0.001907
57(H)	0.002279	0.001147	0.001713	0.001132
58(H)	0.004349	-0.00151	0.001422	0.005855
59(H)	0.010821	0.002907	0.006864	0.007914
60(H)	0.008929	0.000993	0.004961	0.007936
61(H)	0.009477	0.002948	0.006213	0.006529
62(H)	0.004924	0.002699	0.003812	0.002225
63(H)	0.003601	-0.00052	0.001539	0.004124
64(H)	0.002922	0.001357	0.00214	0.001565

Table S5. Condensed Fukui functions calculated by the Hirshfeld charge population for the SA4

Atom	f^+	f	f^\bullet	Δf
1(C)	0.020551	0.073426	0.046989	-0.05288
2(C)	0.04136	0.069336	0.055348	-0.02798
3(C)	0.065436	0.058865	0.062151	0.006571
4(C)	0.028802	0.11841	0.073606	-0.08961
5(C)	0.038058	0.035545	0.036802	0.002513
6(C)	0.038433	0.050227	0.04433	-0.01179
7(O)	0.012007	0.105606	0.058807	-0.0936
8(C)	0.041414	0.027941	0.034678	0.013473
9(C)	0.039228	0.003556	0.021392	0.035672
10(O)	0.01916	0.007598	0.013379	0.011562
11(C)	0.017818	0.012799	0.015309	0.005019
12(O)	0.05343	0.046415	0.049923	0.007015
13(C)	0.008312	0.008172	0.008242	0.00014
14(C)	0.00471	0.006274	0.005492	-0.00156
15(C)	0.005742	0.005517	0.00563	0.000225
16(C)	0.002497	0.003049	0.002773	-0.00055
17(C)	0.003954	0.002912	0.003433	0.001042
18(C)	0.003269	0.001747	0.002508	0.001522
19(C)	0.003156	0.001573	0.002365	0.001583
20(C)	0.003321	0.001093	0.002207	0.002228
21(N)	-0.00014	0.000268	6.6E-05	-0.0004

22(S)	0.005796	0.003521	0.004659	0.002275
23(O)	0.004429	0.005886	0.005158	-0.00146
24(O)	0.007354	0.010233	0.008794	-0.00288
25(C)	-0.00109	-0.00153	-0.00131	0.000438
26(C)	0.000871	-8.1E-05	0.000395	0.000952
27(C)	-0.00017	-0.00047	-0.00032	0.000292
28(C)	0.001948	0.001239	0.001594	0.000709
29(C)	0.002836	0.001887	0.002362	0.000949
30(C)	0.002407	0.002221	0.002314	0.000186
31(C)	0.003257	0.001085	0.002171	0.002172
32(H)	0.054412	0.03535	0.044881	0.019062
33(H)	0.051839	0.038733	0.045286	0.013106
34(H)	0.027991	0.046894	0.037443	-0.0189
35(H)	0.058331	0.029578	0.043955	0.028753
36(H)	0.058648	0.029551	0.0441	0.029097
37(H)	0.04449	0.029677	0.037084	0.014813
38(H)	0.01577	0.010624	0.013197	0.005146
39(H)	0.01942	0.014734	0.017077	0.004686
40(H)	0.015015	0.013577	0.014296	0.001438
41(H)	0.02242	0.016661	0.019541	0.005759
42(H)	0.012163	0.015117	0.01364	-0.00295
43(H)	0.002504	0.004025	0.003265	-0.00152
44(H)	0.008297	0.005198	0.006748	0.003099
45(H)	0.006243	0.006296	0.00627	-5.3E-05
46(H)	0.016072	0.007704	0.011888	0.008368
47(H)	0.003796	0.002288	0.003042	0.001508
48(H)	0.005	0.00357	0.004285	0.00143
49(H)	0.012342	0.003927	0.008135	0.008415
50(H)	0.005193	0.003011	0.004102	0.002182
51(H)	0.004947	0.002106	0.003527	0.002841
52(H)	0.009202	0.00144	0.005321	0.007762
53(H)	0.005031	0.001709	0.00337	0.003322
54(H)	0.009766	0.002393	0.00608	0.007373
55(H)	0.003196	0.001437	0.002317	0.001759
56(H)	0.012287	0.000742	0.006515	0.011545
57(H)	0.002805	0.000787	0.001796	0.002018
58(H)	0.001872	0.000436	0.001154	0.001436
59(H)	0.001385	-0.00013	0.000627	0.001517
60(H)	0.006126	0.001471	0.003799	0.004655
61(H)	0.00338	0.002029	0.002705	0.001351
62(H)	0.008392	0.002808	0.0056	0.005584

63(H)	0.004324	0.001295	0.00281	0.003029
64(H)	0.002751	0.000527	0.001639	0.002224

Table S6. Condensed Fukui functions calculated by the Hirshfeld charge population for the SA5

Atom	f^+	f	f^-	Δf
1(C)	0.020645	0.071933	0.046289	-0.05129
2(C)	0.039376	0.069735	0.054556	-0.03036
3(C)	0.063732	0.056936	0.060334	0.006796
4(C)	0.026908	0.116756	0.071832	-0.08985
5(C)	0.036365	0.035376	0.035871	0.000989
6(C)	0.037567	0.047606	0.042587	-0.01004
7(O)	0.010793	0.103083	0.056938	-0.09229
8(C)	0.030484	0.027291	0.028888	0.003193
9(C)	0.038993	0.003267	0.02113	0.035726
10(O)	0.019217	0.007267	0.013242	0.01195
11(C)	0.016656	0.012478	0.014567	0.004178
12(O)	0.050802	0.04444	0.047621	0.006362
13(C)	0.006837	0.008414	0.007626	-0.00158
14(C)	0.003935	0.006812	0.005374	-0.00288
15(C)	0.003553	0.00602	0.004787	-0.00247
16(C)	0.002342	0.003786	0.003064	-0.00144
17(C)	0.002973	0.003742	0.003358	-0.00077
18(C)	0.004593	0.002625	0.003609	0.001968
19(C)	0.006343	0.002349	0.004346	0.003994
20(C)	0.008278	0.002124	0.005201	0.006154
21(N)	0.000287	-0.00138	-0.00055	0.001666
22(S)	0.004945	0.004784	0.004864	0.000161
23(O)	0.006512	0.01471	0.010611	-0.0082
24(O)	0.008521	0.008931	0.008726	-0.00041
25(C)	-0.00042	-0.00077	-0.0006	0.000348
26(C)	0.002705	0.001642	0.002174	0.001063
27(C)	-0.00025	-0.00181	-0.00103	0.001558
28(C)	0.003306	-0.00068	0.001313	0.003986
29(C)	0.003349	0.002602	0.002976	0.000747
30(C)	0.004569	0.001829	0.003199	0.00274
31(C)	0.001242	-0.00068	0.000282	0.00192
32(C)	0.009458	0.001402	0.00543	0.008056
33(H)	0.043264	0.035064	0.039164	0.0082
34(H)	0.043628	0.037944	0.040786	0.005684

35(H)	0.021772	0.046063	0.033918	-0.02429
36(H)	0.04083	0.029049	0.03494	0.011781
37(H)	0.031723	0.028909	0.030316	0.002814
38(H)	0.044125	0.028945	0.036535	0.01518
39(H)	0.01334	0.013206	0.013273	0.000134
40(H)	0.018467	0.01442	0.016444	0.004047
41(H)	0.014845	0.010376	0.012611	0.004469
42(H)	0.015127	0.016415	0.015771	-0.00129
43(H)	0.010174	0.015132	0.012653	-0.00496
44(H)	0.005744	0.005211	0.005478	0.000533
45(H)	0.001963	0.004603	0.003283	-0.00264
46(H)	0.004442	0.006702	0.005572	-0.00226
47(H)	0.006784	0.007647	0.007216	-0.00086
48(H)	0.005792	0.003733	0.004763	0.002059
49(H)	0.002351	0.003045	0.002698	-0.00069
50(H)	0.006652	0.004042	0.005347	0.00261
51(H)	0.00613	0.003605	0.004868	0.002525
52(H)	0.004121	0.001968	0.003045	0.002153
53(H)	0.017944	0.002359	0.010152	0.015585
54(H)	0.014814	0.002414	0.008614	0.0124
55(H)	0.019725	0.002549	0.011137	0.017176
56(H)	0.015251	0.004694	0.009973	0.010557
57(H)	0.02181	0.001604	0.011707	0.020206
58(H)	0.028263	0.000667	0.014465	0.027596
59(H)	0.003524	0.001995	0.00276	0.001529
60(H)	0.004831	-0.00053	0.002153	0.005357
61(H)	0.004899	0.00184	0.00337	0.003059
62(H)	0.004464	0.002053	0.003259	0.002411
63(H)	-0.00029	-0.00361	-0.00195	0.003312
64(H)	0.001799	-0.00093	0.000434	0.002731
65(H)	0.007774	0.000719	0.004247	0.007055
66(H)	0.01896	0.002492	0.010726	0.016468
67(H)	0.01445	0.002821	0.008636	0.011629

Table S7: Types of interactions and distances (Å) between the ligands and the amino acid residues of cruzain.

Ligand	Receptor	Interaction	Distance (Å)
SA1	ASP158	H-Bond	2.35
	TRP177*	π - π Stacked	5.42
SA2	CYS25*	H-Bond	3.54
	ALA136	Hydrophobic	4.99
	ASP158	π -Anion	4.38
	TRP177*	π - π Stacked	5.55
SA3	TRP177*	Amide- π Stacked	4.58
	ARG8	Hydrophobic	4.90
	VAL13	H-Bond	3.68
	ALA15	Hydrophobic	5.08
SA4	MET142	π -Sulfur	5.05
	TRP177*	π - π Stacked	3.89
	TRP177*	π -Sigma	3.70
SA5	GLN180	H-Bond	3.58
	CYS56	Hydrophobic	4.05
	LYS58	H-Bond	2.40
	CYS63	H-Bond	2.24
	SER64	H-Bond	3.60
	TRP74	Hydrophobic	4.88
	CYS95	Hydrophobic	4.46
CYS95	Hydrophobic	5.08	
A0	ASP18	H-Bond	2.62
	GLY20	H-Bond	2.60
	MET142	π -Sulfur	5.38
	TRP177*	π - π Stacked	4.27
BZN	CYS25*	Hydrophobic	4.99
	TRP177*	π - π Stacked	3.82

CONCLUSION

The SA1-SA5 molecules studied in this work were geometrically optimized by performing DFT using B3LYP/6-311+G (d, p) combinations. The IR and NMR spectroscopy data obtained from the calculations were compared with the experimental data in Reddy's article. The comparison was used by linear regression, checking the theoretical-experimental R2 values. The correlation data showed a minimum of 0.9961 and a maximum of 0.9991, indicating excellent structural correlations of the calculated geometries. The study of local and global reactivity of the derivatives was also performed. The data indicated that the SA1 molecule tended to be the most reactive, while the SA2 molecule tended to be more stable. From the analysis of the boundary orbitals, it was observed that the HOMO orbital of the derivatives was concentrated in the A ring region. While the LUMO orbital, the SA1 molecule, was concentrated on ring A, and the substitution of ring B by an aromatic group influenced the LUMO orbital to spread out on ring B. In the local reactivity analysis, described by the isosurface of the electronic function of Fukui, the region responsible for the nucleophilic and electrophilic attack of the molecule was in ring A, highlighting the ordinary atoms among the derivatives: C3, C5, C8, C9, O10, C11, O12, C18, C19, C20, favoring nucleophilic attack of the molecules, and the atoms: C1, C2, C4, C6, O7, C13, C14, C15, C16, C17, favoring electrophilic attack of the molecules. The MESP indicated that the highest electronic concentration, highlighted by red color, was in the ring A region and the Oxygens of sulfonamide, while the methyl region of the methoxyl group of ring A indicated a lower electronic concentration.

From the molecular docking analysis, the interaction SA1-5 with the enzyme 1F29 observed good interaction energy values, being SA1, SA3, and SA4, with values very close to AA. According to articles, it was verified interaction experimentally. The interaction length values of the derivatives SA1, SA2, and SA4 at the Tpr 177 site were excellent compared to AA. Moreover, at the Asn 175 site, they showed values close to or better than BZN. From the 2D map, the SA1, SA2, and SA4 molecules indicated interactions with the Tpr 177 site, AA, and the BNZ, by pi-stacked, revealing the importance of this region for interactions. These interactions corroborate the global and local reactivity data, where the HOMO orbital and the Fukui function isosurfaces indicated reactivity in this ring.

The molecular dynamics calculations were performed to verify the stability of the molecules in the enzyme cruzaina. The results of interaction energy indicated that the complex 1F29-SA4 had the highest interaction energy -179.217 (kJ.mol⁻¹) about the others, followed by

the complex 1F29-SA1. Between 1F29 and SA4, there are three hydrophobic interactions with Trp 177 and His 159 (distance of 3.74 Å, 3.75 Å, and 3.94 Å, respectively); Moreover, two hydrogen bonds uncharged of moderate strength were registered with the amino acids Gln 19 (1.82 Å), His 159 (2.05 Å), and a weak one with Trp 177 (2.50 Å).

From this perspective, this study obtained promising results, indicating an excellent interaction of sulfonamide derivative from anacardic acid (SA4) with cruzain, and is recommended for future in vitro testing studies.

REFERENCES

- ALVES, F. das C. de S. **Uso de microscopia de força atômica como modelo de estudo em atividades parasitárias e efeito do ácido anacárdico em formas epimastigota e tripomastigota de *Trypanosoma cruzi***. 2018. 80 f. Tese (Doutorado Biotecnologia de Recursos Naturais) - Pró-Reitoria de Pesquisa e Pós-Graduação, Universidade Federal do Ceará, Fortaleza, 2018.
- AZEVEDO JUNIOR., W. de. MolDock Applied to Structure-Based Virtual Screening. **Current Drug Targets**, v. 11, n. 3, p. 327–334, 11 fev. 2010.
- BRITO, A.; FALCÃO, L.; MATIAS, A. *et al.* Um doenças negligenciadas: doença de Chagas e os aspectos atuais do tratamento. **Revista de Ensino, Ciência e Inovação em Saúde**, v. 2, n. 1, p. 9–17, 4 maio 2021.
- CHABI S. K., SINA, H., ADOUKONOU-SAGBADJA, H., AHOTON, L. E. *et al.* Antimicrobial activity of *Anacardium occidentale* L. leaves and barks extracts on pathogenic bacteria. **African Journal of Microbiology Research**, v. 8, n. 25, p. 2458–2467, 2014.
- CHEUKA, P. M.; MAYOKA, G.; MUTAI, P. *et al.* The Role of Natural Products in Drug Discovery and Development against Neglected Tropical Diseases, **Molecules** v. 22, n. 1, p. 58, 31 dez. 2016.
- CLAYTON, J. Chagas disease: pushing through the pipeline, **Nature**, v. 465, n. 7301, p. S12–S15, 23 jun. 2010.
- FERREIRA, A. M.; DAMASCENO, R. F.; MONTEIRO-JUNIOR, R. S. *et al.* Reações adversas ao benzonidazol no tratamento da Doença de Chagas: revisão sistemática de ensaios clínicos randomizados e controlados. **Cadernos Saúde Coletiva**, v. 27, n. 3, p. 354–362, 30 set. 2019.
- JAISWAL, Y. S.; TATKE, P. A.; GABHE, S. Y. *et al.* Antidiabetic activity of extracts of *Anacardium occidentale* Linn. leaves on n-streptozotocin diabetic rats. **Journal of Traditional and Complementary Medicine**, v. 7, n. 4, p. 421, 1 out. 2017.
- KESSELHEIM, A. S. Drug development for neglected diseases — The Trouble with FDA Review Vouchers. **The new England journal of medicine**, v. 359, n. 19, p. 1981–1983, 6 jun. 2009.
- MARINHO, M.M.; DOS SANTOS, R.P.; BEZERRA, E.M. *et al.* Molecular dractionation with conjugate caps study of the interaction of the anacardic acid with the active site of *Trypanosoma Cruzi* Gapdh enzyme: A quantum investigation. **Asian Journal of Pharmaceutical and Clinical Research**, p. 183–189, 2019.
- MARINHO, M. M. **Efeito Tripanocida de substancias presentes no cajueiro (*Anacardium occidentale*): Uma abordagem experimental e teórica**. 2020.138 f. Tese (Doutorado em Ciências Farmacêuticas) - Pró-Reitoria de Pesquisa e Pós-Graduação, Universidade Federal do Ceará, Fortaleza, 2020.
- MARINHO, M. M.; ALMEIDA-NETO, F. W. Q.; MARINHO, E. M. *et al.* Quantum computational investigations and molecular docking studies on amentoflavone. **Heliyon**, v. 7, n. 1, 2021.

- MARTINS-MELO, F. R.; RAMOS, A. N.; ALENCAR, C. H. *et al.* Prevalence of Chagas disease in Brazil: A systematic review and meta-analysis. **Acta Tropica**, v. 130, n. 1, p. 167–174, 1 fev. 2014.
- MINISTÉRIO DA SAÚDE. Departamento de Ciência e Tecnologia. Secretaria de Ciência, Tecnologia e Insumos Estratégicos. Doenças negligenciadas: estratégias do Ministério da Saúde. **Revista de Saúde Pública**, São Paulo, v. 44, n. 1, p. 200-202, fev. 2010. Disponível em Scielo
- OLIVEIRA, M. S. C.; MORAIS, S. M.; MAGALHÃES, D. V. *et al.* Antioxidant, larvicidal and antiacetylcholinesterase activities of cashew nut shell liquid constituents. **Acta Tropica**, v. 117, n. 3, p. 165–170, 1 mar. 2011.
- PAULA, R. S. F.; VIEIRA, R. S., LUNA; F. M. T. *et al.* A potential bio-antioxidant for mineral oil from cashew nutshell liquid: an experimental and theoretical approach. **Brazilian Journal of Chemical Engineering**, v. 37, n. 2, p. 369–381, 2020.
- POSENATO, L.; LUÍS, G.; DE MAGALHÃES, C. G. *et al.* 607 **Epidemiologia das doenças negligenciadas no Brasil e gastos federais com medicamentos.** [s. l.] Disponível em: <http://www.ipea.gov.br>. Acesso em: 25 out. 2021.
- RANGEL, N. V. P.; DA SILVA, L. P.; PINHEIRO, V. S. *et al.* Effect of additives on the oxidative stability and corrosivity of biodiesel samples derived from babassu oil and residual frying oil: An experimental and theoretical assessment. **Fuel**, v. 289, p. 119939, 1 abr. 2021.
- REDDY, N. S.; RAO, A. S.; CHARI, M. A. *et al.* Synthesis and antibacterial activity of sulfonamide derivatives at C-8 alkyl chain of anacardic acid mixture isolated from a natural product cashew nut shell liquid (CNSL). **Journal of Chemical Sciences**, v. 124, n. 3, p. 723–730, 2012.
- SANTOS, R. P. dos.; SÁ, R. A.; MARINHO, M. M. *et al.* Compositional analysis of cashew (*Anacardium occidentale* L.) peduncle bagasse ash and its in vitro antifungal activity against *Fusarium* species. **Revista Brasileira de Biociências**, v. 9, n. 2, p. 1679–2343, 20 jun. 2011.
- SU, C.; YANG, C.; GONG, M. *et al.* Antidiabetic activity and potential mechanism of amentoflavone in diabetic mice. **Molecules**, v. 24, n. 11, p. 1–14, 2019.
- SÜLSEN, V. P.; PUENTE, V.; PAPADEMETRIO, D. *et al.* Mode of action of the sesquiterpene lactones psilostachyin and psilostachyin C on *Trypanosoma cruzi*. **PLOS ONE**, v. 11, n. 3, p. e0150526, 1 mar. 2016.
- ZINSSER, V. L.; HOEY, E. M.; TRUDGETT, A. *et al.* Biochemical characterisation of glyceraldehyde 3-phosphate dehydrogenase (GAPDH) from the liver fluke, *Fasciola hepática*. **Biochimica et Biophysica Acta (BBA) - Proteins and Proteomics**, v. 1844, n. 4, p. 744–749, 1 abr. 2014.

APPENDIX A – AUTHOR'S CURRICULUM DATA



Leonardo Paes da Silva

Endereço para acessar este CV: <http://lattes.cnpq.br/6288308362104199>

ID Lattes: **6288308362104199**

Última atualização do currículo em 16/12/2021

Possui formação de nível médio no Colégio Santa Isabel (2015). Graduado em Química Licenciatura pela Universidade Estadual de Ceará (UECE). Foi bolsista de Monitoria Acadêmica - PROMAC (2016-2017) e FUNCAP (2018-2019). Possui experiência em pesquisa na Química com ênfase na Química Computacional e Química Teórica, com especialidade em métodos DFT (Density Functional Theory). **(Texto informado pelo autor)**

Identificação

Nome	Leonardo Paes da Silva
Nome em citações bibliográficas	SILVA, L. P.; DA SILVA, LEONARDO P.; SILVA, LEONARDO PAES; SILVA, LEONARDO PAES DA; DA SILVA, LEONARDO PAES
Lattes ID	http://lattes.cnpq.br/6288308362104199
Orcid ID	https://orcid.org/0000-0002-9264-4721

Endereço

Formação acadêmica/titulação

2019	Mestrado em andamento em Química (Conceito CAPES 6). Universidade Federal do Ceará, UFC, Brasil. Orientador: Pedro de Lima Neto. Coorientador: Emmanuel Silva Marinho. Bolsista do(a): Coordenação de Aperfeiçoamento de Pessoal de Nível Superior, CAPES, Brasil.
2015 - 2019	Graduação em Química. Universidade Estadual do Ceará, UECE, Brasil. Título: Avaliação do potencial antioxidante da molécula Castanol B: Um estudo termodinâmico teórico em DFT de sua forma neutra e seu ânion carboxilato. Orientador: Emmanuel Silva Marinho. Bolsista do(a): Fundação Cearense de Apoio ao Desenvolvimento Científico e Tecnológico, FUNCAP, Brasil.
2012 - 2014	Ensino Médio (2º grau). Colégio Santa Isabel, CSI, Brasil.

Formação Complementar

2019 - 2019	Modelagem Computacional. (Carga horária: 6h). Universidade Federal do Ceará, UFC, Brasil.
2018 - 2018	ESPECTROMETRIA DE ABSORÇÃO ATÔMICA. (Carga horária: 12h). Universidade Estadual do Ceará, UECE, Brasil.
2018 - 2018	PETROLEO E SEUS DERIVADOS. (Carga horária: 12h). Universidade Estadual do Ceará, UECE, Brasil.
2017 - 2017	INTRODUÇÃO A QUÍMICA COMPUTACIONAL. (Carga horária: 12h). Universidade Estadual do Ceará, UECE, Brasil.
2016 - 2016	Espectrometria de Massas - Potencial e Aplicação. (Carga horária: 6h). Universidade Federal do Ceará, UFC, Brasil.
2016 - 2016	FÍSICA APLICADA AOS SISTEMAS BIOLÓGICOS. (Carga horária: 4h). Universidade Estadual do Ceará, UECE, Brasil.
2016 - 2016	EFICIÊNCIA ENERGÉTICA. (Carga horária: 4h). Universidade Estadual do Ceará, UECE, Brasil.
2016 - 2016	O DESENVOLVIMENTO DA COMPREENSÃO DE TEXTOS ESCRITOS EM INGLÊS, ATRAVÉS DA A. (Carga horária: 4h). Universidade Estadual do Ceará, UECE, Brasil.
2016 - 2016	

2015 - 2015	TEORIA DOS GRUPOS. (Carga horária: 4h). Universidade Estadual do Ceará, UECE, Brasil.
2015 - 2015	ANÁLISES ESPECTRAIS. (Carga horária: 4h). Universidade Estadual do Ceará, UECE, Brasil.
2015 - 2015	FÍSICA APLICADA AO PETRÓLEO. (Carga horária: 8h). Universidade Estadual do Ceará, UECE, Brasil.
2008 - 2008	Operador básico em micro (Windows, Word, Linux, Writer, Excel, Power Point). (Carga horária: 70h). Escola Técnica profissionalizante em informática A&C s/c, A&C, Brasil.

Atuação Profissional

Universidade Estadual do Ceará, UECE, Brasil.

Vínculo institucional

2018 - 2019

Vínculo: Bolsista, Enquadramento Funcional: Iniciação Científica, Carga horária: 20, Regime: Dedicção exclusiva.

Vínculo institucional

2016 - 2017

Vínculo: Bolsista, Enquadramento Funcional: Monitoria, Carga horária: 12, Regime: Dedicção exclusiva.

Outras informações

Monitoria em Química Geral I

Projetos de pesquisa

2018 - Atual

CARACTERIZAÇÃO IN SILICO E AVALIAÇÃO DO POTENCIAL FOTOPROTETOR E ANTIOXIDANTE DE EXTRATO DE CLADÓDIOS E SEMENTES DO FRUTO DA HYLOCEREUS UNDATUS (PITAYA)

Descrição: Descrição: As cactáceas são compostas por um grupo de plantas abundantes nas regiões do semiárido. Apresentam bastante especificidade com relação ao seu habitat e possuem diversas adaptações morfológicas e fisiológicas que permitem a sua sobrevivência em ambientes com déficit em nutrientes e água, além de suportar intensa radiação solar. Muitas espécies de cactáceas produzem frutos comestíveis, como as trepadeiras dos gêneros Hylocereus. No Brasil, existem pequenas áreas para produção de pitaya (cactáceas dos Gêneros Hylocereus e Selenicereus). Atualmente, a região Sudeste do Brasil é a principal produtora do país, mas existem diversos plantios distribuídos por todo o país, sendo alguns desses na região da Chapada do Apodi, nos municípios de Limoeiro do Norte e Quixeré, no estado do Ceará. Muitos princípios ativos sintetizados pelas plantas, exercem diferentes funções no vegetal, como atividade antifúngica, antibactericida, antioxidante e fotoprotetora. Com a crescente preocupação sobre os efeitos deletérios ocasionados pela exposição da pele aos raios ultravioleta, torna-se de grande importância a exploração de testes in vitro capazes de caracterizar as propriedades de um protetor ou testar substâncias com princípios ativos que possam vir a ser utilizados como fotoprotetores. A metodologia a ser empregada, compreende a coleta e obtenção do extrato bruto do material vegetal (cladódios e sementes dos frutos da Hylocereus undatus); análise da capacidade antioxidante pelo método DPPH e capacidade dos extratos como fator de proteção solar - FPS in vitro, caracterização estrutural (comprimentos de ligação), eletrônica (orbitais atômicos) e energética (energia de ligação) dos componentes bioativos, principalmente, pigmentos e compostos fenólicos (metabólitos secundários), presentes no fruto e na polpa, utilizando a teoria da densidade funcional (DFT). Neste contexto, o presente projeto visa caracterizar e avaliar o potencial fotoprotetor e antioxidante do extrato de cladódios e sementes do fruto da Hylocereus undatus (Pitaya), utilizando diferentes concentrações do solvente e diferentes horários de coleta do material vegetal..

Situação: Em andamento; Natureza: Pesquisa.

Alunos envolvidos: Graduação: (1) .

Integrantes: Leonardo Paes da Silva - Integrante / Emmanuel Silva Marinho - Coordenador.

Áreas de atuação

1.

Grande área: Ciências Exatas e da Terra / Área: Química / Subárea: Físico-Química/Especialidade: Química Teórica.

Idiomas

Espanhol

Compreende Razoavelmente, Fala Pouco, Lê Razoavelmente, Escreve Pouco.

Prêmios e títulos

2019	Diploma de Honra ao mérito pela aprovação em 9º lugar na modalidade Química Inorgânica na Olimpíada Cearense do Ensino Superior de Química, Universidade Federal do Ceará.
2019	Diploma de Honra ao mérito pela aprovação em 7º lugar na modalidade Físico-Química na Olimpíada Cearense do Ensino Superior de Química, Universidade Federal do Ceará.
2019	Diploma de Honra ao mérito na classificação geral da Olimpíada Brasileira do Ensino Superior de Química, Programa Nacional de Olimpíadas de Química.
2019	Diploma de Honra ao mérito pela aprovação em 21º lugar na modalidade Química Inorgânica na Olimpíada Brasileira do Ensino Superior de Química, Programa Nacional de Olimpíadas de Química.
2012	1º Lugar Olimpíada Interna de Química, Colégio Santa Isabel.

Produções

Produção bibliográfica

Artigos completos publicados em periódicos

Ordenar por

Ordem Cronológica

1. RANGEL, NELLY V.P. ; **DA SILVA, LEONARDO P.** ; PINHEIRO, VINÍCIUS S. ; FIGUEREDO, IGOR M. ; CAMPOS, OTHON S. ; COSTA, STEFANE N. ; LUNA, FRANCISCO MURILO T. ; CAVALCANTE JR., CÉLIO L. ; MARINHO, EMMANUEL S. ; DE LIMA-NETO, PEDRO ; RIOS, MARIA A.S. . Effect of additives on the oxidative stability and corrosivity of biodiesel samples derived from babassu oil and residual frying oil: An experimental and theoretical assessment. *FUEL JCR*, v. 289, p. 119939, 2021.
Citações: **WEB OF SCIENCE** [™] 1
2. MARINHO, MÁRCIA M. ; ALMEIDA-NETO, FRANCISCO WAGNER Q. ; MARINHO, EMANUELLE M. ; **DA SILVA, LEONARDO P.** ; MENEZES, RAMON R.P.P.B. ; DOS SANTOS, RICARDO P. ; MARINHO, EMMANUEL S. ; DE LIMA-NETO, PEDRO ; MARTINS, ALICE M.C. . Quantum computational investigations and molecular docking studies on amentoflavone. *HELIVON JCR*, v. 7, p. e06079, 2021.
Citações: **WEB OF SCIENCE** [™] 1
3. VASQUES, ROBERTA BASTOS ; LEVY, MARJORY MOREIRA ; RODRIGUES, MATHEUS SOUZA ; QUEIROZ ALMEIDA NETO, FRANCISCO WAGNER ; **SILVA, LEONARDO PAES** ; VAZ, GUSTAVO LEITÃO ; MAGALHÃES, ÁLVARO AUGUSTO OLIVEIRA ; LIMA-NETO, PEDRO ; ARAÚJO, WALNEY SILVA . A theoretical and experimental study of phosphate ester inhibitors for AISI 1018 in carbon dioxide-saturated 3.5-wt% NaCl solution. *MATERIALS AND CORROSION (ONLINE) JCR*, v. 72, p. 1417-1432, 2021.
Citações: **WEB OF SCIENCE** [™] 1
4. FONSECA, ALUÍSIO M. ; **SILVA, LEONARDO PAES DA** ; ALMEIDA-NETO, FRANCISCO WAGNER DE QUEIROZ ; COLARES, REGILANY PAULO ; MACEDO DE OLIVEIRA, MAURO ; LUTHIERRE GAMA CAVALCANTE, ANTÔNIO ; LEMOS, TELMA L. G. ; BRAZ-FILHO, RAIMUNDO ; DE LIMA-NETO, PEDRO ; MARINHO, EMMANUEL SILVA . Synthesis of a new quinine dimer biocatalysed by the coconut water. *BIOCATALYSIS AND BIOTRANSFORMATION JCR*, v. X, p. 1-10, 2021.
5. FROTA, LUCAS SOARES ; ALVES, DANIELA RIBEIRO ; MARINHO, MÁRCIA MACHADO ; **DA SILVA, LEONARDO PAES** ; ALMEIDA NETO, FRANCISCO WAGNER DE QUEIROZ ; MARINHO, EMMANUEL SILVA ; DE MORAIS, SELENE MAIA . Antioxidant and anticholinesterase activities of amentoflavone isolated from *Ouretea fieldingiana* (Gardner) Engl. through in vitro and chemical-quantum studies. *JOURNAL OF BIOMOLECULAR STRUCTURE & DYNAMICS JCR*, v. x, p. 1-11, 2021.
6. PAULA, R. S. F. ; VIEIRA, R. S. ; LUNA, F. M. T. ; CAVALCANTE JR, C. L. ; FIGUEREDO, I. M. ; CANDIDO JUNIOR, J. R. ; **SILVA, L. P.** ; MARINHO, E. S. ; LIMA-NETO, P. ; MAZZETTO, S. E. ; RIOS, M. A. S. . A potential bio-antioxidant for mineral oil from cashew nutshell liquid: an experimental and theoretical approach. *BRAZILIAN JOURNAL OF CHEMICAL ENGINEERING JCR*, v. x, p. xx, 2020.
Citações: **WEB OF SCIENCE** [™] 3
7. ALMEIDA-NETO, FRANCISCO WAGNER Q. ; **DA SILVA, LEONARDO P.** ; FERREIRA, MARIA KUEIRISLENE A. ; MENDES, FRANCISCO ROGÊNIO S. ; DE CASTRO, KEVIN K.A. ; BANDEIRA, PAULO N. ; DE MENEZES, JANE EIRE S.A. ; DOS SANTOS, HÉLCIO S. ; MONTEIRO, NORBERTO K.V. ; MARINHO, EMMANUEL S. ; DE LIMA-NETO, PEDRO . Characterization of the structural, spectroscopic, nonlinear optical, electronic properties and antioxidant activity of the N-{4-[(E)-3-(Fluorophenyl)-1-(phenyl)-prop-2-en-1-one]}-acetamide. *JOURNAL OF MOLECULAR STRUCTURE JCR*, v. 1220, p. 128765, 2020.
Citações: **WEB OF SCIENCE** [™] 7
8. MORAIS FILHO, C. L. ; MARINHO, E. M. ; **SILVA, L. P.** ; MARINHO, M.M. ; MARINHO, E. S. . QUANTUM STUDY OF GEOMETRIC PROPERTIES OF THE ANTHIVCOUMARIN HERACLLENOL: A STUDY OF DENSITY FUNCTIONAL THEORY (DFT).

International Journal of Engineering Technology Research & Management, v. 2, p. 27-37, 2018.

9. **SILVA, L. P.**; MARINHO, E. M. ; MARINHO, M.M. . In Silico Study of Antidepressant Drug Vortioxetine: A Description of their Physical Chemistry Properties using Classical Molecular Mechanics Methods MMFF94. International Journal of Recent Research and Review, v. XI, p. 7-13, 2018.

Trabalhos completos publicados em anais de congressos

1. ★ **SILVA, L. P.**; BEZERRA, L. L. ; MARINHO, M.M. ; MARINHO, E. S. . Caracterização do fármaco antidepressivo Vortioxetine: um estudo in silico usando campo de força clássico MMFF94. In: XXIII Semana Universitaria UECE, 2017, Fortaleza. Encontro de iniciação científica, 2017. v. 1. p. 1-x.
2. ★ **SILVA, L. P.**; SANTOS, W. L. ; MARINHO, M.M. ; MARINHO, E. S. . Estudo DFT do Alcalóide Dincetrina: GAP, HOMO, LUMO, MESP E MULLIKEN. In: III Encontro Internacional de Jovens Investigadores, 2017, Fortaleza. III ENCONTRO INTERNACIONAL DE JOVENS INVESTIGADORES (EDIÇÃO BRASIL), 2017.

Resumos expandidos publicados em anais de congressos

1. SILVA, A. B. F. ; MARINHO, E. M. ; CAMPOS, O. S. ; **SILVA, L. P.** ; MARINHO, M.M. ; MARINHO, E. S. . CARACTERIZAÇÃO DO ORBITAIS DE FRONTEIRA DO ALCALOIDE SOPHALINE F: UMA ETAPA INICIAL PARA ESTUDOS DE REATIVIDADE,, In: XXIV Semana Universitária da UECE, 2019, Fortaleza. CARACTERIZAÇÃO DO ORBITAIS DE FRONTEIRA DO ALCALOIDE SOPHALINE F: UMA ETAPA INICIAL PARA ESTUDOS DE REATIVIDADE,, 2019.
2. ESTACIO, S. P. ; LUCIO, F. N. M. ; MARINHO, E. M. ; CAMPOS, O. S. ; **SILVA, L. P.** ; MARINHO, M.M. . CARACTERIZAÇÃO ESTRUTURAL DA ALTERNAMIDE A: UMA ETAPA INICIAL PARA ESTUDOS DE INIBIÇÃO DO TRYPANOSOMA CRUZI,. In: XXIV Semana Universitária da UECE, 2019, Fortaleza. CARACTERIZAÇÃO ESTRUTURAL DA ALTERNAMIDE A: UMA ETAPA INICIAL PARA ESTUDOS DE INIBIÇÃO DO TRYPANOSOMA CRUZI,, 2019.
3. MARINHO, E. M. ; MENDES, F. R. S. ; FERREIRA, M. K. A. ; **SILVA, L. P.** ; LIMA NETO, P. ; MARINHO, M.M. . ESTUDO FARMACOCINÉTICO DA SOPHORAFLAVONONE G: UMA SIMULAÇÃO DE ADMET. In: XXIV Semana Universitária da UECE, 2019, Fortaleza. ESTUDO FARMACOCINÉTICO DA SOPHORAFLAVONONE G: UMA SIMULAÇÃO DE ADMET, 2019.
4. MARINHO, E. M. ; MENDES, F. R. S. ; COSTA, S. N. ; **SILVA, L. P.** ; LIMA NETO, P. ; MARINHO, M.M. . ESTUDOS DE VIABILIDADE FARMACOCINÉTICA E TOXICOLÓGICA DA LICOCHALCONA A: UM ESTUDO UTILIZANDO O ALGORITMO SWISSADME. In: XXIV Semana Universitária da UECE, 2019, Fortaleza. ESTUDOS DE VIABILIDADE FARMACOCINÉTICA E TOXICOLÓGICA DA LICOCHALCONA A: UM ESTUDO UTILIZANDO O ALGORITMO SWISSADME, 2019.
5. **SILVA, L. P.**; MENDES, F. R. S. ; LIMA NETO, P. ; MONTEIRO, N. K. V. ; MARINHO, E. S. . ESTUDOS INICIAIS DE CARACTERIZAÇÃO ESTRUTURAL DA MOLÉCULA MONO(2- ETILHEXIL)FTALATO. In: XXIII Semana Universitária da UECE, 2018, Fortaleza. ESTUDOS INICIAIS DE CARACTERIZAÇÃO ESTRUTURAL DA MOLÉCULA MONO(2- ETILHEXIL)FTALATO, 2018.
6. **SILVA, L. P.**; BATISTA, G. G. ; BEZERRA, L. L. ; OLIVEIRA FILHO, M. A. C. ; MONTEIRO, N. K. V. ; LIMA NETO, P. ; MARINHO, E. S. . Uso da química quântica computacional para obtenção dos descritores de reatividade global das moléculas encontrada no extrato da *Hyllocereus Undatus*.. In: 58º Congresso Brasileiro de Química, 2018, São Luíz. Uso da química quântica computacional para obtenção dos descritores de reatividade global das moléculas encontrada no extrato da *Hyllocereus Undatus*., 2018.
7. **SILVA, L. P.**; BATISTA, G. G. ; BEZERRA, L. L. ; OLIVEIRA FILHO, M. A. C. ; FERNANDES, A. M. ; MONTEIRO, N. K. V. ; LIMA NETO, P. ; MARINHO, E. S. . Estudo quântico das propriedades geométricas do fármaco Vortioxetine usando DFT. In: 58º Congresso Brasileiro de Química, 2018, São Luíz. Estudo quântico das propriedades geométricas do fármaco Vortioxetine usando DFT, 2018.
8. OLIVEIRA FILHO, M. A. C. ; OLIVEIRA, L. M. ; NASCIMENTO, M. C. ; **SILVA, L. P.** ; OLIVEIRA, S. P. ; MARINHO, E. S. . ESTUDO DE DOCKING MOLECULAR DA PIPERINA COM A PROTEÍNA CYP51: PIPERINA UM POTENCIAL FÁRMACO ANTI-LEISHMANICIDA. In: 58º Congresso Brasileiro de Química, 2018, São Luíz. ESTUDO DE DOCKING MOLECULAR DA PIPERINA COM A PROTEÍNA CYP51: PIPERINA UM POTENCIAL FÁRMACO ANTI-LEISHMANICIDA, 2018.

Resumos publicados em anais de congressos

1. **SILVA, L. P.**; LIMA, K. S. B. ; SANTOS, W. L. . Adaptação de uma aula prática sobre ácidos e bases utilizando materiais e reagentes de fácil acesso na disciplina de Química Geral. In: XXII Semana Universitaria UECE, 2017, Fortaleza. Encontro de monitoria (PROMAC), 2017.
2. BEZERRA, L. L. ; SILVA, J. ; LIMA, A. R. ; **SILVA, L. P.** ; MARINHO, M.M. ; MARINHO, E. S. . Estudos iniciais de modificação molecular (drug design) do fármaco anti-hipertensivo Alprenolol. In: XXII Semana Universitária UECE, 2017, Fortaleza. Encontro de iniciação científica, 2017.
3. SANTOS, W. L. ; **SILVA, L. P.** ; LIMA, K. S. B. . Proposta de Implantação de Aula Prática Sobre Estrutura Atômica na Disciplina de Química Geral. In: XXII Semana Universitária UECE, 2017, Fortaleza. XXII Semana Universitária da UECE, 2017. v. 1. p. 1-x.
4. BEZERRA, L. L. ; SILVA, J. ; LIMA, A. R. ; **SILVA, L. P.** ; MARINHO, M.M. ; MARINHO, E. S. . Caracterização inicial do fármaco antifúngico tavaborole para estudos de modificação molecular (drug design). In: XXII Semana Universitária UECE, 2017, Fortaleza. Encontro de iniciação científica, 2017.
5. **SILVA, L. P.**; TAVARES, C. D. A. . Adaptação de roteiros de aulas práticas na disciplina de Química Geral. In: XXI Semana Universitaria UECE, 2016, Fortaleza. Encontro de monitoria (PROMAC), 2016.

Demais tipos de produção técnica

1. MARINHO, E. S. ; **SILVA, L. P.** ; REGES, M. . SIMULAÇÃO COMPUTACIONAL APLICADA A QUÍMICA TEÓRICA. 2018. (Curso de curta duração ministrado/Extensão).

Eventos

Participação em eventos, congressos, exposições e feiras

1. ACS on Campus. 2019. (Congresso).
2. IX Semana Da Química UFC. 2019. (Congresso).
3. XXIII Semana Universitária da UECE. ESTUDOS INICIAIS DE CARACTERIZAÇÃO ESTRUTURAL DA MOLÉCULA MONO(2-ETILHEXIL)FTALATO. 2018. (Encontro).
4. III ENCONTRO INTERNACIONAL DE JOVENS INVESTIGADORES (EDIÇÃO BRASIL). Estudo DFT do Alcalóide Dincetrina: GAP, HOMO, LUMO, MESP E MULLIKEN. In: III Encontro Internacional de Jovens Investigadores. 2017. (Encontro).
5. XXII Semana Universitária UECE. Caracterização do fármaco antidepressivo Vortioxetina: um estudo in silico usando campo de força clássico MMFF94. 2017. (Encontro).
6. V Semana da Física e I Semana de Astronomia da UECE. 2016. (Encontro).
7. XXI Semana Universitária UECE. Adaptação de roteiros de aulas práticas na disciplina de Química Geral. 2016. (Encontro).
8. IV Semana da Física da UECE. 2015. (Encontro).
9. XX Semana Universitária. 2015. (Encontro).

Página gerada pelo Sistema Currículo Lattes em 18/12/2021 às 20:55:35

[Imprimir currículo](#)

APPENDIX B – PAPERS PUBLISHED

Physical Chemistry Chemical Physics

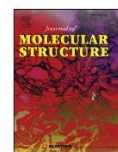


PCCP

Sulfonamide derived from anacardic acid as potential anti-sores: a theoretical approach based on Molecular Docking, Molecular Dynamics, and Density Functional Theory calculations

Journal:	<i>Physical Chemistry Chemical Physics</i>
Manuscript ID	CP-ART-08-2021-003995.R1
Article Type:	Paper
Date Submitted by the Author:	n/a
Complete List of Authors:	da Silva, Leonardo; Universidade Federal do Ceará, Química Analítica e Físico-Química Wagner Queiroz Neto, Francisco; Universidade Federal do Ceará, Analítica e Físico Química Bezerra, Lucas; Universidade Federal do Ceara, Química Analítica e Físico-Química Silva, Jacilene; Universidade Regional do Cariri Monteiro, Norberto; Federal University of Ceará Technology Centre, Marinho, Marcia; Universidade Federal do Ceará, Departamento de Farmácia; dos Santos, Helcio; Universidade Estadual Vale do Acaraú Teixeira, Alexandre; Universidade Regional do Cariri Marinho, Emmanuel; Universidade Estadual do Ceará Lima-Neto, Pedro; Universidade Federal do Ceara, Química Analítica e Físico-Química

SCHOLARONE™
Manuscripts



Characterization of the structural, spectroscopic, nonlinear optical, electronic properties and antioxidant activity of the N-{4'-[(E)-3-(Fluorophenyl)-1-(phenyl)-prop-2-en-1-one]}-acetamide



Francisco Wagner Q. Almeida-Neto^{a,*}, Leonardo P. da Silva^a,
 Maria Kueirislene A. Ferreira^b, Francisco Rogênio S. Mendes^e, Kevin K.A. de Castro^d,
 Paulo N. Bandeira^{c,d}, Jane Eire S.A. de Menezes^b, Hércio S. dos Santos^d,
 Norberto K.V. Monteiro^a, Emmanuel S. Marinho^e, Pedro de Lima-Neto^a

^a Departamento de Química Analítica e Físico-Química, Universidade Federal do Ceará, Campus do Pici, bloco 940, 60440-900, Fortaleza, CE, Brazil

^b Universidade Estadual do Ceará, Centro de Ciência e Tecnologia (CCT), Itaperi Campus, Laboratório de Química de Produtos Naturais - LQPN-S, Fortaleza, CE, Brazil

^c Departamento de Química Biológica, Universidade Regional do Cariri, Crato, CE, Brazil

^d Centro de Ciências Exatas e Tecnologia, Universidade Estadual do Vale do Acaraú, Sobral, CE, Brazil

^e Faculdade de Filosofia Dom Aureliano Matos, Universidade Estadual do Ceará, Ceará, Brazil

ARTICLE INFO

Article history:

Received 12 May 2020

Received in revised form

13 June 2020

Accepted 24 June 2020

Available online 27 June 2020

Keywords:

Bond dissociation energy

Claisen-schmidt aldol condensation

Fukui function

Nonlinear optical

Natural bond orbital

ABSTRACT

The molecule N-{4'-[(E)-3-(Fluorophenyl)-1-(phenyl)-prop-2-en-1-one]} chalcone (PAAPFBA) was recently synthesized due to the growing interest in the chemistry of the chalcone. The quantum chemical calculations were carried out to make a complete theoretical characterization (structural, spectroscopy, nonlinear optical, and electronic properties) employing three Density Functional Theory (DFT) methods like B3LYP, mPW1PW91, and M06-2X at 6-311++G(d,p) basis set. After all these characterizations, the antioxidant activity was studied using the reaction with the compound DPPH in methanol solution and the mechanism was investigated theoretically. All the three DFT methods used can describe with great accuracy the PAAPFBA chalcone: the results of infrared spectroscopy and the ¹H and ¹³C isotropic shielding demonstrate to be in excellent agreement with the experimental data. The nonlinear optical (NLO) properties show that the title chalcone can be used with great potential in NLO devices and this result is in good agreement with the Natural Bond Orbital (NBO) analysis, which shows how the electronic density is delocalized within the molecule. Finally, the experimental data of the antioxidant activity showed a moderate rate of reaction with the DPPH molecule (50.92%) and this fact was proved by the theoretical mechanisms with the Hydrogen Atom Transfer (HAT) mechanism more favorable.

© 2020 Elsevier B.V. All rights reserved.

1. Introduction

Chalcones are natural products considered as the most important subgroup of the flavonoid family. They are chemically characterized by the presence of an open chain with two phenyl rings bonded by α,β -unsaturated carbonyl group (1,3-diphenyl-2-propen-1-ones). For the chalcones, there are two possible

isomers, the E (trans) and Z (cis), being that E isomer occurs naturally and it is thermodynamically more stable [1]. The greatest interest in this class of compound lies in the fact that chalcones have many hydrogen atoms that can be replaced, thus generating the possibility of synthesis routes for several compounds with different possible applications. The chalcone can be used as antileishmanial, antibacterial, antimicrobial, immunosuppressive, antidepressant, anti-inflammatory, anti-obesity, hypnotic, and anticancer [1–11].

Despite these several applications, the chalcones exhibits antioxidant properties. Some examples about the great applicability of chalcone derivatives as antioxidants are given next. Arif et al. [12] studied the antioxidant properties of the 3-(1H-indol-3-yl)-1-p-

* Corresponding author. Departamento de Química Analítica e Físico-Química, Universidade Federal do Ceará, Campus do Pici, Bloco 938/939, 60020-181, Fortaleza, CE, Brazil.

E-mail address: wagnerqueirozneto@gmail.com (F.W.Q. Almeida-Neto).



Contents lists available at ScienceDirect

Heliyon

journal homepage: www.cell.com/heliyon

Research article

Quantum computational investigations and molecular docking studies on amentoflavone



Márcia M. Marinho^{a,*}, Francisco Wagner Q. Almeida-Neto^b, Emanuelle M. Marinho^b, Leonardo P. da Silva^b, Ramon R.P.B. Menezes^a, Ricardo P. dos Santos^c, Emmanuel S. Marinho^d, Pedro de Lima-Neto^b, Alice M.C. Martins^a

^a Departamento de Análises Clínicas e Toxicológicas, Centro de Ciências da Saúde, Universidade Federal do Ceará, Campus Porangabussu, 60430-370, Fortaleza, Ceará, Brazil

^b Departamento de Química Analítica e Físico-Química, Centro de Ciências, Universidade Federal do Ceará, Campus do Pici, Bloco 940, 60440-900, Fortaleza, Ceará, Brazil

^c Engenharia de Computação / Biotecnologia, Universidade Federal do Ceará, Campus de Sobral, 62010-560, Sobral Ceará, Brazil

^d Faculdade de Filosofia Dom Aureliano Matos, Universidade Estadual do Ceará, 62930-000, Limoeiro do Norte, Ceará, Brazil

ARTICLE INFO

Keywords:

Antichagasic agent
Biflavonoid
DFT
Fukui analysis
NLO

ABSTRACT

Chagas disease is a neglected tropical disease caused by the protozoan parasite *Trypanosoma cruzi*, with approximately 6–7 million people infected worldwide, becoming a public health problem in tropical countries, thus generating an increasing demand for the development of more effective drugs, due to the low efficiency of the existing drugs. Aiming at the development of a new antichagasic pharmacological tool, the density functional theory was used to calculate the reactivity descriptors of amentoflavone, a biflavonoid with proven anti-trypanosomal activity in vitro, as well as to perform a study of interactions with the enzyme cruzain, an enzyme key in the evolutionary process of *T. cruzi*. Structural properties (in solvents with different values of dielectric constant), the infrared spectrum, the frontier orbitals, Fukui analysis, thermodynamic properties were the parameters calculated from DFT method with the monomeric structure of the apigenin used for comparison. Furthermore, molecular docking studies were performed to assess the potential use of this biflavonoid as a pharmacological antichagasic tool. The frontier orbitals (HOMO-LUMO) study to find the band gap of compound has been extended to calculate electron affinity, ionization energy, electronegativity electrophilicity index, chemical potential, global chemical hardness and global chemical softness to study the chemical behaviour of compound. The optimized structure was subjected to molecular Docking to characterize the interaction between amentoflavone and cruzain enzyme, a classic pharmacological target for substances with anti-gas activity, where significant interactions were observed with amino acid residues from each one's catalytic sites enzyme. These results suggest that amentoflavone has the potential to interfere with the enzymatic activity of cruzain, thus being an indicative of being a promising antichagasic agent.

1. Introduction

Chagas disease is a tropical disease caused by the protozoan parasite *Trypanosoma cruzi*, classified as neglected by the World Health Organization. The Chagas disease is transmitted to humans by the triatomine insect, popularly known, in Brazil, as the barber [1]. Currently, there are approximately 6–7 million infected people in the world and it is estimated that 70 million people will be able to contract this disease. This is an endemic disease in Latin America, Africa and Asia, but also found in

non-endemic developed countries such as Canada, Spain, Japan and Australia [2,3]. Currently, benznidazole and nifurtimox are the only drugs used for the pharmacological treatment of Chagas disease, developed almost fifty years ago, have limited effectiveness in the chronic phase of the disease. However, these drugs led to the occurrence of several side effects, such as polyneuritis, bone marrow depression, lymphoma and dermatitis [4]. Therefore, it is necessary to look for new bioactive substances, as well as therapeutic strategies that promote

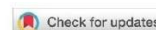
* Corresponding author.

E-mail address: marinho.marcia@gmail.com (M.M. Marinho).

<https://doi.org/10.1016/j.heliyon.2021.e06079>

Received 27 October 2020; Received in revised form 1 December 2020; Accepted 20 January 2021

2405-8440/© 2021 Published by Elsevier Ltd. This is an open access article under the CC BY-NC-ND license (<http://creativecommons.org/licenses/by-nc-nd/4.0/>).



Received: 16 February 2021 | Revised: 24 February 2021 | Accepted: 27 February 2021

DOI: 10.1002/maco.202112365

ARTICLE

Materials and Corrosion

A theoretical and experimental study of phosphate ester inhibitors for AISI 1018 in carbon dioxide-saturated 3.5 wt% NaCl solution

Roberta Bastos Vasques¹ | Marjory Moreira Levy¹ |
Matheus Souza Rodrigues¹ | Francisco Wagner de Queiroz Almeida Neto² |
Leonardo Paes da Silva² | Gustavo Leitão Vaz³ |
Álvaro Augusto Oliveira Magalhães³ | Pedro de Lima-Neto² |
Walney Silva Araújo¹

¹Departamento de Engenharia Metalúrgica, Universidade Federal do Ceará, Fortaleza, Ceará, Brazil

²Departamento de Química Analítica e Físico-Química, Universidade Federal do Ceará, Fortaleza, Ceará, Brazil

³Centro de Pesquisa da Petrobras CENPES, Rio de Janeiro—RJ, Brazil

Correspondence

Roberta B. Vasques, Departamento de Engenharia Metalúrgica, Universidade Federal do Ceará, Campus do Pici, Fortaleza, CE 60440-900, Brazil.
Email: robertavasques@yahoo.com.br

Funding information

Petrobras, Grant/Award Number: 2017/00402-2

Abstract

Phosphate ester was investigated as a corrosion inhibitor for AISI 1018 carbon steel in carbon dioxide-saturated chloride solutions at different temperatures and pressures. The corrosion tests were realized by electrochemical techniques, weight loss measurements, bubble tests, and a high-pressure/high-temperature autoclave system. The corrosion tests demonstrated that the investigated molecule is an excellent corrosion inhibitor. The inhibiting effect is even bigger at high pressure and temperature than at atmospheric pressure and room temperature. The thermodynamic parameters were calculated and determined to obey the Langmuir isotherm. Polarization studies revealed that the evaluated inhibitor is a mixed type.

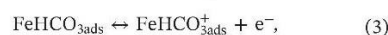
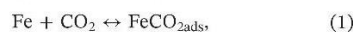
KEYWORDS

carbon dioxide, corrosion inhibitors, phosphate ester, temperature, pressure

1 | INTRODUCTION

Corrosion caused by CO₂ in the aqueous phase is a common problem in carbon steel pipelines used in oil and gas transportation. The formation of corrosion products is usually an essential process in the CO₂ corrosion mechanism, and their presence can significantly change the corrosion rate.^[1,2] For the cathodic process, some papers have proposed two mechanisms: the buffering effect,^[5–7] which relates the impact of the pH on the dissociation of carbonic acid and hydrogen evolution, from a combination of H⁺, H₂CO₃⁻, HCO₃⁻, and H₂O.^[3,4,8–10] However, steel dissolution accounts for the anodic process.

In 1996, Nescic et al.^[11] proposed different anodic mechanisms for steel dissolution in CO₂ solutions at a pH range from 2.5 to 6. The author proposed six reactions at pH < 4, 4 < pH < 5, and pH > 5 (Equations (1)–(6)). Then, for carbon steel, CO₂ corrosion rates are strongly influenced by many factors, such as flow velocity, temperature, pH, gas-liquid rates, oil-water ratio, CO₂ partial pressure, and chemical composition of the produced water^{[12–14]:}





Contents lists available at ScienceDirect

Fuel

journal homepage: www.elsevier.com/locate/fuel

Full Length Article

Effect of additives on the oxidative stability and corrosivity of biodiesel samples derived from babassu oil and residual frying oil: An experimental and theoretical assessment

Nelly V.P. Rangel^a, Leonardo P. da Silva^b, Vinícius S. Pinheiro^a, Igor M. Figueredo^{a,c}, Othon S. Campos^c, Stefane N. Costa^d, Francisco Murilo T. Luna^e, Célio L. Cavalcante Jr.^e, Emmanuel S. Marinho^f, Pedro de Lima-Neto^b, Maria A.S. Rios^{a,*}

^a Grupo de Inovações Tecnológicas e Especialidades Químicas, Centro de Tecnologia, Universidade Federal do Ceará, Campus do Pici, Bloco 714, CEP 60440-554 Fortaleza, CE, Brazil

^b Departamento de Química Analítica e Físico-Química, Centro de Ciências, Universidade Federal do Ceará, Campus do Pici, Bloco 940, CEP 60440-900 Fortaleza, CE, Brazil

^c Departamento de Química e Física, Universidade Federal do Espírito Santo, Campus Guararema, CEP 29500-000 Alegre, ES, Brazil

^d Programa de Pós-Graduação em Engenharia Metalúrgica e de Materiais, Universidade Federal do Ceará, Fortaleza, CE, Brazil

^e Grupo de Pesquisa em Separações por Adsorção, Núcleo de Pesquisas em Lubrificantes, Departamento de Engenharia Química, Universidade Federal do Ceará, Fortaleza, CE CEP 60455-900, Brazil

^f Faculdade de Filosofia Dom Aureliano Matos, Universidade Estadual do Ceará, CEP 62930-000 Limoeiro do Norte, Ceará, Brazil

ARTICLE INFO

Keywords:
FUKUI index
DFT
PDA
IONOL
Hydrogenated cardanol

ABSTRACT

The objective of this work is to evaluate the effect of the addition of N,N'-di-sec-butyl-p-phenylenediamine (PDA), IONOL, and hydrogenated cardanol (HC) (500 mg/kg, each) on the oxidative stability and corrosivity of biodiesel obtained from babassu oil (BB) and from residual frying oil (BRFO). Oxidative stability was assessed by induction period (IP) using the Rancimat method (EN 14112), while the corrosivity was assessed by the mass losses of copper coupons immersed in the biodiesel samples (ASTM TM0169/G31-12a (2010)). The most severe corrosion was observed for the fresh biodiesel samples without any additives (4.85 mpy for BB, and 5.00 mpy for BRFO). Using PDA, IONOL, and HC as additives inhibited the copper corrosion in both biodiesel samples (between 0.61 and 3.09 mpy for BB, and between 2.19 and 4.69 mpy for BRFO). The use of IONOL and PDA as additives, besides showing a decrease in corrosion rates, also improved the oxidative stability (IP values) for both biodiesel samples (by 66 and >100 h, for BB; and by 3.31 and 7.23 h, for BRFO, respectively), demonstrating that these additives have bi-functionality in these biodiesel samples. Conversely, the use of HC increased the oxidative stability for BB (by 10.82 h) but also presented a pro-oxidant effect on biodiesel obtained from residual frying oil, decreasing its IP value by ca. 18%. Finally, theoretical studies were carried out based on the formalism of the functional density theory, which confirmed that PDA has indeed the highest anti-corrosion potential among the studied additives.

1. Introduction

The gradual depletion of fossil fuel reserves, the increase of oil prices, and environmental concerns have accelerated the need to find fuels that meet technical and sustainable requirements given the consequences of the greenhouse effect on human health. In this perspective, based on the principles of green chemistry for the use of renewable energies, biodiesel has stood out as an alternative to petrodiesel. This fuel is biodegradable and may be produced from different fatty raw materials [1,2].

Considered environmentally friendly because it is sulfur-free, non-toxic, and derived from renewable sources, biodiesel is however susceptible to oxidation, and this represents one of the biggest challenges in its production and commercialization [3]. In the production of biodiesel, triacylglycerols are converted into esters by transesterification to obtain a fuel that has properties similar to petrodiesel [4]. Among the main advantages, it possesses higher flash point than petrodiesel, which facilitates its transport [5], is biodegradable, and generates fewer emissions [6].

However, due to its chemical structure and the presence of double

* Corresponding author.

E-mail address: alexandrarios@ufc.br (M.A.S. Rios).

<https://doi.org/10.1016/j.fuel.2020.119939>

Received 20 August 2020; Received in revised form 28 November 2020; Accepted 1 December 2020

Available online 16 December 2020

Synthesis of a new quinine dimer biocatalysed by the coconut water

Aluísio M. Fonseca^{a,b}, Leonardo Paes da Silva^c, Francisco Wagner de Queiroz Almeida-Neto^c, Regilany Paulo Colares^b, Mauro Macedo de Oliveira^{a,d}, Antônio Luthierre Gama Cavalcante^c, Telma L. G. Lemos^e, Raimundo Braz-Filho^f, Pedro de Lima-Neto^c and Emmanuel Silva Marinho^{c,g}

^aMestrado Acadêmico em Sociobiodiversidades e Tecnologias Sustentáveis – MASTS, Instituto de Engenharias e Desenvolvimento Sustentável, Universidade da Integração Internacional da Lusofonia Afro-Brasileira, Acarape, Brazil; ^bInstituto de Ciências Exatas e da Natureza, Universidade da Integração Internacional da Lusofonia Afro-Brasileira, Acarape, Brazil; ^cGrupo de Química Teórica, Departamento de Analítica e Físico-Química, Universidade Federal do Ceará, Fortaleza, Brazil; ^dDepartamento de Química, Centro Universitário Paraíso – UNIFAP, Juazeiro do Norte, Brazil; ^eLaboratório de Biocatálise e Produtos Naturais, Departamento de Química Orgânica e Inorgânica, Universidade Federal do Ceará, Fortaleza, Brazil; ^fCentro de Ciências e Tecnologias, Universidade Estadual do Norte Fluminense Darcy Ribeiro, Campos Dos Goytacazes, Brazil; ^gFaculdade de Filosofia Dom Aureliano Matos - FAFIDAM, Universidade Estadual do Ceará, Centro, Brazil

ABSTRACT

The obtaining of bis-quinine, a novel alkaloid dimer, has been successfully achieved starting from quinine and the raw coconut juice (*Cocos nucifera*) as biocatalyst dimerization-like reaction, in mild conditions, with a mass yield of 64.7% in 72 h. The structural elucidation was made based on the spectral data, mainly by a high-field NMR and a mass spectrometry. In a second step, theoretical calculations were performed, an optimised energy structure of the new compound was obtained, the energy gap of the boundary orbitals (HOMO and LUMO) as well as the chemical reactivity descriptors were estimated.

GRAPHICAL ABSTRACT

ARTICLE HISTORY

Received 23 August 2020
 Revised 7 May 2021
 Accepted 23 May 2021

KEYWORDS

Quinine; biotransformations;
 crude enzyme;
 coconut water

1. Introduction


In the recent decades, the current model of economic, scientific and technological development, combined with unrestrained consumerism, has generated a significant increase in the consumption of goods and raw materials, as well as an unbridled growth in industrial production and the usage of synthetic chemicals (Chi et al. 2019). This actions have generated an unseen picture of environmental degradation leading to an environmental crisis. Therefore, it is necessary to develop processes and actions that would minimise the harmful entropic effects in the natural and human environments (Faber et al. 2019; Schwarz 2017).

With the purpose to maintain and improve the quality of life around the planet and considering the need for continuous sustainable economic, social and environmental developments, a new chemical conduct would become imperative for the improvement of the techniques and methodologies with the rising generation of toxic residues and effluents. This particular trend, known as Green Chemistry, can be defined as "the creation, development and application of

chemicals, as well as the processes to reduce or eliminate the use in the generation of substances that are harmful to human health and the environment" (Irvani 2011; Lazar 2008; Lewandowski 2014). Hence, this previously mentioned way, provides enzymes that will increasingly replace many conventional catalysts, since they are a sustainable path, because they are ecologically more viable. The usage of enzymes (isolated from vegetables or microorganisms) as catalysts to promote specific changes in a given substrate, is known as biocatalysis, which is considered an interdisciplinary area by correlating studies in organic chemistry and biology, therefore, contributing to the development of new synthetic strategies with the use of easily accessible raw materials (Sheldon and Woodley 2018).

Previous studies have reported the presence of enzymes in all parts of fruits that have been used as biocatalysts in several organic reactions (Chittamuru et al. 2016). Research continues to find sources of enzymes in the Brazilian plants for a later use in biocatalysis, such as the juice of *Cocos nucifera* L. Among

CONTACT Aluísio M. Fonseca aluismi@unilab.edu.br Institute of Exact and Nature Sciences – ICEN, University for the International Integration of the Afro-Brazilian Lusophony, Acarape, CE, CEP 62785-000, Brazil

 Supplemental data for this article can be accessed [here](#).

© 2021 Informa UK Limited, trading as Taylor & Francis Group



A potential bio-antioxidant for mineral oil from cashew nutshell liquid: an experimental and theoretical approach

Rubem S. F. Paula¹ · Rodrigo S. Vieira¹ · F. Murilo T. Luna¹ · Célio L. Cavalcante Jr.¹ · Igor M. Figueredo^{1,5} · José R. Candido Jr.² · Leonardo P. Silva² · Emmanuel S. Marinho³ · Pedro de Lima-Neto² · Diego Lomonaco⁴ · Selma E. Mazzetto⁴ · Maria A. S. Rios⁵

Received: 9 January 2020 / Revised: 19 April 2020 / Accepted: 5 May 2020
© Associação Brasileira de Engenharia Química 2020

Abstract

The objective of the present work was to evaluate the antioxidant potential of a mixture of saturated, monoene, diene, and triene cardanols derived from the cashew nutshell liquid in naphthenic mineral oil. A mineral naphthenic oil sample was doped with the cardanols mixture at concentrations of 500, 2000, and 5000 mg/kg and evaluated using differential scanning calorimetry (DSC) and the accelerated oxidative method (PetroOXY), following ASTM standards (E2041-18, E1970-16, E537-12, and E698-18). The addition of cardanols increased the oxidative stability of the mineral oil by a factor of 4 to 5. To evaluate the antioxidant potential of each particular cardanol present in the mixture, structural analysis and specific antioxidant mechanisms were investigated by density functional theory (DFT). Each molecular structure was optimized with the hybrid functional B3LYP with a basis set 6-31G (d, p), and the antiradical mechanisms (HAT, SPLET, and SET-PT) were evaluated. The HAT was the best observed mechanism, standing out for the cardanol monoene that showed presented better antiradical activity. Concerning the global reactivity study, it was concluded that the increase of the unsaturations in the side chain of the molecules contributes significantly to their increased general reactivity. When evaluating the Fukui index, it was confirmed that, for the cardanol monoene, the reactivity prevails in the aromatic ring with an emphasis on oxygen

Electronic supplementary material The online version of this article (<https://doi.org/10.1007/s43153-020-00031-z>) contains supplementary material, which is available to authorized users.

✉ Maria A. S. Rios
alexandrarios@ufc.br

¹ Grupo de Pesquisa em Separações por Adsorção,
Departamento de Engenharia Química, Núcleo de Pesquisas
em Lubrificantes, Universidade Federal do Ceará, Fortaleza,
CE CEP 60455-900, Brasil

² Departamento de Química Analítica e Físico-Química,
Centro de Ciências, Universidade Federal do Ceará,
Fortaleza, CE CEP 60440-900, Brasil

³ Departamento de Química/FAFIDAM, Universidade
Estadual do Ceará, Limoeiro do Norte, CE CEP 62930-000,
Brasil

⁴ Laboratório de Produtos e Tecnologia em Processos,
Departamento de Química Orgânica e Inorgânica, Centro
de Ciências, Universidade Federal do Ceará, Fortaleza,
CE CEP 60440-900, Brasil

⁵ Grupo de Inovações Tecnológicas e Especialidades
Químicas, Departamento de Engenharia Mecânica, Centro
de Tecnologia, Universidade Federal do Ceará, Fortaleza,
CE CEP 60440-554, Brasil

Published online: 20 May 2020



Antioxidant and anticholinesterase activities of amentoflavone isolated from *Ouratea fieldingiana* (Gardner) Engl. through *in vitro* and chemical-quantum studies

Lucas Soares Frota^a, Daniela Ribeiro Alves^b, Márcia Machado Marinho^c, Leonardo Paes da Silva^c, Francisco Wagner de Queiroz Almeida Neto^c, Emmanuel Silva Marinho^d and Selene Maia de Morais^e

^aPrograma de Pós-graduação em Biotecnologia, Rede Nordeste de Biotecnologia, Faculdade de Veterinária, Universidade Estadual do Ceará, Fortaleza, Brasil; ^bPrograma de Pós-graduação em Ciências Naturais, Faculdade de Veterinária, Núcleo de Pesquisa em Sanidade Animal, Universidade Estadual do Ceará, Fortaleza, Brasil; ^cDepartamento de Química Analítica e Físico-Química, Centro de Ciências, Universidade Federal do Ceará, Fortaleza, Brasil; ^dGrupo de Química Teórica e Eletroquímica, Faculdade de Filosofia Dom Aureliano Matos, Universidade Estadual do Ceará, Limoeiro do Norte, Brasil; ^eCurso de Química, Renorbio, Universidade Estadual do Ceará, Fortaleza, Brasil

Communicated by Ramaswamy H. Sarma

ABSTRACT

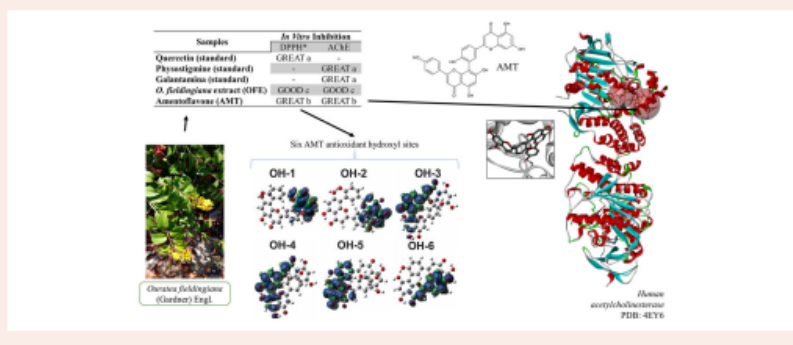
Ouratea fieldingiana, popularly known as batiputá, is a tree species easily found in the coastal part of northeastern Brazil. Its leaves are rich in biflavonoids, its major compound being amentoflavone. Biflavonoids are well studied due to their high antioxidant capacity. Alzheimer's disease (AD) is a disease characterized by the progressive loss of neurons. Currently, the pharmacological treatment of AD has four drugs: donepezil, galantamine, rivastigmine and memantine. Where these drugs, with the exception of memantine, are inhibitors of acetylcholinesterase, thus inhibiting the enzyme that destroys acetylcholine, thus increasing the availability of this neurotransmitter. This article aims to determine *in vitro* and *in silico* the antioxidant and anticholinesterase action of amentoflavone isolated from the leaves of *Ouratea fieldingiana*. The antioxidant capacity of amentoflavone was evaluated using the DPPH[•] free radical scavenging method, with an IC₅₀ of 5.73 ± 0.08 µg/mL. The antiradical properties of the molecule were also studied *in silico* through several HAT, SET-PT and SPLET mechanisms via DFT M06-2X/6-311++G(d,p). It was found that in the hydrogen atom transfer mechanism (HAT) the best trend was obtained as an anti-radical mechanism. Amentoflavone has the ability to inhibit acetylcholinesterase when tested *in vitro*, having an IC₅₀ of 8.68 ± 0.73 µg/mL, corroborating its effect in the *in silico* test, presenting four strong covalent hydrogen bonds for having a bond length up to 2.5 Å. Thus, amentoflavone is an important target for further testing against Alzheimer's disease.

ARTICLE HISTORY

Received 15 September 2021
 Accepted 7 December 2021

KEYWORDS

Amentoflavone; antioxidant; density functional theory; enzymes; natural products; quantum chemical calculations



CONTACT Emmanuel Silva Marinho emmanuel.marinho@uece.br Grupo de Química Teórica e Eletroquímica, Faculdade de Filosofia Dom Aureliano Matos, Universidade Estadual do Ceará, Limoeiro do Norte, Brasil.

Supplemental data for this article can be accessed online at <https://doi.org/10.1080/07391102.2021.2017353>.

© 2021 Informa UK Limited, trading as Taylor & Francis Group

APPENDIX C – ELSEVIER AND RSC'S AUTHOR RIGHTS

According to Elsevier's and RSC permission and Author's rights to reproduce copyright work, the author can use the published articles in part or complete when included in a thesis if there are no commercial purposes. The following information was taken from Elsevier's and RSC website accessed on January 06, 2022.

source: <https://www.elsevier.com/about/policies/copyright/permissions>

Author rights in Elsevier's proprietary journals	Published open access	Published subscription
Retain patent and trademark rights	✓	✓
Retain the rights to use their research data freely without any restriction	✓	✓
Receive proper attribution and credit for their published work	✓	✓
Re-use their own material in new works without permission or payment (with full acknowledgement of the original article): 1. Extend an article to book length 2. Include an article in a subsequent compilation of their own work 3. Re-use portions, excerpts, and their own figures or tables in other works.	✓	✓
Use and share their works for scholarly purposes (with full acknowledgement of the original article): 1. In their own classroom teaching. Electronic and physical distribution of copies is permitted 2. If an author is speaking at a conference, they can present the article and distribute copies to the attendees 3. Distribute the article, including by email, to their students and to research colleagues who they know for their personal use 4. Share and publicize the article via Share Links, which offers 50 days' free access for anyone, without signup or registration 5. Include in a thesis or dissertation (provided this is not published commercially) 6. Share copies of their article privately as part of an invitation-only work group on commercial sites with which the publisher has a hosting agreement	✓	✓

source: <https://www.elsevier.com/about/policies/copyright>

Deposition and sharing rights

The following details apply only to authors accepting the standard licence to publish. Authors who have accepted one of the open access licences to publish, or are thinking of doing so, should refer to the [details for open access deposition rights](#).

When the author accepts the licence to publish for a journal article, he/she retains certain rights concerning the deposition of the whole article. This table summarises how you may distribute the accepted manuscript and version of record of your article.

Sharing rights	Accepted manuscript	Version of record
Share with individuals on request, for personal use	✓	✓
Use for teaching or training materials	✓	✓
Use in submissions of grant applications, or academic requirements such as theses or dissertations*	✓	✓
Share with a closed group of research collaborators, for example via an intranet or privately via a scholarly communication network	✓	✓
Share publicly via a scholarly communication network that has signed up to STM sharing principles	⌚	×
Share publicly via a personal website, institutional repository or other not-for-profit repository	⌚	×
Share publicly via a scholarly communication network that has not signed up to STM sharing principles	×	×



source: <https://www.rsc.org/journals-books-databases/author-and-reviewer-hub/authors-information/licences-copyright-permissions/>